DEPENDENCE OF TWO ARBOVIRUSES ON THE HOST MICRORNA PATHWAY

by

Cathaleen King Madsen
A Dissertation
Submitted to the
Graduate Faculty
of
George Mason University
in Partial Fulfillment of
The Requirements for the Degree
of
Doctor of Philosophy
Biosciences

Committee:

_____ Dr. Kylene Kehn-Hall, Dissertation Director

_____ Dr. Fatah Kashanchi, Committee Member

_____ Dr. Barney Bishop, Committee Member

_____ Dr. Norman Lee, Committee Member

_____ Dr. James Willett, Department Chair

_____ Dr. Donna M. Fox, Associate Dean, Office of Student Affairs and Special Programs, College of Science

_____ Dr. Peggy Agouris, Dean, College of Science

Date: _____ Summer Semester 2015
George Mason University
Fairfax, VA

Dependence of Two Arboviruses on the Host MicroRNA Pathway

A Dissertation submitted in partial fulfillment of the requirements for the degree of Doctor of Philosophy at George Mason University

by

Cathaleen King Madsen
Bachelor of Arts
Randolph-Macon Woman's College, 1995

Director: Kylene Kehn-Hall, Associate Professor
Biosciences

Summer Semester 2015
George Mason University
Fairfax, VA

DEDICATION

This work is dedicated to the dear friends and family I lost during my graduate studies, especially these:

Harold Van Carpenter, II (2010), faithful friend, genial host, and stalwart protector of our nation;

Cathaleen "Cici" King-Shelton (2012), beloved mother and the first scientist I ever knew;

Cathaleen Hutchins and Norma Joy (2012), beloved grandmothers-- one my rock, and the other my source of wisdom;

Susan O'Reilly (2014), aunt by marriage, who never let "extended" get in the way of "family,"

And last but not least, our children Bridget (2013) and Max (2014).

Thank you for everything, in this life and beyond.

ACKNOWLEDGEMENTS

I owe a great debt of thanks to all of those who helped make this project a success, especially my dissertation committee. In particular, Dr. Kylene Kehn-Hall, Committee Chair, provided expert guidance, gentle encouragement, hard truth, and strong mentorship as I developed my scientific skills. Committee members Drs. Fatah Kashanchi and Barney Bishop of George Mason University, and Dr. Norman Lee of The George Washington University, provided invaluable tools, insight, and suggestions to strengthen this project. Additional thanks go to Drs. Bi-Dar Wang and Russell Williams, also of GWU, for the microarray hybridization and analysis, and Dr. Catherine Campbell of DCE Consulting for the bioinformatics tools. The current and former members of Kehn-Hall Lab, Dr. Cynthia de la Fuente, Dr. Alan Baer, Dr. Todd Bell, Ashwini Benedict, Jacque Fontenot, Dr. Irene Guendel, Idris Hooper, Lindsay Lundberg, Chelsea Pinkham, and Dr. Nazly Shafagati, provided companionship, advice, and emergency backup sample collection as needed. Drs. Ancha Baranova, Monique Van Hoek, Taissia Popova, and Aarthi Narayanan provided additional necessary advice and encouragement, while Drs. James Willett, Daniel Cox, Larry Rockwood, and Charles Madden kept me funded during the academic terms. The indefatigable administrators Diane St. Germain, Andrea Nikoi, and Jacqueline Houle kept the paperwork running as smoothly as possible. Special thanks are due to Dr. Charles Bailey, Director of the National Center for Biodefense and Infectious Diseases at George Mason University, for his leadership, and to the anonymous donors of our human cell lines, in making our research possible.

On a personal note, I would like to thank my family, that vast Madsen-King-Bowman-Koumoutseas-Hutchins-Johnson-Carlson-O'Reilly-McDowell clan, and the Fairfax Crew, especially the families Wilbur, O'Shea (all three generations), Smith, Van Vleet, and Render-Lyle, along with Patty Hagan, Erin Kelly, Joe Farrell, Cindy Ballentine, Carolyn Henn, and Tony Russo, for the sanity checks, meals, and zombie apocalypse jokes, and to Deirdre Whitford, the wind beneath my wings and the boot beneath my bottom. Extra special thanks go to Mike and Merilew Evers and the late Ruth Balzer for opening their hearts, home, refrigerator, and guest space to me for all these years.

Finally, I wish to thank the three people who have been most instrumental in helping me to get this far: Ruthie Evers, for 26 years of everything from the paracosm to the chicken dinners; Dane Madsen, for daily acts of love and support far too numerous to mention; and to Charlotte, for hanging in there and keeping me grounded as we went through this crazy process together. To them, and to everyone on this list, I give my sincerest gratitude.

TABLE OF CONTENTS

LIST OF TABLES

LIST OF FIGURES

LIST OF ABBREVIATIONS

293-T ..... Human Embryonic Kidney cells strain 293-T
Ago ..... Argonaute protein
a-miR-(number) ..... anti-microRNA (number)
ANOVA ..... Analysis of Variance
BCL11B ..... B-Cell/CLL Lymphoma Protein 11B
BIM (BCL2L11) ..... BCL-like 11
BME 2-Mercaptoethanol
BMPR2 ..... Bone Morphogenic Protein 2
BSA ..... Bovine Serum Albumin
BSL ..... Biosafety Level
CCND1 ..... Cyclin D1
cDNA ..... Complementary DNA
CDC ..... Centers for Disease Control and Prevention
CHIKV ..... Chikungunya Virus
Ct ..... Cycle Threshold
CV ..... Crystal Violet stain
ΔNSm ..... Rift Valley Fever Virus strain lacking NSm protein
ΔNSs ..... Rift Valley Fever Virus strain lacking NSs protein
DDIT4 ..... DNA Damage-Inducible Transcript 4
DGCR8 ..... DiGeorge Critical Region Syndrome 8 protein
DMEM ..... Dulbecco's Modified Eagle's Media
DMEM+++ ..... Dulbecco's Modified Eagle's Media, completed by supplementation
dsRNA ..... Double Stranded RNA
DTT ..... Dithiothreitol
EEEV ..... Eastern Equine Encephalitis Virus
EIF4G2 ..... Eukaryotic Translation Initiation Factor 4, Gamma 2
EMSA ..... Electromobility Shift Assay
ER ..... Endoplasmic Reticulum
Exp-5 ..... Exportin-5
FOX ..... Forkhead Box protein
Gc ..... Glycoprotein at C terminus
Gn ..... Glycoprotein near N terminus
HCV ..... Hepatitis C Virus
HHS ..... Department of Health and Human Services
HIV ..... Human Immunodeficiency Virus
HOX ..... Homeobox

Hpi..... Hours Post Infection
Hpt.....Hours Post Transfection
hsa-(prefix).....Homo sapiens
HSAECS ..... Human Small-Airway Epithelial Cells
IGF1R ..... Insulin-like growth factor 1 receptor
IL-[number].....Interleukin-[number]
IRES.....Internal Ribosome Entry Site
kDa..... kilodalton
L (segment) .....Large segment
Let-7..... Lethal-7 microRNA
M (segment).....Medium segment
MAPK..... Mitogen-Activated Protein Kinase
MEM.....Minimal Essential Media
miR-[number] ..... MicroRNA-[number]
miRNA.....microRNA
mRNA.....Messenger RNA
MOI.....Multiplicity of Infection
MP12.....MP12 strain of Rift Valley Fever Virus (attenuated)
µg .....Microgram
µl ..... Microliter
µM..... Micromolar
N or NP .....Nucleoprotein
NC.....Negative Control
NF-κB .....Nuclear Factor kappa-light-chain-enhancer of activated B cells
nM.....Nanomolar
NSm ..... Nonstructural Protein, Medium Segment
NSs.....Nonstructural Protein, Small Segment
Nt.....Nucleotide(s)
ORF..... Open Reading Frame
PABP1..... Polyadenylate Binding Protein 1
PBS .....Phosphate Buffered Saline
PBST.....Phosphate Buffered Saline with 0.5% TWEEN-20
piRNA.....Piwi-like Interacting RNA
PKR..... Double-Stranded RNA-Dependent Protein Kinase
PTEN.....Phosphatase and Tensin Homolog
PVDF ..... Polyvinylidine Fluoride
qRT-PCR.....Quantitative Real Time Polymerase Chain Reaction
RdRP..... RNA-dependent RNA polymerase
RGS.....Reverse Genetics System
RISC.....RNA induced silencing complex
RNAi.....RNA Interference
RNP.....Ribonucleoprotein Complex
RVFV..... Rift Valley fever virus
S(segment) .....Small segment

SFV ..... Semliki Forest virus
shRNA.....Small Hairpin RNA
SINV .....Sindbis virus
siRNA .....Small Interfering RNA
si(protein name) ..... Small Interfering RNA Against (Protein Name)
SOX..... Sex Determining Region Y Box
TC-83 .....Venezuelan Equine Encephalitis Strain TC-83
TrD .....Venezuelan Equine Encephalitis Strain Trinidad Donkey
TFIIH ..... Transcription Factor II Human
TNF-α.....Tumor Necrosis Factor Alpha
USDA..... United States Department of Agriculture
UTR.....Untranslated Region
VEEV .....Venezuelan Equine Encephalits Virus
vsRNA.....Virally Derived Small RNA
WEEV ..... Western Equine Encephalitis Virus
Wnt..... Wingless Type
WT ..... Wild Type
XPO5..... Exportin-5
ZH501 ..... Rift Valley Fever Virus strain ZH501
ZH548 ..... Rift Valley Fever Virus strain ZH548

ABSTRACT

DEPENDENCE OF TWO ARBOVIRUSES ON THE HOST MICRORNA PATHWAY

Cathaleen King Madsen, Ph.D.

George Mason University, 2015

Dissertation Director: Dr. Kylene Kehn-Hall

Rift Valley fever virus (RVFV) and Venezuelan equine encephalitis virus (VEEV) are two mosquito-borne, select agent viruses with severe effects on humans and livestock, and for which no FDA-approved vaccines or specific treatments exist. To identify potential therapeutic targets, this research focuses on viral interactions with host microRNA (miRNA), a class of small, non-coding RNA which bind to messenger RNA (mRNA) to regulate its endpoint proteins. This study demonstrates dependence of both RVFV and VEEV on the host miRNA pathway through different means. RVFV infection induces upregulation of miR-630 and miR-99a, which downregulate the anti-apoptotic protein IGF1R. Inhibition of these miRNA partially rescues IGF1R and decreases viral replication. Conversely, RVFV NSs protein inhibits the anti-apoptotic miR-17-92 cluster, revealing interplay between NSs and miRNA for control of host functions during infection, while overexpression of this cluster reduces viral replication. In contrast, VEEV replication depends heavily on miRNA processing enzymes including

Drosha, Exportin 5, and Argonaute 2 (Ago2). Knockdown or inhibition of these enzymes leads to decreased replication and production of viral proteins. The Ago2 inhibitor acriflavine (ACF) reduces VEEV replication in both vaccine and virulent strains by approximately 6-$\log_{10}$ in culture, and is similarly effective against Eastern and Western equine encephalitis viruses. Taken together, these data show the importance of the miRNA pathway for several types of virus, suggesting a fine-tuning function for replication in RVFV and an active use of the pathway itself for VEEV and related Alphaviruses.

CHAPTER 1: STATEMENT OF PROBLEM

Rift Valley fever virus (RVFV) and Venezuelan equine encephalitis virus (VEEV) are arthropod-borne, zoonotic diseases, currently identified as select agents of concern for their severe disease courses in humans and animals, lack of specific treatment, and potential to emerge in naïve regions either through natural means or nefarious intent. RVFV produces a characteristic "abortion storm" phenotype among infected livestock herds, while VEEV causes potentially fatal neurological disease in horses and equids. While normally self-limiting in humans, both diseases can cause debilitating illness lasting several weeks, with potential long-term neurological complications and other serious sequelae, and in rare cases, can be fatal. While the molecular biology of RVFV and VEEV are fairly well-characterized, little is known about the exact mechanisms of pathogenicity in mammalian systems. It is hoped that this investigation of viral interactions with host microRNA, a class of molecules highly conserved among vertebrates, will provide both a fuller understanding of viral pathogenesis and an opportunity for therapeutic or preventative measures.

CHAPTER 2: SPECIFIC AIMS

MicroRNA (miRNA) comprises a class of small, non-coding RNA which serve as master regulators of the cell, canonically by binding to messenger RNA (mRNA) and inhibiting production of the endpoint proteins. They are widely conserved among vertebrates and were initially studied for their roles in embryonic development and oncogenesis. Later studies illustrated their roles in viral pathogenesis, specifically for those viruses which interact with the host genome and/or maintain latency, such as hepatitis C virus (HCV) and human immunodeficiency virus (HIV). While the larger picture of miRNA interaction in disease states is being expanded, there is comparatively little information regarding its role in acute viral infections. Specifically, there is a **gap of knowledge** regarding miRNA regulation in Rift Valley fever virus (RVFV) and Venezuelan equine encephalitis infection, and the mechanisms by which such regulation contribute to viral pathogenesis and/or host response. RVFV is known to induce effects consistent with miRNA regulation, such as developmental abnormalities in livestock[1] and activation of DNA damage response in cultured cells[2], while differential regulation of miRNA regulation has been reported for VEEV in the brains of infected mice[3]. Therefore, **we hypothesize** that miRNA alteration is a significant factor in RVFV and VEEV pathogenesis in a human cell model. To test these hypotheses, we performed two broad sets of experiments, the first focused on RVFV and the second on VEEV.

In the first set of experiments, microarray analysis of miRNA isolated from RVFV-infected human small-airway epithelial cells (HSAECs) showed a significant subset of miRNA which were up- or down-regulated by twofold or greater compared to the levels in uninfected controls. Bioinformatic analysis predicted multiple "significant pathways" targeted by these miRNA, comprised largely of two overall groups: cytokines and developmental genes. Additional bioinformatic analysis combined with literature search supported this latter category, as well as linking developmental and cell-cycle control genes to several of the most highly regulated miRNA. This is noteworthy due to the characteristic "abortion storm" phenotype shown in RVFV infection of livestock[4], as well as the RVFV-induced regulation of cell cycle and DNA damage response pathways[2,5] previously demonstrated by our research group.

The second set of experiments focused on interaction of VEEV with host miRNA machinery, and demonstrated a significant decrease in viral replication with the loss of nuclear component Drosha, but not cytoplasmic Dicer. In particular, the inhibition of Ago-2, a component of the RNA-induced silencing complex (RISC), induced a major decrease in VEEV replication. Taken together, these experiments suggest a significant role for miRNA mediation of acute viral infections, and represent a significant opportunity to characterize several factors of host-pathogen interaction. We therefore propose the following objectives:

2.1: Aim 1— Confirm highly regulated miRNA and identify potential links to specific pathogenic processes in RVFV.

Regulation of highly up-regulated and down-regulated miRNA, as well as other miRNA of potential interest, will be confirmed by qRT-PCR. Bioinformatic databases and literature search will be used to identify connections to known pathogenic processes of RVFV such as cell cycle dysregulation, apoptosis, viral protein expression, or replication.

2.2: Aim 2— Investigate specific regulation of pathogenic processes by confirmed miRNA.

Subaim 2.2.1: Connect regulation of miR-630 and miR-99a to apoptosis and cell cycle effects.

miR-630 and miR-99a were identified bioinformatically as potential mediators of cell cycle and apoptosis. Specific gene targets of these miRNA will be identified through bioinformatics and literature search. Regulation of these gene targets will be confirmed by qRT-PCR as described above, and/or by western blot for the endpoint protein(s). Effect on viral replication will be assessed by antagonism of miR-630 and/or miR-99a in HSAECs prior to infection with RVFV. Collected supernatants from these experiments will be assessed by plaque assay in Vero cells to determine viral replication. Finally, specific regulation by miRNA will confirmed by assessing rescue or reversal of endpoints, using antagonism of the miRNA in question, followed by qRT-PCR or western blot as described above.

Subaim 2.2.2: Assess interplay between the miR-17-92 cluster and NSs in RVFV infection

Expression of the miR-17-92 cluster is reportedly suppressed by p53, previously shown to be activated in RVFV infection in an NSs-dependent manner[5]. This interplay will be investigated first through infection with virus encoding or lacking NSs, with regulation of miR-17-92 cluster members and their gene targets assessed by qRT-PCR. Finally, the cluster will be overexpressed prior to infection. Regulation of cluster members and targets will be assessed by qRT-PCR, and effects on viral replication will be assessed through qRT-PCR and plaque assay.

2.3: Aim 3— Assess interactions of VEEV with cellular miRNA machinery

While differential expression of miRNA is reported in VEEV-infected mice, little is known about its interactions with cellular miRNA machinery. To assess viral effects on miRNA machinery, mock or VEEV-infected samples will be assessed by western blot for the expression levels of the miRNA machinery proteins. To assess viral dependence on miRNA machinery, siRNA will be used to induce targeted knockdown of machinery proteins prior to infection, and replication will be determined by plaque assay. Supporting studies will use null cell lines and chemical inhibitors to confirm viral dependence on the miRNA pathway. Finally, chemical inhibition will be performed in fully-virulent strains of VEEV and in related Alphaviruses to determine effects on replication, as measured by plaque assay.

CHAPTER 3: A BRIEF BACKGROUND OF RIFT VALLEY FEVER VIRUS

3.1 Etiology and epidemiology

RVFV was first described in the Rift Valley of Kenya in the early 1900s, but not isolated until 1930[6]. In 1931 it was first published as an "enzootic hepatitis" affecting both humans and livestock in regions of eastern Africa[7]. In humans, the disease course normally presents as a mild to moderate febrile illness, which may include significant weight loss at early onset of symptoms, and lasting several days to a week, with full recovery after two weeks[6, 8]. However, in a subset of cases, symptoms may progress to ocular damage, encephalitis, coma, and/or a hemorrhagic form, with the latter two symptoms being potentially fatal[8]. While the mortality rate of RVFV has traditionally been low, approximately 1% of those infected[8], more recent outbreaks have shown significantly higher mortality, as in the 2007 outbreak in Kenya which resulted in a mortality rate of approximately 29%[9]. This statistic is closely tied to the disease course in livestock, which classically presents with near-100% abortion rates in pregnant animals and significant mortality of neonates, thus presenting ample opportunity for herders and caretakers to come into contact with infectious fluids and tissues[6,8,9].

More typically, the virus is spread by mosquitoes, which remain infected for life following a tainted blood meal, and may spread the disease either horizontally while feeding from a naïve host, or vertically during production and laying of eggs. This latter

characteristic enables the mosquito larvae to act as a sort of reservoir for the virus, which causes cyclical outbreaks following seasonal rains in endemic regions[6]. The horizontal route is largely responsible for outbreaks in previously naïve regions, as viremic humans and animals traveling to these regions can introduce the disease into a new population of mosquitoes, which then become vectors for spreading the virus. It has been suggested that a single viremic animal entering a naïve region could trigger a major outbreak before health officials even knew the disease had been introduced[10]. The cycle of transmission from animals (or humans) to mosquitoes and back again has already been responsible for a significant spread of the disease beginning in the latter half of the 20th century, emerging as an epizootic in Egypt in 1977[11], and reaching the island of Madagascar in the early 1980s[12], Sudan in the 1990s[13], and the Arabian Peninsula in 2000[14], with periodic re-emergence described in the first three locales. European Union countries bordering the endemic regions have grown rightfully concerned about the possible incursion of the virus into areas with robust populations of potential hosts and vectors, with Spain being identified as a likely target and Spanish researchers using sophisticated computational methods to predict regions of possible emergence[15].

In addition to these naturally-occurring routes of infection, RVFV has also been demonstrated to spread through the aerosol route, either by accidental exposure in a laboratory setting[8] or deliberate attempts to weaponize the virus[16]. This potential, combined with the severe disease course in humans and livestock, as well as the lack of specific therapeutic treatment or approved vaccine, has led to the classification of RVFV in the United States as a Category B pathogen by the National Institutes of Health, and an

overlap select agent by the Centers for Disease Control and Prevention (CDC) and the United States Department of Agriculture (USDA)[17,18]. This cross-agency classification points to the "triple threat" potential of RVFV entering the United States: biodefense, for the significant level of concern and disruption associated with such an emergence; public health, for the severe disease course and the potential for establishment of a native reservoir leading to repeated outbreaks; and economy, for the devastating effect on the U.S. livestock industry. A recent article by Pendell *et al* supports these assertions and recommends a "one-health" approach to treating a U.S. outbreak of RVFV[19]; however, it is important to note that the current endemic regions include many poor and/or developing nations which lack the coherent infrastructure to mount a robust "one-health" response. Subsistence herders in these regions face the double jeopardy of losing their major food source even if they survive the virus. Therefore, the development of effective medical countermeasures is expected to remain a priority for some time.

3.2 Genome and structure of RVFV

RVFV is a member of the family *Bunyaviridae*, genus *Phlebovirus*. Like others in its family, it has a tripartite genome comprised of single-stranded RNA in the negative-sense or ambisense orientation, packaged into a capsid which is surrounded by a glycoprotein envelope[20]. The virions themselves are approximately 90-110 nm in size[21], with an outer structure of 122 capsomers arranged in T=12 icosahedral quasi-symmetry (Figure 1)[20, 22].

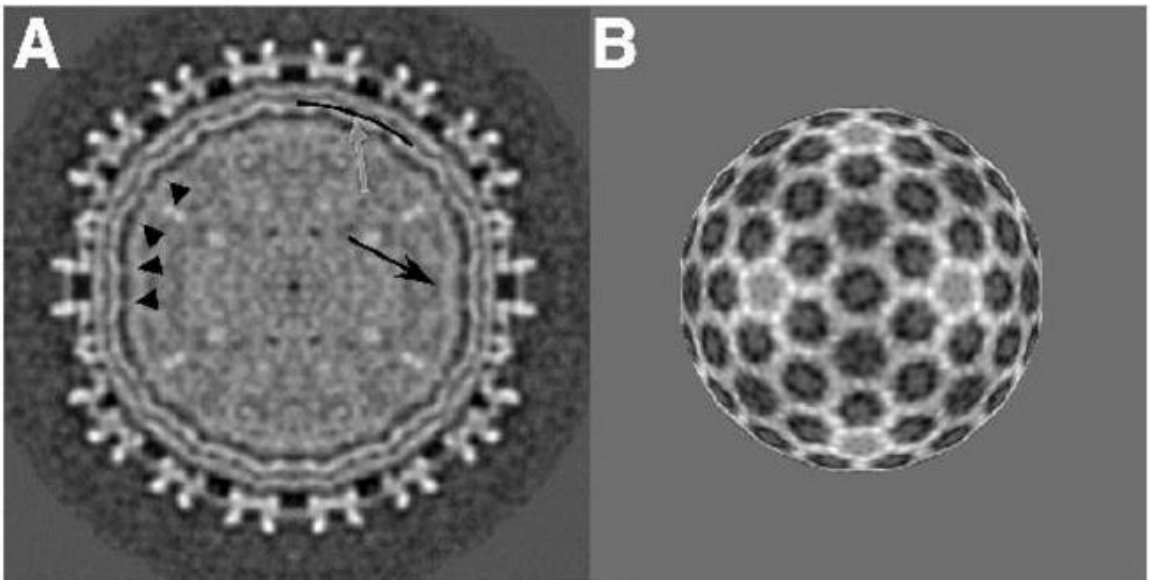

Figure 1: Cryo-electron micrograph of RVFV.
Panel A: Virion is contains a RNP core, surrounded by glycoprotein spikes and a double lipid envelope. The black arrow indicates a high density area thought to represent the outer portion of RNP core, while smaller arrowheads indicate areas corresponding to penetration of RNP by cytoplasmic tails of glycoproteins. Panel B: Outer surface of virion shows proteins crossing the lipid envelope; protein clusters demonstrate alternating fivefold and sixfold arrangements surrounding a central cluster, in a pattern resembling that of a soccer ball. Source: Sherman, *et al*. 2009[22].

Inside the virion are packaged the genome segments, termed by size as L, M, and S, for Large, Medium, and Small, respectively, and which collectively encode seven proteins (Figure 2). The viral L protein serves as the RNA-dependent RNA polymerase and is encoded in one open reading frame (ORF) on the L segment, in negative-sense orientation. The two envelope glycoproteins, Gn and Gc, a non-structural protein called NSm, and an additional 78-kDa protein, are encoded in a single ORF on the M segment, also in negative-sense orientation. Finally, the viral nucleoprotein is encoded on the S segment in negative-sense orientation, while the non-structural protein NSs is encoded in the opposite direction, making this segment ambisense[23].

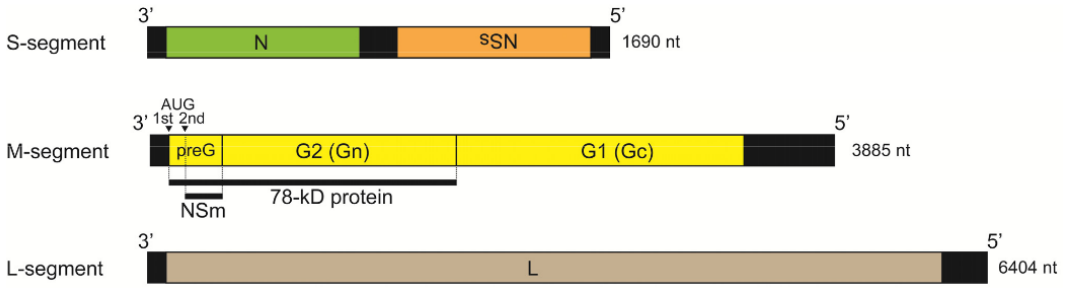

Figure 2: Genome of Rift Valley Fever Virus.
The three genomic segments are shown in order of decreasing size from top to bottom. The larger two segments are encoded in negative-sense orientation, while the smallest is ambisense. The L segment encodes the viral L protein and polymerase in one ORF. The M segment encodes non-structural protein NSm and the two envelope glycoproteins, Gn and Gc. The S segment encodes the viral nucleoprotein in negative-sense, and the non-structural NSs protein in opposite sense. Source: Ikegami, 2012[24] (adapted).

3.3 Viral proteins

3.3.1 L protein

The RVFV L protein, also called L-polymerase, is a 237.7 kDa protein comprised of 2092 amino acids[25]. It functions as the viral RNA-dependent RNA polymerase (RdRP), which allows RNA-to-RNA transcription and replication of the viral genome without the need for a DNA stage[20, 26]. The central C motif is responsible for nucleotide polymerization[25], while the N-terminal domain contains an exonuclease responsible for cap-snatching[27], the process by which the 5' cap essential for transcription is removed from host mRNA and used by the virus. This domain is conserved among Bunyaviruses and is similar in structure and function to the cap-snatching exonuclease of influenza[27]. It is a major component of the ribonucleoprotein complex in which the L and nucleoproteins associate with viral genomic RNA to form a replication competent structure[28].

3.3.2 Envelope glycoproteins

The M segment of the RVFV genome encodes a polyprotein which is cleaved in the endoplasmic reticulum (ER) during translation to produce non-structural proteins and the two envelope glycoproteins[29, 30], termed Gn and Gc for their positions near the amino and the carboxy terminus, respectively. The glycoproteins form heterodimers[31] which comprise spikes on the outside of the virion, and share similarity to the surface glycoproteins of other viruses.

The Gn and Gc proteins function largely in viral trafficking to and across membranes, including mediation of endocytosis[20], localization to the Golgi apparatus[20], and viral maturation and budding[29]. The Golgi localization signal has been experimentally determined to reside in Gn, but is not present in Gc, which localizes to the endoplasmic reticulum (ER) in the absence of Gn[32].

In addition to their role in viral trafficking, the glycoproteins have been proposed to mediate genome packaging through interactions with the RNP complex, as occurs with other Bunyaviruses such as Uukuniemi[33] and Bunyamwera[34]. Cryo-electron microscopy confirms that this interaction occurs in RVFV as well, with the cytosolic tail domains of the glycoproteins clearly crossing the lipid bilayer between the envelope and the core region[22]. Therefore, it is likely that this interaction serves a similar function in RVFV[28].

3.3.3 NSm proteins

The polyprotein translated from the M segment also produces two non-structural proteins, having molecular weights of 14 and 78 kDa and originally termed NSm1 and NSm2, respectively[35]. More recent nomenclature recognizes the smaller protein as NSm

and the larger by its mass or by its composition as NSm-Gn [36] or LGp for "large glycoprotein"[37]. The two proteins are non-essential for replication in mammalian cell culture[35, 38]. However, NSm in particular is considered a pathogenic factor due to its ability to suppress host apoptosis[39], which it does through a localization signal in the C-terminal region which targets the protein to the mitochondrial outer membrane[40]. Despite its anti-apoptotic function, NSm has also been shown to upregulate the p38/MAPK response in host cells, and to induce inhibition of superoxide dismutase 1 (SOD1), an antioxidant molecule normally expressed to reduce oxidative stress such as occurs during infection[41].

Contrary to their dispensability in mammalian infection, NSm proteins appear to be crucial for establishing and maintaining infection in mosquitoes. Recent studies show both that the 78-kDa protein is packaged into virions established in C6/36 mosquito cells, but not mammalian cells, in culture[37], and that the experimental deletion of the NSm gene reduces midgut replication and ease of transmission *in vivo* in a mosquito model[36, 42]. As mosquitoes can function both as primary vectors for horizontal transmission and *de facto* reservoirs for vertical transmission, the requirement for NSm in this model has a profound implication for controlling the spread of the virus.

3.3.4 Nucleoprotein

The RVFV nucleoprotein, or N protein, is encoded in negative-sense orientation on the smallest segment of the viral genome. It has a mass of approximately 27 kDa[43] and is the most abundant of the viral proteins[44]. The major functions reported for N protein include forming a protective coat around viral RNA and associating with the viral

RNA and L protein to form replication-competent RNP complexes[28]. It has also been suggested that an increase in cytoplasmic concentration of N protein triggers the change between primary transcription, which produces the replication complex, and secondary transcription, which produces the complementary strand of RNA used as a template for genomic replication[44]. Early studies demonstrated that N protein forms functional dimers through interactions between the N-terminal domains of the two monomers, and that this function seems to be conserved among Bunyaviruses[44]. A later study showed that N protein forms two types of functional hexameric rings, one comprised of α monomers, and the other comprised of dimers containing alternating β and γ monomers, with the two hexamers facing in opposite directions[28]. The outer surface of the hexamer contains a positively charged patch which has been confirmed as the RNA binding site[28]. This hexameric structure is in accordance with that produced by the N protein of Toscana virus, another Bunyavirus native to the Mediterranean regions of Europe, which forms the RNP complex by winding genomic RNA around a groove in the N protein hexamers, which rearrange upon the binding to form a helical structure[45]. Therefore, it is reasonable to suggest that a similar winding of the RNP might take place in RVFV as it does in Toscana virus.

3.3.5 NSs protein

NSs is a non-structural protein, approximately 38 kDa in mass, encoded on the S segment in positive-sense orientation. This orientation means that NSs, unlike the other viral proteins, can be translated promptly upon infection[46]. Although dispensable for

replication in a mammalian cell model[47, 48], it is perhaps the single greatest determinant of RVFV pathogenicity, and certainly the most well-studied of the Bunyavirus proteins. Curiously for a virus which replicates in the cytoplasm, one notable effect of RVFV NSs is the formation of large filaments in the nucleus[49, 50]. Many functions have been identified for NSs, beginning with its effect as a general inhibitor of host transcription, especially of interferon-β (IFN-β)[51] through degradation of the p62 subunit of host transcription factor TFIIH[52]. Additional studies have shown that NSs binds to many promoter regions on the host genome, many of which are predictably related to host transcription, but also including regions related to known factors of RVFV pathogenesis, such as Wnt, FOX, SOX, and HOX (embryonic development), semaphorins and plexins (neuronal guidance signaling), membrane-bound sulfotransferase (coagulation and inflammation), and a number of G protein coupled receptors, important for cell signaling[53].

NSs serves to control host translation as well as transcription, through the degradation of double-stranded-RNA dependent protein kinase (PKR)[51], which would otherwise phosphorylate the protein eIF2a and cause a shutdown of mRNA translation for both host and virus[54]. At the same time, NSs is reported to induce the localization of polyadenylate binding protein 1 (PABP1) to the nucleus, where it is less able to facilitate binding of mRNA to the ribosomes. This state favors translation of viral mRNAs, which are not polyadenylated and therefore do not require PABP1[55].

Although RVFV does not cause DNA damage, the expression of NSs in the nucleus causes chromosomes to stick together during replication, resulting in segregation

defects[49]. NSs has also been shown to activate the DNA damage response pathway[2], specifically in the activation of p53 to induce apoptosis[5]. This latter response represents an important point of host-pathogen interaction, as the induction of apoptosis is a classical antiviral response, yet the removal of p53 by mutation causes a decrease in both apoptosis and viral replication[5]. Because of its many antagonistic effects against host response, NSs is under frequent consideration as a potential drug target.

3.4 Viral replication cycle

Natural infection with RVFV commonly occurs through the skin, either from the bite of infected arthropods or through the handling of infectious materials. According to this model, viral entry is achieved by receptor-mediated endocytosis, in which the surface glycoproteins bind to the dermal-cell-specific receptor DC-SIGN[56] and are internalized along with the receptor through the action of caveolin[57]. Once in the endosome, the virus detaches from the receptor. The acidic environment of the endosome protonates a histidine residue on Gc, triggering a rearrangement which enables fusion of the viral envelope with the endosomal membrane[58]. Replication of the virus takes place in the cytoplasm. Because RVFV has a tripartite genome, each virion must contain one of each segment in order to be infectious. The signal which induces co-packaging of the three segments has not been fully characterized, but appears to require a sophisticated interaction between all three viral segments[59]. As previously discussed, the viral RNA is encapsidated by the N protein. Assembly of components and maturation of the virus takes place in the Golgi[60]. The mature virion buds from the Golgi and is released to the extracellular matrix either upon degradation of the cell[61], or by trafficking to the surface

membrane through the Golgi network. The replication cycle of RVFV in HSAECs is complete in approximately 8 hours[62], and in Vero cells, approximately 13 hours[61].

CHAPTER 4: A BRIEF BACKGROUND OF VENEZUELAN EQUINE ENCEPHALITIS VIRUS

4.1 Etiology and epidemiology

Venezuelan equine encephalitis virus (VEEV) was first isolated from horses in 1938 and from humans in 1943[63]. Interestingly, although natural infection of humans was suspected prior to 1943, the two confirmatory cases occurred as a result of laboratory exposure[63], thus underscoring the ease of transmission in an occupational or healthcare setting. More typically, the virus is spread by the bite of infected mosquitoes. As reviewed by Taylor and Paessler, natural transmission takes place in both enzootic cycles, between a rodent reservoir and a mosquito vector, and epizootic cycles, in which infection of horses, donkeys, or related equids, and sometimes humans[64], leads to viral amplification[65].

The enzootic and epizootic strains are associated with particular serotypes during infection: types IAB and IC are associated with epizootic outbreaks; and types ID, II, III, and IV, which do not amplify in equines, are therefore not associated with such outbreaks[66, 67]. The potential for amplification and epizootic transmission is also associated with two different species of vector, with *Culex* mosquitoes primarily carrying the enzootic strains, and *Aedes* mosquitoes carrying the epizootic strains[68]. Vertical transmission from mosquitoes to ova has not been reported for VEEV. However, a shift in vector can bring about a change in virulence, leading to epizootic outbreaks from a

formerly enzootic strain, as illustrated by a 1993 outbreak in Chiapas, Mexico. This was caused by infection with Type IE , previously thought to be non-epizootic, but transmitted by the *Aedes* vector rather than the more typical *Culex*[68, 69]. Regardless of their effects in equines, all strains are capable of causing disease in humans, and the equine-avirulent serotypes have been isolated from human hosts during outbreaks of these strains[67].

The disease course of VEEV in humans normally results in a non-specific, self-limiting, febrile illness which is often clinically indistinguishable from dengue[70]. Given the latter disease's nickname of "breakbone fever" for its severe joint and muscle pain, it is not surprising that infection with VEEV, while rarely fatal, can be quite debilitating. Symptoms of headache, fever, and malaise may be associated with vomiting and diarrhea, and involvement of kidney and liver. Once established, overt encephalitis may progress to neurological complications including seizure, and in rare cases, coma and death[71, 72]. Effects in equines are much more severe, as illustrated by the 1993 Chiapas outbreak which demonstrated approximately 50% mortality for infected horses[69]. As previously discussed for RVFV, direct transmission can occur between animals and humans through aerosol exposure or contact with infectious bodily fluids, thus posing a substantial risk to those involved in animal husbandry, particularly the veterinarians. Also as with RVFV, the ubiquitous presence of competent mosquitoes in the Americas illustrates the potential for emergence of VEEV into previously naïve regions, as occurred during a 1969 outbreak that began in Guatemala and reached Texas in 1971[73]. However, as demonstrated by the Chiapas outbreak, emergence of VEEV in a naïve

region also carries the added risk of a shift in vector causing added virulence and a more serious outbreak.

In addition to its natural means of transmission, VEEV infection can also occur through human intervention, either by accident or by design. Occasional laboratory-acquired infections have been reported[63, 74, 75], though the incidence in the United States has diminished since the end of the offensive biological weapons program in 1969[75]. During that era, VEEV was experimentally weaponized by both the U.S. and the former Soviet Union. It is still considered of high risk as a potential bioweapon, due to its ability to produce high viral titers, ease of lyophilization, and potential for aerosol transmission, with one source unfortunately describing it as "user friendly"[76].

There is currently no FDA-approved vaccine against VEEV. Although an attenuated strain called TC-83 is used to vaccinate high-risk workers, it is of limited protective capacity, associated with significant side effects, and both costly and potentially hazardous to produce[77, 78]. Similarly, there is no specific treatment for VEEV. This lack of specific preventatives and therapies, combined with the severe disease course in humans and equines, high likelihood of new emergence, and potential for aerosol transmission, has led to the classification of VEEV as Category B select agent by the NIH/NIAID[79] and an overlap select agent of concern by HHS (CDC) and USDA[18]. Development of novel vaccine and therapeutic candidates for VEEV is likely to remain a priority for the foreseeable future.

4.2 Genome and structure

VEEV belongs to the family *Togaviridae*, genus Alphavirus, which is further subdivided into Old-world and New-world Alphaviruses based on geographical distribution. The Old-world Alphaviruses include Sindbis virus (SINV), Semliki Forest virus (SFV), and Chikungunya virus (CHIKV)[80], the latter of which is of particular interest due both to a VEEV-like vector-associated shift in virulence[81, 82] and its recent emergence in the Americas[83]. The New-world Alphaviruses are categorically encephalitic and include Eastern and Western equine encephalitis viruses (EEEV and WEEV) in addition to VEEV[80]. While the molecular pathology of VEEV is less well characterized compared to the robust data available for the Old-world Alphaviruses, the major proteins and genetic components appear to be largely conserved across all Alphaviruses, thus suggesting similar roles for these components in VEEV.

Unlike Bunyaviruses, Alphaviruses have a non-segmented, positive sense, RNA genome which includes a 5' cap and a poly-A tail[84]. The genome is surrounded by two concentric shells, the inner comprised of nucleocapsid protein and the outer of glycoprotein, with a host-derived envelope between them. Both the nucleocapsid and the glycoprotein shells are composed of 80 subunits with T=4 arrangement of vertices[85, 86]. The size of the virion is approximately 65-70 nm in diameter[87].

The Alphavirus genome encodes a total of nine "standard" proteins (Figure 3). Four are non-structural and are labeled nsP1-nsP4 according to their position on the genome, while the other five are structural, including the capsid protein, the E1, E2, and E3 glycoproteins, and the 6K protein[78]. At the start of the 6K region is a so-called

slippery codon motif, which sometimes induces -1 ribosomal frameshifting to produce a tenth protein called the transframe protein (TF)[88]. The structural and non-structural proteins are encoded on two separate ORFs separated by a junction region containing a subgenomic promoter, allowing the non-structural proteins to be translated early in infection, and the structural proteins from the 26S RNA as shown below[78], which occurs following new positive-strand synthesis[89].

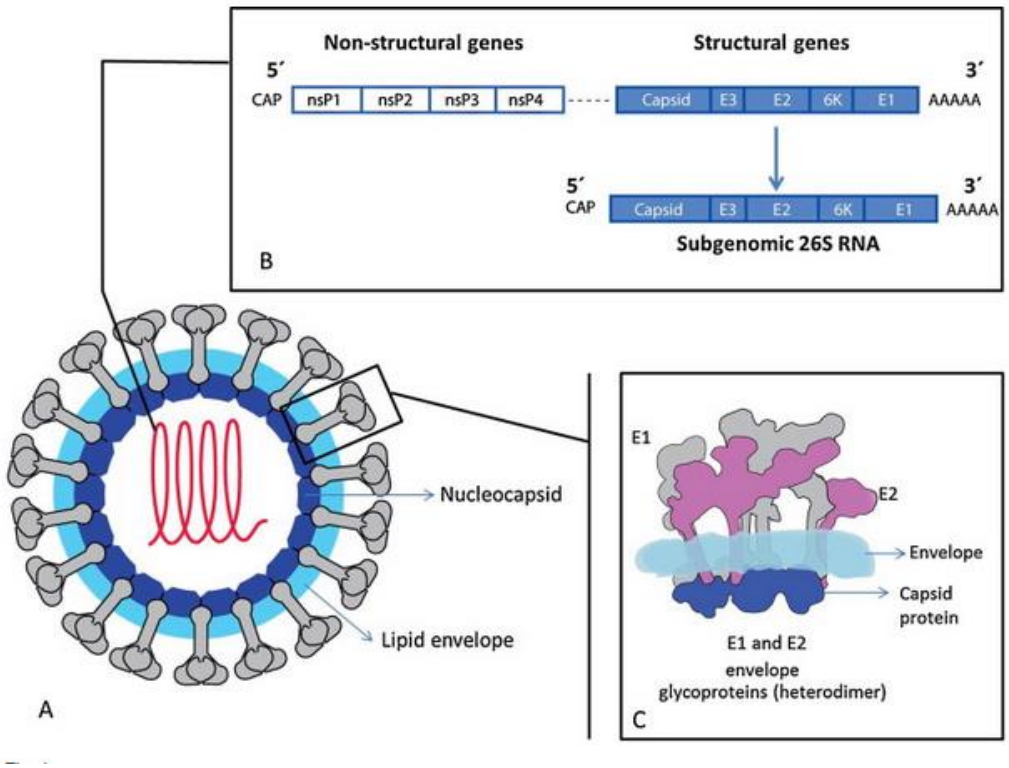

Figure 3: Alphavirus structure and genome.
Panel A: Schematic diagram of the virion structure, including genome at core, surrounded by glycoprotein spikes. The dark inner band represents the nucleocapsid while the lighter outer band indicates the envelope through which the glycoproteins protrude. Panel B: Schematic of genome, showing two ORFs which encode the non-structural and structural proteins. The two ORFs are separated by a junction region encoding the subgenomic promoter. Transframe protein is not shown. Panel C: Expanded view of viral shell capsomer,showing nucleocapsid at bottom, envelope at center, and glycoproteins at surface. Figure source: Carossino *et al*, 2014[78].

In addition to coding for the viral proteins, the Alphavirus genome contains four conserved sequence elements, or CSEs, which have specific functions in viral replication[87]. CSE1, located near the 5' end, is a stem-loop structure which acts as a promoter for synthesis of the positive strand, and is slightly upstream of CSE2, which acts as a promoter for the negative strand. CSE3 is the subgenomic promoter located between the two ORFs, and CSE4 is the co-promoter for negative strand synthesis, acting in concert with CSE2[87].

4.3 Non-structural viral proteins

The four non-structural proteins, nsP1-nsP4, comprise the viral replication complex[90], with nsP1 involved in RNA capping, nsP2 containing the helicase and protease domains, nsP3 controlling cell-specific replication[80] and acting in RNA synthesis, and nsP4 serving as the RdRp[87]. .The nsP1234 polyprotein is translated from a single open reading frame early in infection, as the individual proteins are needed for production of the negative-stranded replication intermediate[87], and are also necessary at later stages of infection for the efficient packaging of the viral genome into the virions[91]. In VEEV, as well as several other Alphaviruses including Ross River and O'nyong-nyong, this ORF contains a UGA or "opal" stop codon, which allows for the translation of either nsP123 or nsP1234 polyprotein[87, 92-94]. The individual proteins are cleaved through the protease action of nsP2, with nsP4 first being cleaved *in cis*, and the others *in trans* by another nsP123 complex[87]. Several models of Alphavirus infection have been used to investigate the individual proteins in depth, as discussed below.

Viral protein nsP1 targets the replication complex to the host membrane[95] by an uncharacterized mechanism, and is also critical for the capping of viral transcripts, allowing them to be processed by host machinery. Studies in Old-world Alphaviruses SINV and SFV have demonstrated that this capping occurs through the action of nsP1, which possesses both guanyltransferase and methyltransferase activity[87, 96, 97].

The role of nsP2 is not fully characterized in VEEV[89], although studies in other Alphaviruses illuminate a multifunctional role including helicase, replicase, and protease[87], end of minus strand synthesis[98], and in Old-world Alphaviruses, shutdown of host transcription[99] (fulfilled in New-world Alphaviruses by capsid protein)[100]. Specifically for VEEV, nsP2 is known to function in genome packaging, and has a complex interaction with the capsid protein, such that mutations in capsid generate compensatory mutations in nsP2[101, 102]. Because of its multifunctionality in both Old- and New-world Alphaviruses, nsP2 continues to be investigated as a novel target for vaccines and therapeutics[89, 103].

NsP3 is poorly characterized compared to other nonstructural proteins, though it has been linked to late-stage RNA synthesis and temperature-sensitive infectivity of SINV[104, 105]. The N terminal region contains a macro domain, or so-called “X domain”, comprising the first 160 amino acids of the protein, which is remarkably conserved across many forms of life and serves to bind adenosine[106, 107] . Phosphorylation of a hypervariable domain (HVD) in the C-terminal region is required for VEEV replication in cultured mosquito cells, but not in mammalian cells, suggesting that this domain may be involved in viral adaptation to new environments and different cell types[80]. NsP3 is

predicted to interact with IKKβ, an upstream component of the NF-κB pathway which is critical for VEEV infection of mammalian cells in culture[108].

NsP4 is the Alphavirus RdRp[87]. Studies in Old-world variants implicate nsP4 as a significant factor for viral infectivity and replication. In both SFV and SINV, it forms a complex with nsP1 to enable minus-strand synthesis[95, 109] , and has been shown in SINV to bind both the genomic and subgenomic promoters to enable transcription[110, 111]. Differences in nsP4 have been used to determine genetic and evolutionary links between enzootic strains of VEEV in Argentina[112], suggesting that a similar study in epizootic strains may illustrate important factors of pathogenicity differentially controlled by nsP4.

4.4 Structural viral proteins

The Alphavirus structural proteins are encoded within a single ORF near the 3' end of the genome, downstream of a subgenomic promoter which allows transcription of the protein-encoding region as a 26S RNA from the negative-stranded intermediate[87, 94]. These proteins include the capsid, which encloses the genomic material, acts as a protease[113] , and contributes to shutdown of host transcription[114, 115]; the three glycoproteins E3, E2, and E1, which comprise the surface spikes and mediate endocytosis; the 6k protein, which acts in glycoprotein processing and membrane trafficking[116, 117]; and a transframe protein, which has yet to be fully characterized but appears to have viroporin activity and to mediate trafficking functions in a manner similar to 6k[88]. The existence and function of TF protein have been experimentally verified in SINV and in CHIKV, but as of this writing, remain unverified in VEEV. As with the non-structural proteins, the structural proteins are initially expressed as a single

polyprotein and cleaved subsequently, and individual functions have been investigated through multiple models of infection. These are discussed in greater depth below.

4.4.1 Capsid

The VEEV capsid protein is reported by Watowich, *et al*. to be a trimer measuring 157 amino acids in length between its first two subunits, (PubMed Protein, unpublished data), and likely has a full length of approximately 270 amino acids as reported for SINV[118]. During replication, the individual capsid proteins assemble through interaction with genomic RNA to form the complete nucleocapsid, which is composed of 80 capsomers (240 individual proteins) arranged in T=4 symmetry, with an alternating pattern of pentons and hexons[119, 120]. As reviewed in Leung, *et al*, studies in SINV reveal that RNA binding takes place via arginine, lysine, and proline residues near the N-terminal end of the capsid protein[121]. However, assembly of VEEV capsid in particular appears to be a somewhat plastic process, as capsid intermediates isolated prior to budding show a range of sizes and inconsistent symmetry, suggesting that the final, mature form is influenced by interactions with the glycoproteins and lipid envelope[120]. These have yet to be fully characterized; however, earlier studies in SINV confirm interaction between the nucleocapsid and the cytoplasmic domain of the E2 envelope glycoprotein[122]. Although there are structural differences between the nucleocapsids of Old- world and New-world Alphaviruses[100], it is likely that a similar association links the two proteins in VEEV as well.

In addition to its main function of enclosing the viral genome, capsid protein is known to induce shutdown of host transcription and interfere with trans-nuclear

signaling. This is done through the formation of a tetrameric complex, comprised of capsid, nuclear export receptor CRM1, and nuclear import receptor importin α/β, which blocks the nuclear pore and prevents export of karyopherin signaling molecules[123]. The interaction of capsid with the nuclear pore is mediated by the short sequence C_{VEE}33-68, and mutations in this sequence are associated with differing levels of pathogenicity in the several VEEV strains[115].

VEEV capsid presents a potentially valuable therapeutic target. The cytopathic effect (CPE) associated with capsid expression points to its high level of immunogenicity, a valuable trait for the development of vaccines. A recent study has demonstrated the experimental effectiveness of VEEV capsid mutants, capable of replicating the genome but not incorporating it into the viral particles, in stimulating the innate immune response without the possibility of introducing infectious revertants into the transmission cycle[76]. Other studies have focused on disrupting the interaction between VEEV capsid and the host nuclear membrane. As capsid is indispensable for viral replication, highly immunogenic, and effectively targeted by existing drugs, it is likely to be the subject of continuing investigations in the prevention and treatment of VEEV.

4.4.2 Glycoproteins, 6k, and transframe protein

As described for SINV, the Alphavirus glycoproteins are assembled in the ER as heterodimers of E1 and pE2, the latter being the precursor of the E2 and E3 protein. From the ER, the heterodimers are transported to the Golgi, where pE2 is cleaved by furin into the mature E3 and E2[87, 124], and where the E2 and E1 proteins are glycosylated

before transport to the membrane surface[125]. On the surface of the virion, the glycoproteins form 80 spikes composed of heterodimers (or trimers, where E3 is present), mirroring the structure of the nucleocapsid beneath[125].

E1 and E2 are reported to have a similar leaf-like shape, with the blade of the "leaf" distal to the stalk which comprises the main body of the molecule[87, 124]. However, their placement at the viral surface illustrates their different functions: E2, which protrudes radially to form the tip of the spike, mediates attachment to the host cell membrane, while E1 lies tangentially to the viral surface and mediates membrane fusion[87, 125]. Specifically shown in VEEV, the E2 protein forms a loop structure which traverses the lipid bilayer, such that the "hanging" portion of the loop interacts with a hydrophobic pocket on the capsid protein, thus completing the linkage between viral RNA, capsid protein, and envelope[85]. Unlike the interaction reported in Bunyaviruses, the Alphavirus glycoproteins are not reported to act directly with the viral RNA.

The 6k protein, named for its molecular mass, has been identified as a viroporin, a type of molecule that interacts with host membranes to increase permeability to ions[126, 127]. This membrane interaction allows for the insertion of E1 and pE2 into the membrane of the ER[128] and has profound implications for the efficiency of viral budding[126, 129], virion assembly, and packaging of viral cores[130]. Studies in SFV have also shown 6k to be important in formation of glycoprotein spikes, as this process is mediated by the 6k/E1 interaction[129] . However, this has not been conclusively shown for VEEV.

The transframe protein (TF, Figure 4) was first conclusively identified in 2008 as the source of the doublet band seen when separating the 6K protein on electrophoresis

gels[131]. It is formed through a -1 ribosomal frameshift in the 6K region, which occurs at a conserved UUUUUUA site and is induced by a species-specific 3' stimulatory sequence which often forms a hairpin or pseudoknot structure[131, 132]. The stimulatory sequence in VEEV forms a hairpin structure considered "exceptionally stable", with a stem consisting of 9 G-C pairs[131, 133]. As described in SFV, the ribosomal frameshifting occurs with approximately 10-18% efficiency and produces a transframe protein approximately 8KDa in mass[131]. The specific functions of TF have not been fully characterized. However, studies in SINV show that TF exhibits ion channel activity similar to 6K, and that mutations in TF are associated with reduced particle release in cultured cells and reduced lethality in a mouse model[88].

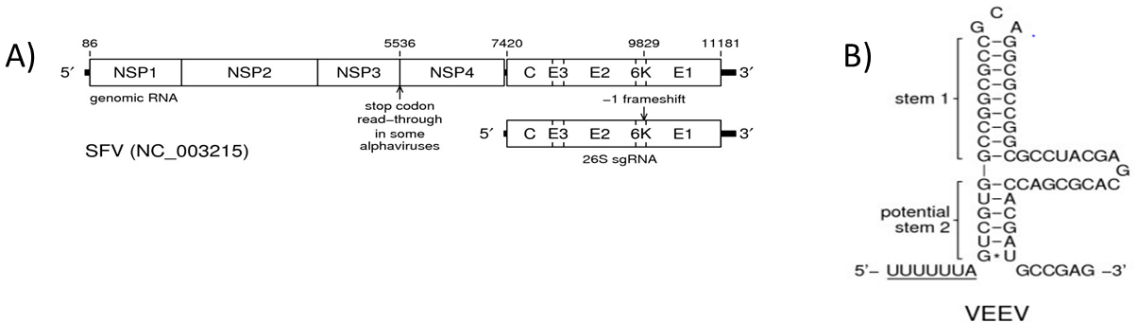

Figure 4: Genomic structure of transframe protein.
Panel A: Genome of SFV showing site of ribosomal frameshift which produces transframe protein. Panel B: 3' stimulatory structure of VEEV. Note Stem 1 site with stable arrangement of 9 GC pairs. Figure source: Firth, *et al*, 2008[131] (adapted).

4.5 Viral replication cycle

Alphaviruses were originally thought to enter host cells through the process of receptor-mediated, clathrin-dependent endocytosis[121, 134]. Under this model, the process begins with binding of the E2 viral protein[87, 121] to a host surface protein, triggering formation of the clathrin-coated pit. The virus is trafficked to an endosome, where low

pH induces a conformational change. As described for SFV, the E1-E2 dimer dissociates, allowing E1 to form homotrimers which act to form pores in the endosomal membranes[135-137], enabling release of the nucleocapsid (viral core) into the host cytoplasm for disassembly without the need for endosomal membrane fusion[138]. A 2013 study by Vancini, *et al*. confirmed the direct infection by SINV of host cells in cultures through pore formation at the cell membrane, in a time- and temperature-dependent process[139]. It is currently unknown whether the entry mechanisms are species-specific or whether a single species can switch between such mechanisms in response to outside factors, nor has either process been experimentally demonstrated as specific to VEEV.

The next step in the infection process is disassembly of the nucleocapsid core and release of the viral genome. According to the proposed model, this takes place in four stages: 1) priming of the core, through exposure of a proteolytic cleavage site in the linker region of the nucleocapsid protein; 2) exposure of the viral RNA to host transcriptional machinery; 3) binding of host 60S ribosomal subunit to capsid proteins and simultaneous transfer of those proteins or fragments thereof to the 28S rRNA; and 4) inactivation of steps 2 and 3 later in the viral replication cycle, possibly through binding of newly-synthesized capsid to the 28S rRNA[140].

Following disassembly of the capsid, the viral genome and proteins are synthesized by a multi-step, interconnected process. The non-structural proteins are translated first, as a polyprotein from a single ORF as previously described, and proteolytically cleaved through the action of nsP2. This first cleaves nsP4 from the polyprotein *in cis*, whereas subsequent cleavage is performed *in trans* by the nsP2 of a

second polyprotein[87]. NsP1 and nsP4 then interact with nsP2 and nsP3 to form the replication complex[95, 109-111], which interacts with host transcription machinery in turn to produce the negative stranded intermediate. This intermediate is used to transcribe both full-length RNA from the genomic promoter, and the 26S RNA from the subgenomic promoter. Finally, the 26S RNA is translated to produce the structural polyprotein, which is subsequently cleaved following translation to produce the individual proteins [87,121,141].

Assembly of the viral particles begins with the assembly of the E1-pE2 polyproteins in the ER. These are then trafficked to the Golgi, where furin cleaves the pE2 into E2 and E3 proteins, and where E1 and E2 are glycosylated before transport to the membrane surface[124, 125]. The genomic RNA is encapsidated through interaction with three subdomains at the amino-terminal domain of capsid protein[101], and is trafficked to the cell surface. Finally, the mature virus acquires its glycoprotein coat through interaction between E2 and a hydrophobic pocket on the capsid protein as the virion buds from the plasma membrane[142]. As reviewed by Martinez, et al, the budding process specifically excludes host proteins from the viral envelope[143], in contrast to viruses such as influenza, which incorporate them[144]. However, the host proteins may have a role in enabling viral transmission: a recent study in SINV has shown the production of long, filopodia-like extensions from the cell membrane in conjunction with budding, suggesting a means of infecting adjacent cells with minimal exposure to the extracellular anti-viral defenses[143]. It is possible that similar extensions form during budding of VEEV, although this has not been confirmed as of this writing.

CHAPTER 5: INTRODUCTION TO MICRORNA

5.1 Background

miRNA are small, non-coding RNA which act as master regulators of the cell, canonically downregulating endpoint proteins through targeting and degrading of messenger RNA (mRNA). First described in 2001 for their regulatory roles in development of the roundworm *C. elegans*[145, 146], they appear to be broadly conserved among eukaryotes, and serve a variety of functions in both normal and disease states. The miRNA are normally produced as primary transcripts in the cell nucleus and processed through a series of precisely regulated enzymatic steps to yield asymmetrical, ladder-like structures approximately 22 base pairs in length. These dissociate into separate strands, one of which associates with the RNA-induced silencing complex, or RISC, facilitating its binding to the target mRNA, while the other is normally degraded. The fate of the miRNA/mRNA complex is determined by complementarity; an imperfect match will lead to an inhibition of translation, while a perfect match will target the mRNA for degradation[147].

In mammalian cells, miRNA regulation has been linked to a variety of chronic disease states, including cancer[148-151], diabetes[152-154], heart disease[155-157], and neurological dysfunction[158-160], among many others. In plants and invertebrates, which lack the multi-tiered functionality of the mammalian immune response, miRNAs form an important part

of the host response against infection [161-164]; however, early investigations into the mammalian response focused largely on the role of miRNA in chronic infections, such as those occurring with HIV[165-168], and herpes virus [169-172]. Since that time, the picture has enlarged considerably to include such concepts as positive viral regulation through a host miRNA[173-175], virally-derived miRNA and similar small interfering RNA[176-178], and altered regulation in acute viral infections[3, 179, 180], along with a variety of non-canonical means of processing. Given the ubiquitous role of miRNA in regulating a variety of cellular processes across multiple states, it was hypothesized that such regulation would form an important point of host-pathogen interaction in RVFV and VEEV infection as well.

5.2 Biogenesis and function

Canonical miRNA function is a subset of a process known as RNA interference, or RNAi, which also includes the actions of many other types of small RNA, such as small interfering RNA (siRNA), piwi-interacting RNA (piRNA), and small hairpin RNA (shRNA). As described by Cullen[147], canonical miRNA processing begins in the nucleus, with the formation of a primary transcript containing a hairpin-shaped precursor known as pri-miRNA (Figure 5). The 11-base pair sequence of single-stranded RNA immediately flanking the hairpin is thought to serve as a signal for nuclear enzyme DGCR8[181], which forms a trimeric complex in order to recruit a second enzyme called Drosha[182]. Drosha cleaves the hairpin from the primary transcript, leaving a ladder-like structure with an asymmetric overhang of two base pairs at the free end. This structure, now called pre-miRNA, is exported from the nucleus by Exportin 5 (Exp-5 or XPO5)[147].

Once in the cytoplasm, the pre-miRNA binds with the enzyme Dicer, a molecule shaped roughly like a numeral 7, which uses a pair of magnesium ions as a molecular scissors to trim the loop from the hairpin[183]. A cofactor called TRBP recruits the Dicer-RNA complex to the next step in the process, which is binding to enzyme Argonaute-2 (Ago-2)[184]. Ago2 catalyzes the dissociation of the two strands of RNA into the guide strand, which remains attached to Ago2, and the passenger strand, which is degraded[185, 186]. As reviewed by Kawamata and Tomari, strand fate is determined by thermodynamic stability of the strands' 5' ends, with the less-stable strand becoming incorporated into the RNA-induced silencing complex, or RISC[187]. Depending on the need, either strand may fulfill this function. The complete structure of the mammalian RISC has yet to be fully characterized, but appears to require an association between the small RNA, Ago2, and cofactor TRBP[188, 189], along with chaperone proteins such as Hsp70 and Hsp90, and is ATP-dependent[190]. Both Dicer-dependent and Dicer-independent interactions have been proposed for assembly of the RISC[187].

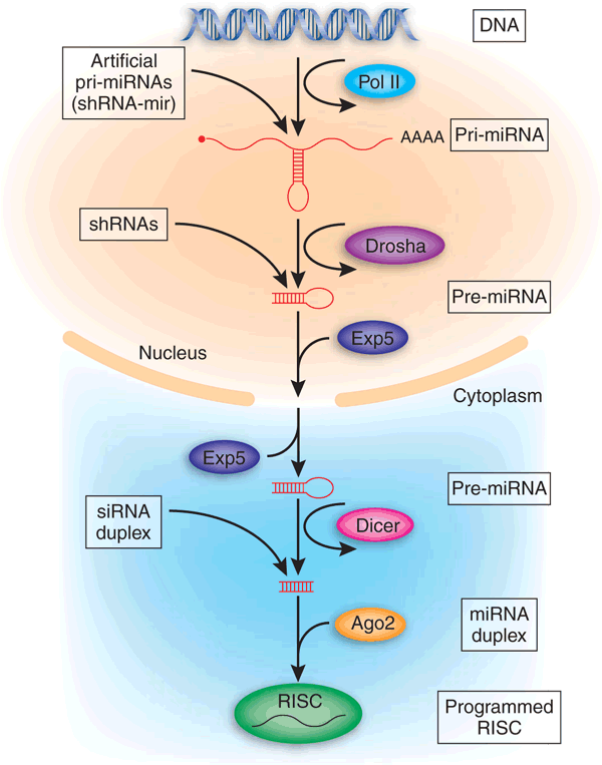

Figure 5: Biogenesis of miRNA.
MiRNA is processed from a primary transcript through a series of enzymatic steps which serially cleave the structure, ending in a ladderlike duplex. This binds to Ago2 and dissociates, with incorporation of the guide strand into the RISC and passenger strand degraded. . Figure source: Cullen, 2005[147]

Once attached, the guide strand of miRNA is used as a template to recognize target sites at the 3' UTR of complementary mRNA.[191, 192]. Recent research by Li *et al.* has demonstrated a mRNA recognition sequence within Ago2 itself which is thought to aid in miRNA recognition of target sequences with high specificity[193]. Classically, perfect complementarity enables so-called slicing activity by the RISC, cleaving the mRNA at the point where it is bound to residues 10-11 of the miRNA[192]; however, this exact pairing rarely occurs in animals[194]. Instead, a slight mismatch induces a bulge in the nucleotide 9-12 region, which acts either to inhibit transcription, or to enable

nucleolytic decay[194] through the deadenylation of the mRNA[195, 196], resulting in reduced production of the endpoint protein.

In addition to the canonical pathway described above, several non-canonical pathways have been described for the biogenesis of miRNA. One of these, called the mirtron pathway, makes use of the splicesome to process short intronic sequences into hairpin precursors, independently of Drosha, which are then exported from the nucleus and processed according to canonical methods[197]. First described in nematodes and flies, this pathway is now known to occur in mammals as well[197, 198]. As with canonical miRNA, either strand of the mirtron may be processed into mature miRNA for RISC association and mRNA regulation[199]. Another type of small RNA called a simtron can be processed by a specialized pathway requiring Drosha, but not requiring DGCR8, Exp-5, or Dicer. These simtrons readily associate with all four Ago proteins, are incorporated into the RISC, and participate in gene silencing in a similar manner to that of miRNA and mirtrons.

While miRNA is well-studied for its role in gene silencing as described above, several studies have demonstrated its alternative role in promoting translation[201]. This can obviously occur indirectly, either through downregulation of the miRNA which would otherwise target and degrade the mRNA[202], or through canonical repression of an inhibitor[203, 204]. However, miRNA can also serve directly in this role, as in a 2007 study demonstrating miRNA-induced recruitment of Ago2 and Fragile X mental retardation-related protein 1 (FRX1) to the 3' AU-rich element (ARE) of TNF-α, to increase its translation efficiency under serum-starvation conditions[205]. The same study

demonstrated that miRNA may switch roles according to the cell cycle, repressing translation during cell proliferation, and activating translation during the G_0/G_1 arrest phase which precedes differentiation, through recruitment of the necessary proteins[205].

A notable series of studies has focused on hepatitis C virus (HCV), a DNA virus which does maintain latency, but uses miRNA regulation in a novel way. In contrast to its canonical role in repressing translation, miRNA studies in HCV have described positive regulation through use of miR-122, which facilitates better binding of the ribosome to the viral IRES[174, 206-208]. This raises the question of similar positive regulation occurring in other viruses, such as RVFV or VEEV.

It is worth noting that canonical miRNA-associated regulation is highly redundant, according to several factors. First, the short target sequences and tolerance of central nucleotide mismatches allow for multiple potential binding sites within each target mRNA. This presents not only an increased chance of binding a given miRNA, but the potential to bind multiple different miRNA. As an example, the target prediction program TargetScan (www.targetscan.org) lists three potential binding sites within the 3' UTR of the insulin-like growth factor 1 receptor (IGF1R), with 11-13 different miRNA predicted to target each one[209-211]. Second, these target sequences are highly conserved[210], allowing one miRNA to bind and regulate many different genes. As an example, the human miRNA hsa-miR-99a has been experimentally validated to target five different mRNAs, with an additional 145 interactions described through *in silico* methods such as microarray and next-generation sequencing[212]. Third, the transcripts targeted by miRNA may themselves induce changes in abundance or transcription of

other miRNA, for instance, by targeting a processing molecule as in the targeting of Dicer by miR-103[213]. Therefore, the miRNA/mRNA interactions are characteristically "many to many" rather than "one to one," an arrangement that allows for subtle control of responses, but makes experimental characterization of such interactions exceedingly difficult.

5.3 Virally-encoded miRNA and vsRNA

The potential to generate miRNA and other small, regulatory, non-coding RNA is not restricted to the cellular model. Several viruses are known to encode miRNA and miRNA-like elements, though the specific term "miRNA" is restricted by convention to those transcripts which are produced in the nucleus and processed according to the canonical pathway. Therefore, it is most commonly used in conjunction with those viruses which replicate in the nucleus, such as the DNA-based herpes viruses [e.g. Herpes Simplex-1 (HSV-1)[214], Epstein-Barr Virus (EBV)[215], and Kapsosi's Sarcoma Associated Herpesvirus (KSHV)[216]], and the RNA-based retroviruses (e.g. HIV)[176]. Several distinct roles of viral miRNA have now been established, such as control of latency in herpes infections[215, 217, 218], activation of cellular proliferation and/or apoptosis pathways, control of angiogenesis, and immune invasion in KSHV infections [216, 219], and chromatin remodeling and enhancement of viral replication in HIV infection[220, 221].

Viruses which do not replicate in the nucleus may also encode similar small regulatory RNA; however, these transcripts are considered non-canonical by virtue of their cytoplasmic processing, and therefore are normally described as vsRNA or virally-induced siRNA rather than miRNA. A 2010 paper describes the experimental production

of vsRNA from six viruses and 41 host systems, and lists several characteristic differences from canonical miRNA, including their relative abundance and amount of asymmetrical overhang, but does not investigate potential roles for these vsRNA[178]. Later studies confirming the presence of vsRNA in various plant and arthropod systems have illustrated several potential roles. For instance, Cauliflower mosaic virus infection of *Arabidopsis* produces great quantities of vsRNA which are thought to serve as molecular decoys against the plant's natural antiviral response [222]. In contrast, Dengue virus infection and RVFV infection of mosquito cells each produce vsRNA which appear to serve an autoregulatory function for the virus[223, 224]. While Dengue and RVFV are both transmissible to mammalian hosts, there is currently no published confirmation of vsRNA expression by these viruses during *in vivo* mammalian infection.

5.4 Nomenclature

The first two types of miRNA to be characterized were found in the roundworm *C. elegans*: lin-4 in 1993[225] and let-7 (a contraction of "lethal") in 2000[226]. Since that time, several hundred miRNAs have been identified across multiple organisms, each miRNA differing in sequence, origin, abundance, and degree of RISC incorporation within each organism. Therefore, the names of each miRNA must convey this information in a clear and concise manner. The naming convention outlined below is taken from miRBase (www.mirbase.org) in accordance with the guidelines suggested by Ambros, *et al*. in 2003[227].

The number of a miRNA denotes the order in which it was published; for instance, the next miRNA to be described after miR-350 would be called miR-351. Two

major exceptions are the members of Let-7 and Lin-4 families of miRNA, which retain these designations out of tradition.

The species in which the miRNA occurs is denoted by a three letter prefix referring to its taxonomical name. For instance, human miRNAs are denoted with hsa- for *Homo sapiens*, while mouse miRNAs are denoted with mmu- for *Mus musculus*. Identical numbers denote identical sequences in the two different species (e.g. hsa-miR-17 and mmu-miR-17).

Identical miRNA sequences processed from two distinct precursors are denoted with the suffixes -1 and -2. For instance, miR-92a-1 and mir-92a-2 have identical sequences but are processed from separate chromosomes (13 and X, respectively)[228]. Closely related sequences which are not identical are denoted with lettered suffixes, such as –a and –b. For instance, miR-20a and miR-20b have identical seed sequences but differ in the non-seed regions[228].

miRNA which derive from opposite arms of the precursor are named according to relative abundance, with the less abundant partner denoted by an asterisk (*), such as miR-56 and miR-56*. These latter are sometimes called star strands. When the relative abundance is not clear, the two miRNA are differentiated according to which end of the sequence produced them, for instance -3p or -5p. Designations may change from star format to “p” format as additional miRNA are described and characterized.

Capitalization is sometimes used to differentiate miRNA, such as miR for a mature RNA and mir for a precursor, or MIR for a plant miRNA; however, this is not a universal practice.

Virally-encoded miRNAs are typically denoted by a three-letter or four-letter prefix indicating the virus of origin, but are named according to the portion of the genome from which they derive, rather than the order in which they were discovered. For instance, the miRNAs described for Herpes simplex 1 virus are denoted as HSV-1-miR-H1 through –H4[229], while miRNAs described for Epstein-Barr virus have the form EBV-miR-BART (from BamHI-A region rightward transcript) or EBV-miR-BHRF1 (from BamHI Fragment H rightward open reading frame 1)[230]. Where sequence homology occurs between a viral and a cellular miRNA, the original names are retained for each, to aid in differentiation.

5.5 The miR-17-92 cluster

The miR-17-92 cluster represents some of the most widely-studied miRNAs, with over 300 entries listed in PubMed at the time of this writing. The cluster is considered an oncomir [231] for its association with cancer, specifically for its ability to promote proliferation and angiogenesis while reducing apoptosis[232]. It is also associated with a variety of normal cellular processes including development and differentiation[231]. The cluster is transcribed from a common promoter, located on Chromosome 13[231]. There are six recognized members of the cluster: the predominant strands miR-17-5p, miR-18a-5p, miR-19a-3p, miR-19b-1-3p, miR-20a-5p, and miR-92-a1-3p; and their opposite-arm strands miR-17-3p, miR-18a-3p, miR-19a-5p, miR-19b-1-5p, miR-20a-3p, and miR-92a-1-5p, respectively. A paralog known as the miR-106a/363 cluster is located on the X chromosome and encodes miR-106a, miR-18b, miR-20b, miR-19b-2, miR-92a-2, and miR-363. A second paralog encodes three additional members, miR-106b, miR-

93, and miR-25 on Chromosome 7[228]. These miRNAs share sequence homology of their seed regions. Based on that characteristic, the predominant strands can be sorted into the families of miR-17, miR-18, miR-19, and miR-92 as shown below (Figure 6)[228].

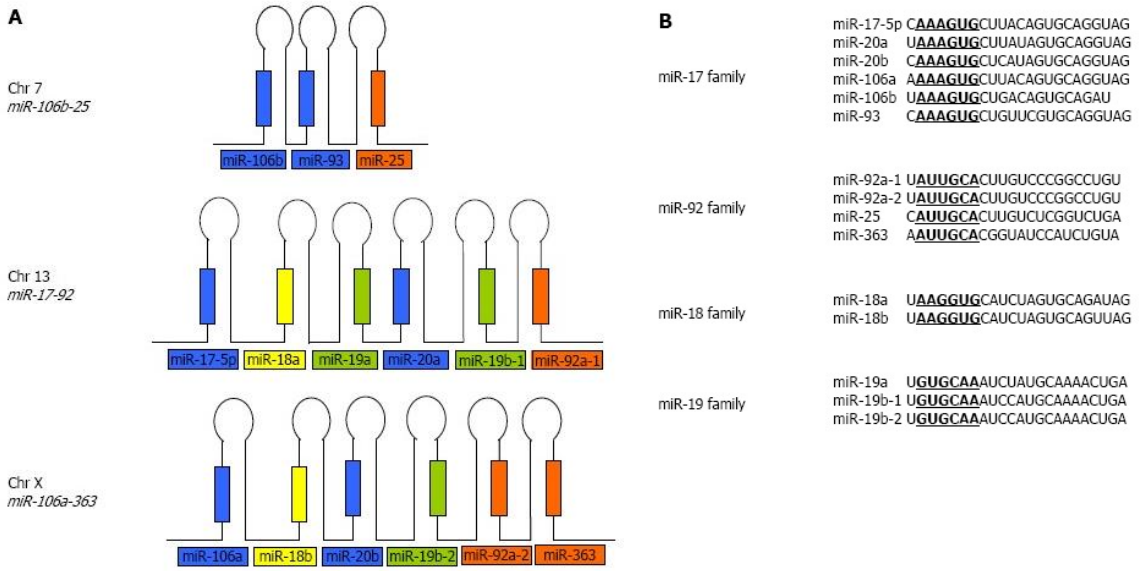

Figure 6: miR-17-92 cluster and paralogs.
Panel A: The miR-17-92 cluster is transcribed from a common promoter on Chromosome 13, with paralogs located on Chromosomes 7 and X. Panel B: Members of the cluster and its paralogs share homology in the seed region, allowing for sorting into four distinct families. Adapted from Tan *et al*, 2014[228]

As an oncomir, the miR-17-92 cluster is reported to act through a variety of mechanisms, including regulation of multiple genes, associated with DNA replication, cell cycle regulation, and chromosome organization, in response to Myc activation[233]. In normal cellular processes, the cluster is known to regulate T-cell activation[234], monocyte-to-macrophage differentiation[235], branching of embryonic lung[236], signaling of bone morphogenic protein in neurons[237], and regulation of neuronal stem cells[238], among other processes. Deletion of the cluster results in embryonic lethality in a mouse model[239] and

is associated with skeletal abnormalities in humans[240], underlining its fundamental role in developmental regulation.

Compared to the studies in cancer and development, there are relatively few studies relating miR-17-92 regulation to viral infection, and most of those have been in viruses which promote transformation and/or associate with host DNA, such as EBV[241], HCV[242], KSHV[243], and HIV[166, 244, 245]. However, one recent study associated upregulation of miR-17 with H7N9 avian influenza in humans[246], supporting the idea that changes in miR-17-92 cluster could occur in acute infection as well. Specifically for this study, the embryonic lethality and developmental defects associated with cluster deletion seem highly significant in light of the deleterious reproductive effects known to occur with RVFV. Combined with the cluster's role in mediating apoptosis and neuronal effects, this suggests the possibility of miR-17-92 cluster involvement in RVFV pathogenesis as well.

CHAPTER 6: CHARACTERIZATION OF MIRNA PROFILE DURING RVFV INFECTION (AIM #1)

6.1 Introduction

Changes in the host miRNA profile have been reported for a number of disease states, most notably those already known to produce transcriptional changes, such as cancer and chronic viral infections (e.g. HIV and herpes). Recent studies have expanded the picture to include miRNA involvement in acute viral infections, such as VEEV[3], rabies[179], and influenza[246]. However, such studies are comparatively few, and the association of changes in miRNA regulation with changes in gene and protein expression or other relevant endpoints remains poorly characterized in acute viral infections.

RVFV infection produces characteristic changes which are highly suggestive of miRNA regulation, including reproductive and neuronal anomalies *in vivo*[247], and activation of apoptotic and DNA-damage response pathways *in vitro*[2, 5]. To investigate these, we performed microarray analysis of miRNAs extracted from mock-infected or RVFV-infected HSAECs at 6, 24, and 48 hours post infection. Microarray analysis is widely regarded as a "hypothesis generator"[248], as it provides the means to determine regulation of hundreds of miRNAs (or genes or proteins) at once, though further analysis is often needed to determine patterns and confirm regulation. Therefore, the resulting data were analyzed bioinformatically to identify significantly regulated pathways warranting further investigation. Our study identified over 170 differentially-regulated

miRNAs, including a significant subset up- or down-regulated by 2-fold or greater, which mapped to pathways associated with known features of RVFV pathogenesis, including development, apoptosis, and regulation of cytokines. To our knowledge, this represents the first investigation of miRNA profile in a mammalian model of RVFV infection.

6.2 Materials and methods

6.2.1 Cells and virus

Human Small Airway Epithelial Cells (HSAECs) were obtained from Cambrex, Inc. in Walkersville, MD. Cells were cultured in Ham's F-12 media supplemented with 10% fetal bovine serum, 1% L-glutamine, 1% penicillin-streptomycin (pen-strep), 1% sodium pyruvate, 1% non-essential amino acids, and 0.1% 1000X 2-mercaptoethanol (HSAEC media), and were maintained in a humidified atmosphere at 37°C and 5% CO_2. Rift Valley fever virus strain MP12 is a well-characterized model for the fully-virulent strains and was generated by serial passage of the ZH-548 strain in the presence of the mutagen 5-fluorouracil[249]. This strain differs from the parent strain by 12 nucleotides and 7 amino acids, including mutations of all three segments[250] and the presence of a novel AUG stop codon upstream of the ORF encoding the glycoproteins[251]. The MP12 strain was obtained from Dr. Sina Bavari, USAMRIID. An additional strain, called arMP12, was obtained from Dr. Shinji Makino, at University of Texas Medical Branch. This strain is reported to have the same sequence as MP12[35], and was used to replace older MP12 stocks. Laboratory stocks of MP12 and arMP12 were generated by passage in Vero cells.

6.2.2 Plaque assay

Confluent cultures of HSAECs in 6-well plates were treated in triplicate by mock infection (media only) or infection with RVFV MP12 at MOI=3, for one hour. Following infection, the cells were washed with PBS and re-fed with fresh media. Supernatants were collected at 6, 16, 24, and 48 hours post infection (hpi). Viral supernatants were serially diluted, and applied at 200 µl to confluent cultures of Vero cells in 12-well plates, for one hour prior to immobilization in agarose. Immobilization and staining were performed as described in Kehn-Hall, *et al*[252]. Plaque assays were assessed at three days post infection.

6.2.3 Cell viability

HSAECs were seeded in a 96-well, white-walled plate, and mock-infected or infected as described above, at MOI=3 for one hour. Cell viability was assessed at 6, 16, 24, and 48 hpi using the CellTiter-Glo reagent (Promega, catalog #7571) according to the manufacturer's instructions. Viability was determined via fluorescence as compared to the control sample, using a Beckman-Coulter DTX-800 Multimode Detector with Multimode Analysis Software platform.

6.2.4 Western blot

Triplicate cultures of HSAECs were mock-infected or infected as described above, and collected in lysis buffer at 8, 16, 24, and 48 hpi. Protein samples of 50 µg (clear lysis buffer) or 20 µl (blue lysis buffer) were separated, transferred, and subsequently processed as described in Austin, *et al*[5]. Membranes were blocked and

primary antibody to cleaved caspase-3 (Cell Signaling Technologies, catalog #9661) was prepared in 3% bovine serum albumin (BSA) in PBS with 0.5% Tween-20 (PBST). β-actin conjugated with horseradish peroxidase was used as a loading control.

6.2.5 Infection and miRNA extraction

Confluent cultures of HSAECs in 6-well plates were treated in triplicate by mock infection (media only) or infection with RVFV MP12 at MOI=3, for one hour. Following infection, the cells were washed with PBS and re-fed with fresh media. Samples were collected at 6, 24, and 48 hours post infection (hpi) and miRNA extracted using Ambion's *mir*Vana^{tm} kit (Life Technologies, catalog #AM1560), following the manufacturer's protocol. Briefly, collected cells were lysed and lysates phase-separated using acid phenol-chloroform. The aqueous phase was removed and RNA was immobilized on a glass-fiber filter. The filter was washed several times with the supplied wash buffers. miRNA was eluted from the filter using ultra-pure RNAse-free water or the supplied elution buffer, at 95°C. Extracted miRNA was stored at -80°C until use, and was shipped on dry ice for microarray analysis.

6.2.6 Microarray hybridization and analysis

Hybridization and analysis were performed by the laboratory group of Dr. Norman Lee, The George Washington University. To determine presence of miRNA, samples of 250 ng were hybridized onto the chip for 20 hours at 55°C. Hybridization signal was assessed using the Agilent Feature Extraction software package and values uploaded into Gene Spring GX 10.0 for statistical and genomic analysis. Poor

hybridization values were marked as "A" for "absent" and were eliminated from further analysis. Signal values were $\log_2$ transformed and subjected to two-way ANOVA comparing across timepoints and infection status. Finally, samples were normalized to 75th percentile values. The change vs. mock was assessed for each miRNA per timepoint using the equation: $2^{(\text{average mock value-individual RVFV value})}$, and standard deviations were assessed for each triplicate. Statistical outliers, as determined by Grubb's test, were removed from fold changes prior to calculation of averages and standard deviations.

6.2.7 qRT-PCR confirmation of miRNA

Triplicate cultures of HSAECs in 12-well plates were mock infected or infected at MOI=3 for one hour, then washed and refed. Samples were collected at 8, 16, 24, and 48 hpi, and the miRNA extracted using the *mir*Vana^{tm} kit as previously described. miRNA was quantified using the NanoDrop 2000 system. Volumes of miRNA were normalized to the lowest concentration to give equivalent final concentrations of cDNA. cDNA was prepared using the miScript II RT kit (Qiagen, catalog # 218160 and #218161) with the included HiSpec buffer and cycled on the LabNet MultiGene thermocycler, model TC9600G, according to the miScript protocol . qRT-PCR was performed using the miScript SYBR Green qRT-PCR kit (Qiagen, catalog #218073) and individual primer assays for each miRNA of interest. miRNA values were normalized to the endogenous control RNU6B and quantitated using the ΔΔCt method developed by Livak and Schmittgen[253]. Fold changes were considered statistically significant if the difference between infected and mock values had a P value of 0.05 or less, as measured by Student's unpaired t-test.

6.2.7 Significant pathways and bioinformatic analysis

Lists of genes targeted by miRNA for each timepoint were generated by Gene Spring software versions GX 10.0 and GX 12.5 and the programs' associated TargetScan analysis platform, using parameters of 2-fold or greater regulation of miRNA, up- or down-regulated, and 90% conservation. These lists were re-imported into Gene Spring to generate the tables of significant pathways targeted by up- or down-regulated miRNAs for each timepoint.

6.3 Results

6.3.1 RVFV infection induces significant changes in host miRNA profile

To establish replication kinetics of RVFV in HSAECs, cells were infected at MOI=3 for one hour and collected at the timepoints shown (Figure 7). Replication was determined by plaque assay (Figure 7A) and showed a time-dependent increase, from approximately 10^4 pfu/ml at 8 hpi to a maximum of 10^7 at 24 hpi and a plateau thereafter. This correlated with a time-dependent decrease in cell viability as compared to mock-infected controls at the same timepoints, decreasing by approximately 20% at 24 hpi, and approximately 40% at 48 hpi (Figure 7B). This correlated in turn with cleavage of caspase-3 (casp-3), a classical marker of apoptosis, as assessed by western blot (Figure 7C). Image analysis shows an increase in cleaved casp-3 beginning at 8 hpi with a level 31-fold greater than mock values, rising to approximately 600-fold over mock values by 48 hpi. Taken together, this demonstrates that RVFV replicates robustly in HSAECs, and that replication is correlated with a substantial decrease in cell viability and increase in apoptosis.

To determine miRNA expression, miRNAs were extracted from HSAECs which had been mock-infected or infected with RVFV MP12 strain at an MOI of 3, at 6, 24, or 48 hours post infection. The miRNAs were analyzed vs. 961 possible matches, resulting in 95 successful hybridizations. Two-way ANOVA was performed using the parameters of time point and infection status, to produce a set of data normalized to the 75th percentile. Fold changes were assessed for the 75th percentile data using the formula:

Fold Change= 2^(individual Infected value-average Mock value)

Among the 6 hour samples, 30/174 miRNAs demonstrated regulation of twofold or greater in infected vs. mock samples. Of that group, 1 miRNA was down-regulated and the remainder up-regulated. Among the 24 hour samples, 48/174 miRNAs demonstrated regulation of twofold or greater, with 22 miRNAs up-regulated and 26 down-regulated. Among the 48 hour samples, 52/174 miRNAs demonstrated regulation of twofold or greater, with 37 miRNA up-regulated and 15 down-regulated (Figure 8, Table 1 and Table 2). miR-630 showed the greatest up-regulation at 24 hpi and was still significantly up-regulated at 48 hpi, with infected sample values of 6.27 and 5.18-fold, respectively, above the mock values. Significantly, the five miRNAs with greatest down-regulation in MP12-infected samples at 24 hours included two members of the miR-17-92 cluster (miR-19b-1-5p and -92a-1-5p), which were also the two most down-regulated miRNAs at 48 hpi

The overall pattern of regulation in microarray was illustrative as well, with early upregulation of miRNAs seen at 6 hpi, followed by apparent suppression at 24 hpi, and recovery at 48 hpi. This is suggestive of early response being carried out under host

control, but suppressed by NSs at 24 hpi. Curiously, despite the significant cell death reported at 48 hpi, there was a substantial increase in both the numbers of up-regulated miRNAs, and the degree of upregulation for several miRNAs such as miR-1224-5p and miR-188-5p (both over 11-fold at 48 hpi). Additionally, results for individual miRNAs show several examples which are up- or down-regulated across several timepoints, for instance the consistent increase in miR-630 over time, or the continued low expression of several members of the miR-17-92 cluster from 24-48 hpi (Table 1).

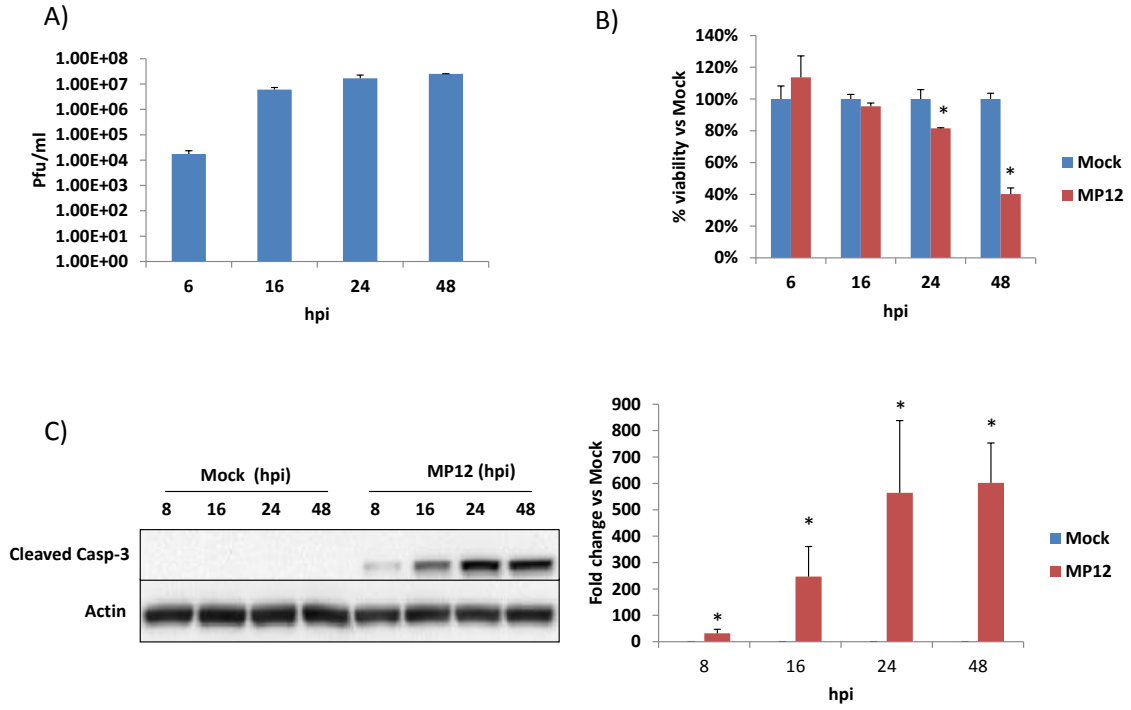

Figure 7: RVFV replication in HSAECs.
HSAECs were infected at MOI=3 and analyzed as follows. Panel A: Time course of replication as measured by plaque assay. Panel B: Time course of cell viability as measured by CellTiter Glo assay. Panel C: Time course of cleaved Casp-3 expression, a classical marker of apoptosis. Left panel shows a representative blot. Actin was used as a loading control Right panel shows quantitation of triplicate samples. All infections performed at MOI=3.

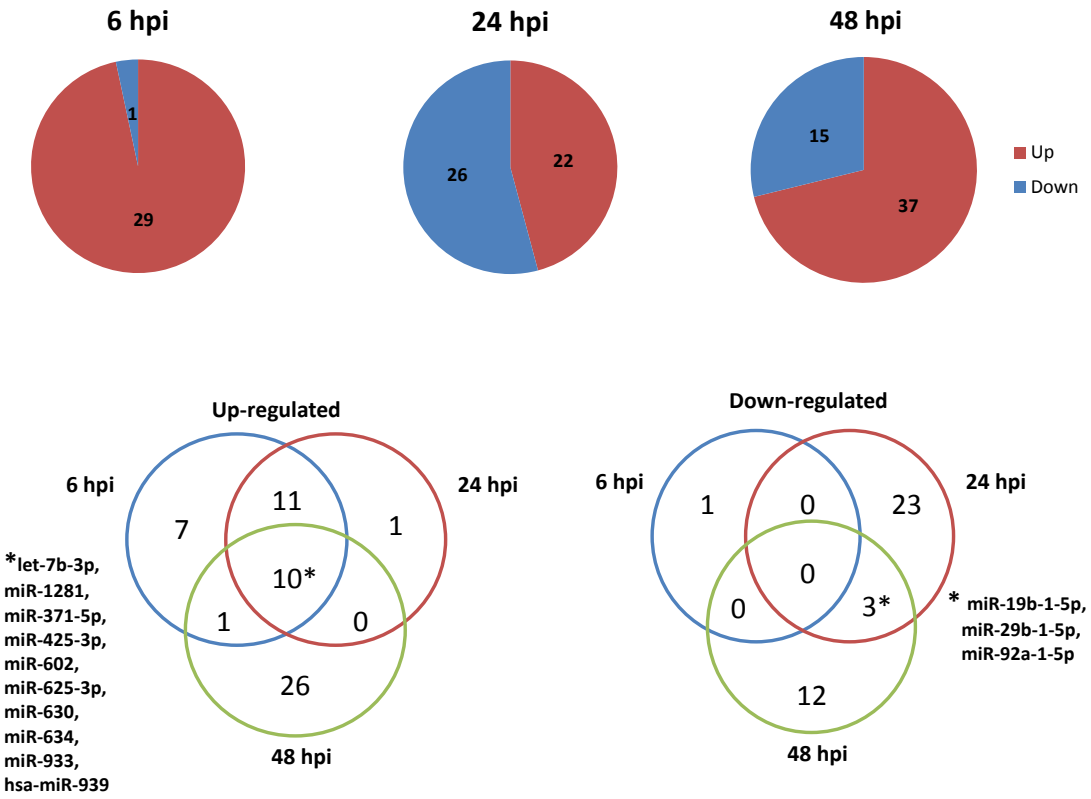

Figure 8: miRNA regulation changes significantly following RVFV infection.
miRNA was collected at 6, 24, and 48 hpi from HSAECs infected with RVFV at MOI=3, and was assessed by microarray for differential regulation. Top panel: number of miRNA which were up- or down-regulated by twofold or greater in infected vs. mock samples. Bottom panel: Venn diagrams showing distribution of regulation across the three timepoints.

Table 1: Up-regulated miRNA at each timepoint.
Table shows those miRNA which are up-regulated by 2-fold or greater compared to Mock values. Continued on following page.

6 hr up		24 hr up		48 hr up	
miRNA	**Change vs. Mock**	**miRNA**	**Change vs. Mock**	**miRNA**	**Change vs. Mock**
hsa-let-7b-3p	4.61	hsa-let-7b-3p	2.26	hsa-let-7a	2.98
hsa-let-7f-1-3p	4.22	hsa-let-7f-1-3p	2.30	hsa-let-7b-3p	3.00
hsa-miR-1224-5p	3.14	hsa-miR-1225-3p	2.53	hsa-let-7c	2.11
hsa-miR-1225-3p	3.64	hsa-miR-1237	2.28	hsa-let-7f	3.25
hsa-miR-1228	3.45	hsa-miR-1238	2.43	hsa-let-7g	2.43
hsa-miR-1234	3.40	hsa-miR-1281	2.23	hsa-miR-10a	2.27
hsa-miR-1237	4.57	hsa-miR-129-1-3p	2.22	hsa-miR-1224-5p	11.04
hsa-miR-1238	4.32	hsa-miR-129-2-3p	2.53	hsa-miR-127-3p	2.13
hsa-miR-1281	4.39	hsa-miR-1539	2.27	hsa-miR-1281	3.01
hsa-miR-129-1-3p	4.12	hsa-miR-1825	2.21	hsa-miR-1308	5.18
hsa-miR-129-2-3p	4.40	hsa-miR-191-3p	2.44	hsa-miR-134	8.94
hsa-miR-1539	4.85	hsa-miR-223	2.03	hsa-miR-141	2.01
hsa-miR-1825	5.48	hsa-miR-371-5p	2.27	hsa-miR-150-3p	5.37
hsa-miR-191-3p	3.34	hsa-miR-425-3p	2.29	hsa-miR-16	2.20
hsa-miR-223	4.81	hsa-miR-602	2.25	hsa-miR-181b	3.21
hsa-miR-296-5p	3.24	hsa-miR-625-3p	2.14	hsa-miR-181d	2.07
hsa-miR-328	3.55	hsa-miR-630	6.27	hsa-miR-188-5p	11.60
hsa-miR-33b-3p	4.61	hsa-miR-634	2.05	hsa-miR-192	2.33
hsa-miR-371-5p	3.84	hsa-miR-92b	2.03	hsa-miR-194	2.37
hsa-miR-425-3p	4.63	hsa-miR-933	2.03	hsa-miR-29c	2.10
hsa-miR-550	4.35	hsa-miR-939	2.24	hsa-miR-31	2.69
hsa-miR-563	4.45	hsa-miR-99a	3.50	hsa-miR-371-5p	4.94

6 hr up		24 hr up		48 hr up	
miRNA	**Change vs. Mock**	**miRNA**	**Change vs. Mock**	**miRNA**	**Change vs. Mock**
hsa-miR-602	4.13			hsa-miR-409-3p	2.10
hsa-miR-625-3p	4.03			hsa-miR-425-3p	2.83
hsa-miR-630	2.30			hsa-miR-494	3.49
hsa-miR-634	4.41			hsa-miR-574-5p	2.80
hsa-miR-92b	4.70			hsa-miR-602	3.38
hsa-miR-933	4.42			hsa-miR-625-3p	2.94
hsa-miR-939	4.06			hsa-miR-630	5.18
				hsa-miR-634	2.74
				hsa-miR-663	2.23
				hsa-miR-671-5p	3.81
				hsa-miR-7	4.92
				hsa-miR-874	3.33
				hsa-miR-886-3p	2.46
				hsa-miR-933	2.76
				hsa-miR-939	29.45

Table 2: MiRNA down-regulated at each timepoint.
Table shows miRNA down-regulated by 2-fold or greater (0.5 or less) compared to Mock values.

6 hr down		24 hr down		48 hr down	
miRNA	**Change vs. Mock**	**miRNA**	**Change vs. Mock**	**miRNA**	**Change vs. Mock**
hsa-miR-494	0.49	hsa-let-7a	0.10	hsa-miR-140-5p	0.50
		hsa-let-7d	0.31	hsa-miR-181a-2-3p	0.32
		hsa-let-7e	0.38	hsa-miR-19b-1-5p	0.12
		hsa-let-7f	0.07	hsa-miR-24-1-5p	0.43
		hsa-let-7g	0.42	hsa-miR-27a	0.34
		hsa-miR-125a-5p	0.29	hsa-miR-29b-1-5p	0.26
		hsa-miR-126	0.38	hsa-miR-301b	0.42
		hsa-miR-128	0.48	hsa-miR-30a-3p	0.33
		hsa-miR-15b	0.34	hsa-miR-30b-3p	0.46
		hsa-miR-183	0.42	hsa-miR-30e-3p	0.23
		hsa-miR-19b-1-5p	0.29	hsa-miR-34c-5p	0.42
		hsa-miR-20a	0.38	hsa-miR-362-5p	0.46
		hsa-miR-20b	0.45	hsa-miR-379	0.43
		hsa-miR-221	0.43	hsa-miR-92a-1-5p	0.18
		hsa-miR-224	0.42	hsa-miR-935	0.50
		hsa-miR-23a	0.50		
		hsa-miR-23b-5p	0.33		
		hsa-miR-27b	0.38		
		hsa-miR-29b-1-5p	0.23		
		hsa-miR-30b	0.48		
		hsa-miR-361-5p	0.50		
		hsa-miR-374b	0.41		
		hsa-miR-424	0.47		
		hsa-miR-455-3p	0.43		
		hsa-miR-660	0.42		
		hsa-miR-92a-1-5p	0.11		

To strengthen the case for differential regulation, representative up-regulated and down-regulated miRNAs identified in microarray were confirmed in qRT-PCR (Figures. 9-11). From the up-regulated group, miR-630, miR-99a, miR-1225-3p, and miR-1238 were chosen for confirmation (Figure 9). Results for miR-630 largely corroborated the microarray data (Figure 9A), showing an upregulation of approximately 6-fold at 24 hpi and 4-fold at 48 hpi above mock values (Figure 9B). In contrast, miR-99a did not appear significantly regulated vs. mock. Results in miR-1225-3p showed trends of downregulation at 24 hpi and moderate upregulation thereafter, while miR-1238 showed trends of downregulation at 16 hpi and upregulation thereafter, though statistical analysis showed these values not to be significantly different from the mock.

The down-regulated miRNAs included many members of the miR-17-92 cluster, whose microarray values are shown in Figure 10A. Three members of this cluster were selected for confirmation: miR-17-5p, miR-19b-1-5p, and miR-92a-1-5p. qRT-PCR values largely correlated with microarray at 24 hpi, showing statistically significant downregulation compared to mock values (Figure 10B). However, the apparent upregulation of miR-17-5p at 48 hpi in microarray was not confirmed; rather, all miRNA showed significant downregulation at 48 hpi. Notably, those miRNA located further downstream from the promoter, as illustrated in Figure 10C, showed the most significant downregulation. Interestingly, position-dependent regulation has also been described for the paralog miR-106a/363 located on the X chromosome, in differentiated macrophages following transfection with an HIV-1 plasmid. However, this generally produced greater suppression in upstream members, and the mechanism was uncharacterized[254]. In the

case of miR-17-92, the pattern suggests that initial transcription is occurring in order to produce the upstream miRNA such as miR-17-5p, but that the process of elongation, necessary to produce the downstream miRNA, is not occurring efficiently

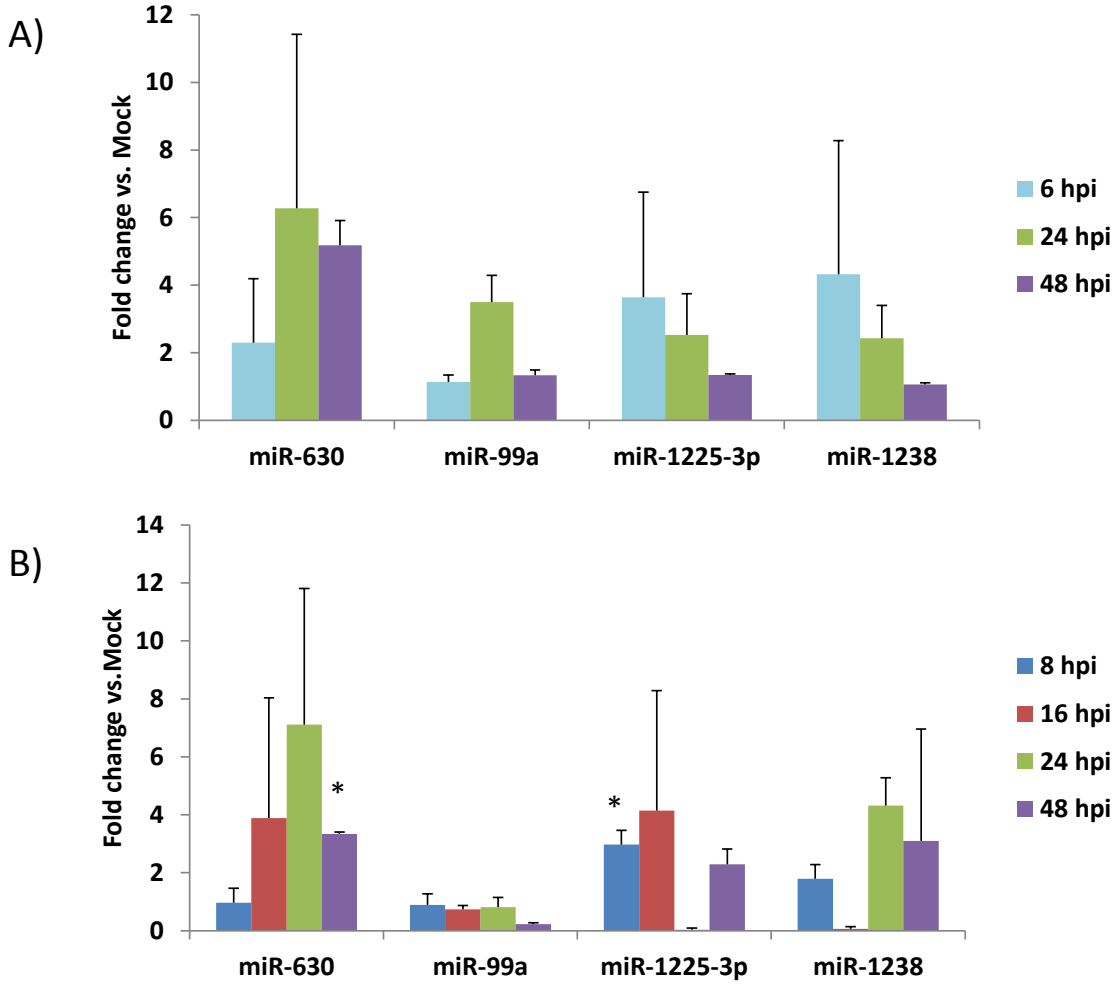

Figure 9: Up-regulated miRNA.
MiRNA was extracted from HSAECs infected with RVFV at MOI=3 and analyzed by microarray and qRT-PCR. Selected values are shown. Panel A: Microarray data at 6, 24, and 48 hpi. Panel B: qRT-PCR results at 8, 16, 24, and 48 hpi. Asterisk (*) indicates statistical significance where P=0.05 or less by Student's t-test.

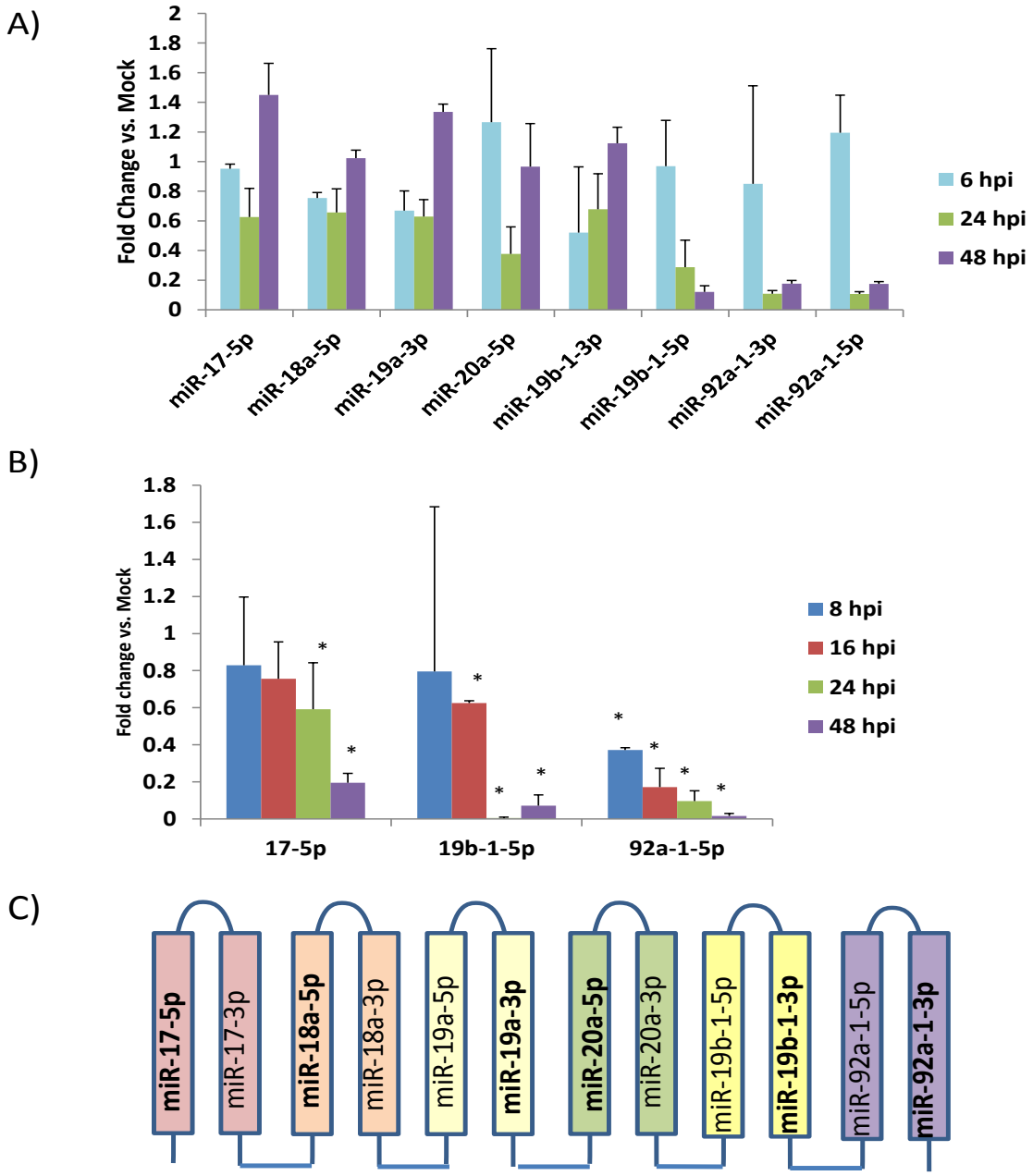

Figure 10: Down-regulated miRNA;miR-17-92 cluster.
MiRNA was extracted from RVFV-infected HSAECs as discussed in Fig. 8. Panel A: microarray data. Panel B: qRT-PCR data. Asterisk (*) indicates statistical significance when P=0.05 or less. Panel C: Diagram of miR-17-92 cluster showing position and distance from the promoter. Bold print indicates canonical members of the cluster; normal text shows complementary strands which were formerly considered "passenger" or with lower levels of expression. Drawing adapted from Tan, *et al.*[228]

6.3.2 Differentially regulated miRNAs map to significant pathways associated with development, apoptosis, and cytokine regulation.

Having confirmed the differential regulation of miRNAs in RVFV infection, the next step was to link these data to known features of pathogenesis. The hybridization data were analyzed using the Gene Spring/TargetScan platform to produce lists of approximately 4,000 potential target genes regulated by significantly changed miRNAs at each timepoint. These lists were then sorted to remove "completer" genes not directly associated with the miRNAs, and re-imported to produce tables of significant pathways over-represented by the targeted genes (Table 3). Approximately half the targeted pathways are associated with cytokines and the remainder with developmental regulators for each timepoint, with the number of entries increasing over time, in keeping with the miRNA regulation data.

Table 3: Significant pathways targeted by miRNA at each timepoint.
Search parameters used to generate the table included both up-regulated and down-regulated miRNA at each timepoint.

6 hpi			24 hpi			48 hpi		
Pathway	Nodes targeted by changed miRNA	p-Value	Pathway	Nodes targeted by changed miRNA	p-Value	Pathway	Nodes targeted by changed miRNA	p-Value
Kit Receptor	24	1.32E-08	TGFBR	20	2.45E-08	EGFR1	44	0.00E+00
IL-9	7	6.40E-05	EGFR1	21	4.55E-07	NOTCH	16	3.02E-06
IL-7	8	8.03E-05	Wnt	14	8.87E-06	BCR	22	7.08E-06
IL-1	9	4.25E-04	NOTCH	10	1.49E-04	Kit Receptor	13	5.99E-05
Hedgehog	6	1.72E-02	TNF-α/NF-kB	16	6.38E-04	Androgen Receptor	15	2.47E-04
			Kit Receptor	8	1.26E-03	Hedgehog	6	8.40E-04
			BCR	12	1.69E-03	IL-7	5	1.48E-03
			IL-3	8	2.24E-03	IL-3	11	2.04E-03
			α-6-β-4 Integrin	6	5.71E-03	IL-6	9	2.34E-03
			Androgen Receptor	8	1.22E-02	IL-4	8	5.82E-03
			IL-7	3	1.43E-02	IL-2	8	1.58E-02
			TCR	9	2.43E-02	IL-9	3	2.70E-02
			IL-1	3	4.27E-02	IL-5	5	3.64E-02
						IL-1	4	4.37E-02

6.3.3 Pathway data indicate regulation through indirect rather than direct means.

After generation of the pathway tables, the next step was to determine regulation of individual nodes in each pathway by particular miRNA. Beginning with the cytokines, a list of nodes was generated for each pathway, with each node representing a potential gene target. This list was compared to the master list of genes generated by Gene Spring/ TargetScan from the microarray data, to identify miRNAs potentially regulating each node. It was hoped that this action would show highly regulated miRNAs directly affecting major pathway nodes; however, this was not the case. Instead, the data showed peripheral nodes in the pathway targeted by multiple miRNAs, many of which were only moderately regulated, and sometimes in opposing directions. IL-6 is shown as an example below (see Figure 11), with cytokines IL-2, IL-3, IL-4, IL-7, and IL-9 showing similar patterns of multiple, moderately-regulated miRNAs targeting peripheral nodes (data not shown). Table 4 shows the miRNAs which are predicted to target the boxed nodes in Figure 11, and the regulation for each. While several miRNAs are up-regulated to the 2-3-fold range above mock values, the majority are down-regulated or do not differ notably from mock values, indicating a complex system of control. The picture is further complicated by the significant overlap between pathways, with notable regulatory molecules such as JAK/STAT members involved in mediation of multiple cytokines. Taken together, this indicates that while bioinformatic tools predict significant targeting of cytokine pathways, actual regulation by miRNA is subtle and therefore will be difficult to demonstrate conclusively through antagonism or overexpression of miRNA of interest.

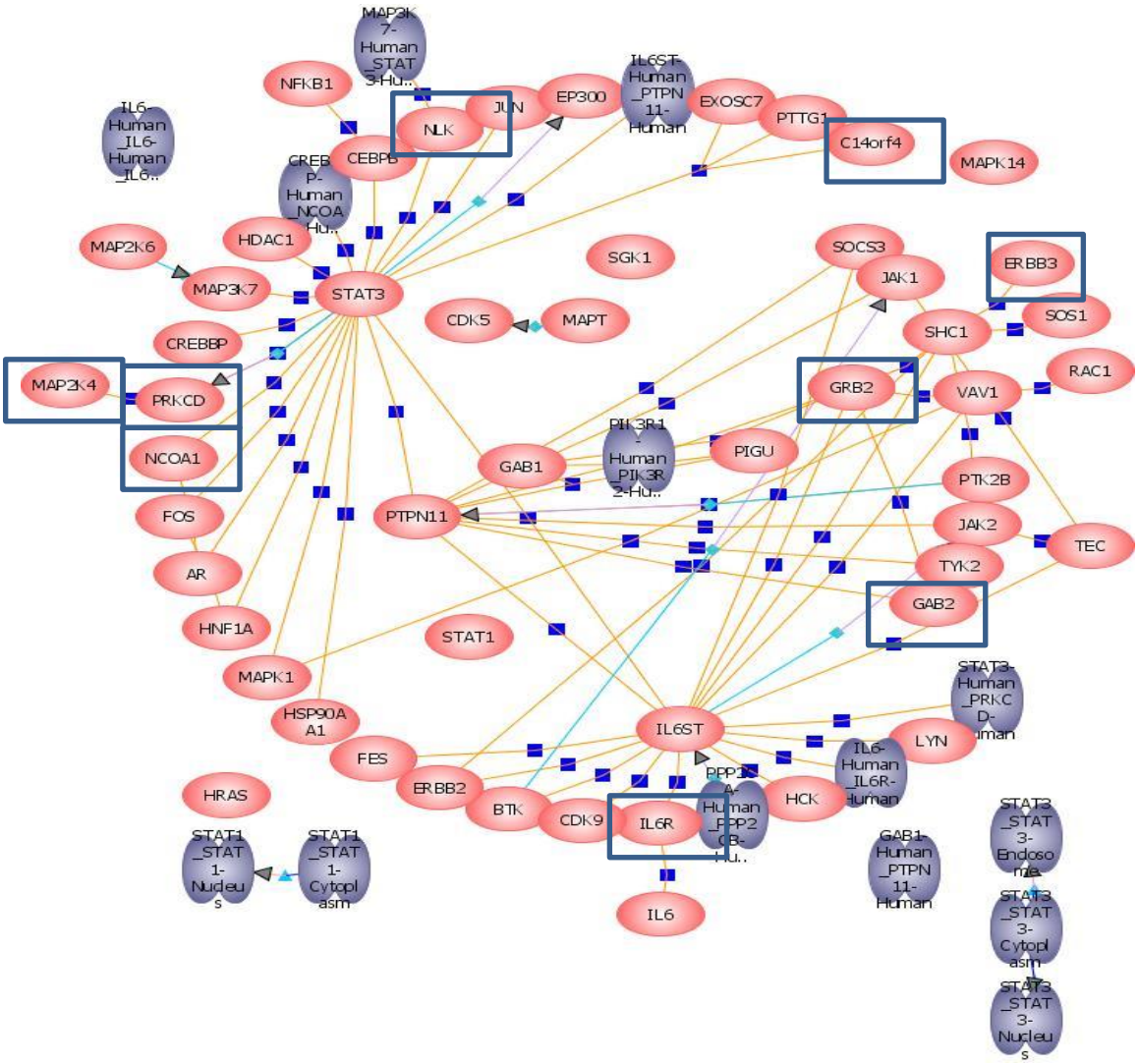

Figure 11: Pathway data indicates regulation by indirect means.
The above graphic, a representation of the IL-6 pathway generated by Gene Spring, shows multiple nodes targeted by the miRNA listed in Chapter 6 (blue boxes). Data is for the 48 hpi timepoint.

Table 4: Nodes targeted by differentially-regulated miRNA.
The 9 nodes predicted in pathway analysis for IL-6 are targeted by multiple miRNA as shown below. Data is from 48 hpi timepoint of HSAECs infected at MOI=3.

Gene	miRNA	Change vs Mock
C14orf4	hsa-miR-193a-3p	0.61
ERBB3	hsa-miR-1237	0.99
GAB2	hsa-miR-149	0.64
GRB2	hsa-miR-141	2.01
	hsa-miR-27a	0.34
	hsa-miR-27b	1.06
IL6R	hsa-miR-34a	1.06
	hsa-miR-34c-5p	0.42
MAP2K4	hsa-miR-141	2.01
	hsa-miR-92b	0.99
	hsa-miR-27a	0.34
	hsa-miR-27b	1.06
NCOA1	hsa-miR-130a	1.11
NLK	hsa-miR-92b	0.99
	hsa-miR-1825	1.16
	hsa-miR-140-5p	0.5
PRKCD	hsa-miR-181b	3.21
	hsa-miR-181c	1.89
	hsa-miR-181d	2.07
	hsa-miR-26b	1.23

6.4 Conclusions

The hypothesis of differential regulation in RVFV infection was strongly supported by initial microarray data, and confirmed by results in qRT-PCR, though the magnitude of change for each miRNA differed somewhat between the two assays. Consistent up- or down-regulation of individual miRNAs, particularly miR-630 and the miR-17-92 cluster, suggests that these molecules are specifically involved in the host-pathogen response.

Bioinformatic analysis of hybridization data linked changed miRNAs to pathways consistent with RVFV infection, including cytokines involved in antiviral response and signaling molecules involved in embryonic development, which provided further support for the hypothesis. However, closer analysis of pathway data revealed a complex, overlapping pattern in which peripheral nodes were targeted by multiple miRNAs with differing degrees and directions of regulation. This “many to many” association of miRNAs with target mRNAs is characteristic of this type of regulation in other systems. While not disproving the core hypothesis, it does pose a challenge in linking individual miRNAs with specific pathogenic processes. Interestingly, several highly regulated miRNAs such as miR-630 were not implicated in the targeting of Gene Spring-determined significant pathways, raising the question of their particular roles during RVFV infection.

The difference in expression between 6 and 24 hpi is particularly noteworthy, as it suggests a change between host and viral control or miRNA regulation during that time. Assuming that miRNAs are acting in their canonical role, this would indicate a

downregulation of host mRNAs at 6 hpi, and a potential upregulation at 24 hpi. Pathway analysis was not detailed enough to reveal overt differences in the targeting pattern, likely due to the many-to-may regulation of miRNAs on targets. The picture is further complicated by the presence of NSs, a known transcriptional inhibitor. While not specifically addressed by this analysis, it is likely that NSs acts to suppress expression of both miRNAs and target mRNAs, especially given the general decrease in miRNA expression at 24 hpi. Further experimentation will be needed to determine the effects of NSs on miRNA regulation in RVFV infection, as well as the roles played by highly-regulated miRNAs.

CHAPTER 7: MEDIATION OF AND BY MIRNA IN THE PATHOGENIC PROCESSES OF RVFV (AIM #2)

7.1 Introduction

To address the challenges posed by the "many to many" regulation of target mRNAs by miRNAs, as well as potential effects from NSs, a series of literature searches was performed to determine association between specific miRNA, potentially relevant transcripts, and pathogenicity factors of RVFV. Several findings emerged to narrow the focus of this study. First, miR-630, the most highly up-regulated miRNA at 24 and 48 hpi, was identified as a regulator of apoptosis via its control of IGF1R[255]. Second, the miR-17-92 cluster, widely studied for its roles in cancer and embryonic development, was reported to be down-regulated by the pro-apoptotic protein p53[256, 257]. As the NSs protein of RVFV is known to induce p53-dependent apoptosis, these two findings appeared likely candidates for further investigation, as well as suggesting a possible cross-talk between regulation of and by the two types of miRNA.

Based on the observed regulation of the miRNAs, the published literature, and the bioinformatic prediction, the following hypotheses were formed: First, that inhibition of miR-630, or overexpression of miR-17-92, would decrease RVFV replication; second, that downregulation of miR-17-92 cluster members was due to the effects of NSs, and that levels would recover in the absence of NSs; third, that mRNA targets of miRNAs would be regulated in canonical fashion (e.g. down-regulated when miRNA were up, and

vice versa); and fourth, that antagonism of up-regulated miRNA, or overexpression of down-regulated miRNA, would reverse the regulation of the target genes.

7.2 Materials and methods

7.2.1 Cells and virus

HSAECs were obtained from Cambrex, Inc. and maintained as described in Chapter 6. Vero cells were obtained from American Type Culture Collection (ATCC) in Manassas, Virginia. Vero is a well-characterized line of monkey kidney epithelial cells, widely used in viral research as it allows for robust growth of viruses due to the lack of Type I interferon response[258-261]. Vero cells were cultured in Dulbecco's Modified Eagle's Media supplemented with 10% FBS, 1% Pen-Strep, and 1% L-glutamine.(DMEM+++). BSR-T7/5 cells were obtained from Dr. Ursula Buchholz, National Institute of Allergy and Infectious Disease, at the National Institutes of Health. This cell line is a BHK-21 line stably expressing the T7 promoter[262], and was cultured in Glasgow minimal essential media supplemented with10% FBS, 1% L-glutamine, 2% non-essential amino acids, 1% Pen-Strep (BSR media); and 1 mg/ml geneticin at every other passage. . All cells were maintained in humidified atmosphere at approximately 37°C and 5% CO_2.

RVFV strain MP12 was obtained from Dr. Sina Bavari as described in Chapter 6. Strains ΔNSs and ΔNSm were obtained from Dr. Shinji Makino at University of Texas Medical Branch. The ΔNSs strain is an experimentally-derived mutant lacking the entire NSs gene[48], while the ΔNSm strain is an experimentally-derived mutant lacking the 21/384 region of the M segment, upstream of the Gn region[39]. Flag-tagged (NSs-Flag)

and V5-tagged (LV5) MP12 were also obtained from Dr. Shinji Makino. All viruses were passaged in Vero cells and maintained at -80°C until use.

An additional strain of virus was generated in-house from cDNA by Dr. Cynthia de la Fuente, using the reverse genetics system developed by Ikegami, *et al*[48, 263]. Virus strains were initially prepared in BSR-T7/5 cells as described in Benedict, *et al*[62]. Viral titers were determined by plaque assay in Vero cells. Further laboratory stocks were generated by infection of Vero cells at MOI=0.1 for one hour.

7.2.3 Transfection of miRNA mimics and inhibitors

For infection at 24 hours post-transfection, cultures of HSAECs were seeded at 6 x 10^5 cells per well in a 6-well plate, or 3 x 10^5 per well in a 12-well plate. Transfection complexes were prepared using Ham's F-12 media (serum-free), miRNA mimics or inhibitors (obtained from Qiagen) at the indicated concentrations, and HiPerfect transfection reagent (Qiagen) at 7 µl per 1 ml final concentration. Cells were transfected concurrently with seeding using the manufacturer's Fast-Forward protocol. For infection 4 hours post transfection, cultures were seeded at 1.5 x 10^5 per well in a 12-well plate and incubated overnight. Transfection complexes were prepared as described above and applied dropwise to cell cultures from which the media had been removed. Complete HSAEC media was added to bring the final volume to 1 ml. In both cases, infection was performed as described in Chapter 6, to the indicated MOI, for one hour.

7.2.4 Plasmid transfections

The miR-17-92 plasmid (pcDNA3.1/V5-His-TOPO-mir17-92) was obtained through Addgene (plasmid #21109) through the kind gift of Joshua Mendell[264], and contains the complete miR-17-92 sequence under control of the CMV promoter. Control plasmid was pcDNA 3.1+. Plasmids were expanded in *E. coli* strain DH5α and isolated using the Qiagen Plasmid Midi Kit or Maxi Kit. Purified plasmids were quantified using the NanoDrop 2000 system.

To transfect the miR-17-92 plasmid, HSAECs were seeded at 1.5×10^5 per well, in complete HSAEC media in 12-well plates. On Day 2, cells were transfected using 1.2 µg per well of miR-17-92 plasmid or pcDNA 3.1+ (negative control) using the Attractene transfection reagent (Qiagen, catalog # 301005) and traditional protocol. On Day 3, at 16 hours post transfection, cells were mock-infected or infected with RVFV MP12 at MOI=3 for one hour, washed with PBS, and re-fed with complete media. Supernatants were collected for plaque assays at 8, 16, and 24 hpi. Protein samples were collected at 16 and 24 hpi in blue lysis buffer as described in section 7.2.6. Samples for miRNA and RNA assessment were collected in *mir*Vana^{tm} kit lysis-binding buffer and extracted as previously described.

7.2.5 Plaque assays

Viral supernatants were serially diluted, and applied at 400 µl in duplicate to confluent cultures of Vero cells in 6-well plates, or 200 µl to confluent cultures of Vero cells in 12-well plates, for one hour prior to immobilization in agarose. Immobilization and staining were performed as described in Narayanan, *et al*[265] for neutral red staining,

or by Kehn-Hall, *et al*[252] for crystal violet staining. Plaque assays were assessed at three days post infection.

7.2.5 qRT-PCR

miRNA was extracted as described in Chapter 6. Full-length RNA was extracted concurrently with miRNA using the *mir*Vana^{tm} kit according to manufacturer's protocol, or from a separate culture using the RNeasy Mini Kit (Qiagen, catalog # 74104 or 74106). Quantitation for both species was performed by NanoDrop as previously described. cDNA preparation and qRT-PCR of miRNA were performed as previously described. cDNA was prepared from full-length RNA using the Applied Biosystems High Capacity RNA-to-cDNA kit (catalog #4387406), and qRT-PCR was performed using Applied Biosystems SYBR Green PCR Master Mix (catalog #4344463). Primer pairs designed using Primer3 (http://biotools.umassmed.edu/bioapps/primer3_www.cgi) were obtained from Integrated DNA Technologies (Table 5). RVFV probe, used with RVFV primers, was obtained from Applied Biosciences (Catalog # 5426725-1).

Table 5: Primer Sequences.
Table shows sequences of primers used for qRT-PCR.

Target	Primer sequence
BCL11B	Fwd: 5'-CCA CCT ACC AGA CCC TGA AA-3'
	Rev: 5'- CGG ACT GGC TGG TTT CTT TA-3'
BIM (BCL2L11)	Fwd: 5'- GAG ATA TGG ATC GCC CAA GA-3'
	Rev: 5'-GTG CTG GGT CTT GTT GGT TT-3'
BMPR2	Fwd: 5'-CTA CCT CTC CTC AGC CTT CG-3'
	Rev: 5'-TTC GGT GCT TCC TTC ACT CT-3'
CCND1	Fwd: 5'-AAC TAC CTG GAC CGC TTC CT-3'
	Rev: 5'- CCA CTT GAG CTT GTT CAC CA 3'
DDIT4	Fwd: 5'-GTG CCA TCT GGG TCT TCC AT-3'
	Rev: 5'-ATC AAG TGT ATT CAT GAA CAG TGA G-3'
EIF4G2	Fwd: 5'-CCA AAG TGG AGA GTG CGA TT-3'
	Rev: 5'-CTT CGT GCA GGA ATC CAT TT-3'
IGF1R	Fwd: 5'-GCC GCT CAT TCA TTT TGA CT-3'
	Rev: 5'-GGG GGA AAA CTG CAA AGA A-3'
PTEN	Fwd: 5'- TTC TCT CCT CTC GGA AGC TG-3'
	Rev: 5'-AGA GGC TGC ACG GTT AGA AA-3'
18S RNA	Fwd: 5'-TGA GAA ACG GCT ACC ACA TC-3'
	Rev: 5'-TTA CAG GGC CTC GAA AGA GT-3'
RVFV	Antisense: 5'-CAC TTC TTA CTA CCA TGT CCT CCA AT-3'
	Sense: 5'-AAA GGA ACA ATC GAC TCT GGT CA-3'

7.2.6 Western blot

Protein samples of 50 µg (clear lysis buffer) or 20 µl (blue lysis buffer) were separated, transferred, and subsequently processed as described in Austin, *et al*[5]. Membranes were blocked and primary antibody to IGF1R was prepared in 3% bovine serum albumin (BSA) in PBST. β-actin conjugated with horseradish peroxidase was used as a loading control.

.

7.2.7 Statistical analysis

Triplicate or higher-order samples were tested for cohesiveness using Grubbs' test for outliers. A value was considered an outlier if the P value was greater than 0.05. Sample sets were tested for significance using Student's unpaired t-test, and were considered significant if the P value was less than 0.05.

7.3 Results—miR-630 and miR-99a

7.3.1 Regulation of miR-630/IGF1R in RVFV infection.

Literature search identified the anti-apoptotic protein IGF1R as a direct target of miR-630, and specific base-pairing was predicted by TargetScan (www.targetscan.org). To confirm changes *in vitro*, triplicate cultures of HSAECs were mock-infected or infected with RVFV at MOI=3, and collected at 8, 16, 24, or 48 hpi. Differential expression of miR-630 and of IGF1R mRNA was assessed by qRT-PCR. miR-630 data were consistent with microarray analysis, showing strong upregulation at 24 hpi (Figure 12a). In contrast, the IGF1R data showed significant downregulation, with levels decreasing to less than 5% of mock value at 48 hpi (Figure 12b). This is consistent with regulation by miR-630. To confirm these results further, a second infection was performed and triplicate samples assessed by western blot. The results were consistent with the qRT-PCR data, showing a decrease of IGF1R in RVFV-infected samples to approximately 40-50% of the mock value (Figure 12c and 12d). Taken together, these results clearly demonstrate altered expression of both molecules during RVFV infection, and suggest the downregulation of IGF1R through the upregulation of miR-630.

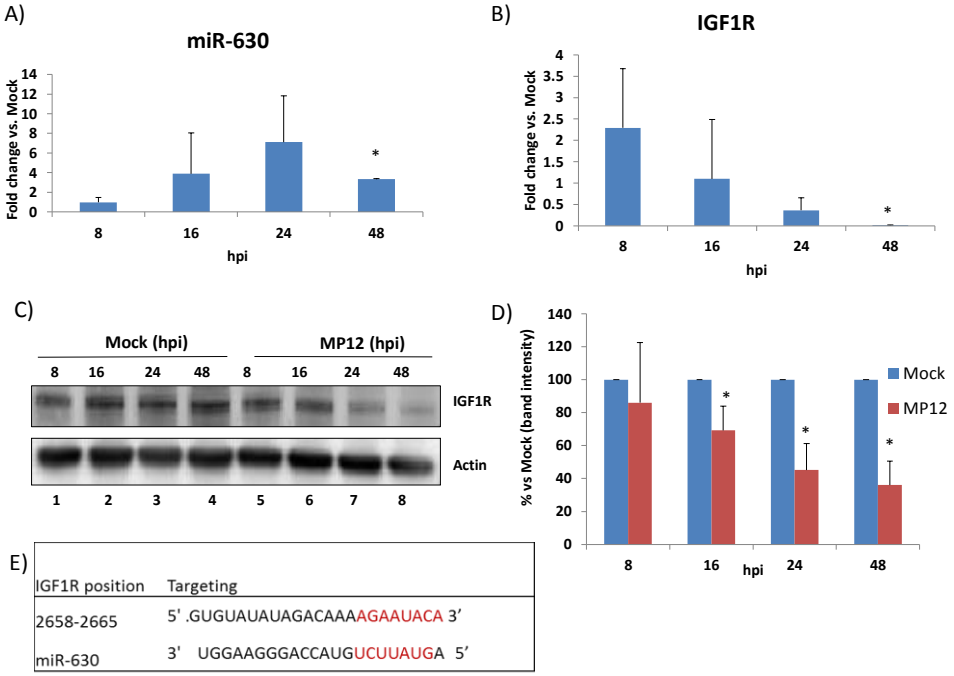

Figure 12: regulation of miR-630 and IGF1R in RVFV infection.
HSAECs were infected at MOI=3 and samples collected at multiple timepoints as shown. Panel A: qRT-PCR results for miR-630 expression over time. Panel B: qRT-PCR results for IGF1R expression over time. Panel C: Western blot results for IGF1R expression in RVFV infection. Single representative trial is shown. Panel D: Quantitation of triplicate western blot samples. For A-D, asterisk (*) indicates statistical significance where P=0.05 or less. Panel E: TargetScan prediction of miR-630 binding sites on IGF1R.

7.3.2 Co-inhibition of miR-630 and miR-99a induces a trend of rescue for IGF1R in RVFV infection.

To confirm that IGF1R suppression was due to the effects of miR-630, a series of transfections were performed in HSAECs, using a miR-630 inhibitor (a-miR-630) or a negative control. Cultures were infected at MOI=3 at 24 hours post transfection, and IGF1R expression was assessed by Western blot. Initial experiments failed to show rescue (data not shown), so the time between transfection and infection was shortened to 4-5 hours. At this point, there was a trend of rescue; however, these results were not consistent. Therefore, additional literature search was performed in order to identify additional miRNAs which targeted IGF1R. Several papers identified miR-99a as a

regulator of IGF1R[266-268], and the specific base pairing was determined by TargetScan as was done for miR-630 (Figure 13B). As discussed in Chapter 6, miR-99a was shown in microarray to be up-regulated in RVFV infection (13A), which appeared consistent with the role described in literature. Therefore, it was hypothesized that inhibition of IGF1R was partially due to upregulation of miR-99a in RVFV infection.

To test this hypothesis, triplicate cultures of HSAECs were treated with 100 nM of NC, a-miR-630, or a-miR-99a, or with 50 nM each of a-miR-630 and a-miR-99a, 4-5 hours prior to infection at MOI=3. Samples were collected at 24 hpi (29-30 hours post transfection) and rescue was assessed by western blot. Similarly to results for a-miR-630 alone, a-mir-99a alone did not produce consistent rescue (Figure 13C). However, co-transfection with a-miR-630 and a-miR-99a appeared to produce moderate rescue, from approximately 50% reduction as seen in with infected, NC treated samples, to approximately 74% with infected, co-transfected samples (Fig. 13 C). Taken together, this supports the hypothesis of miR-99a being a factor in regulation of IGF1R during RVFV infection; however, antagonism of either miRNA alone is insufficient to induce rescue.

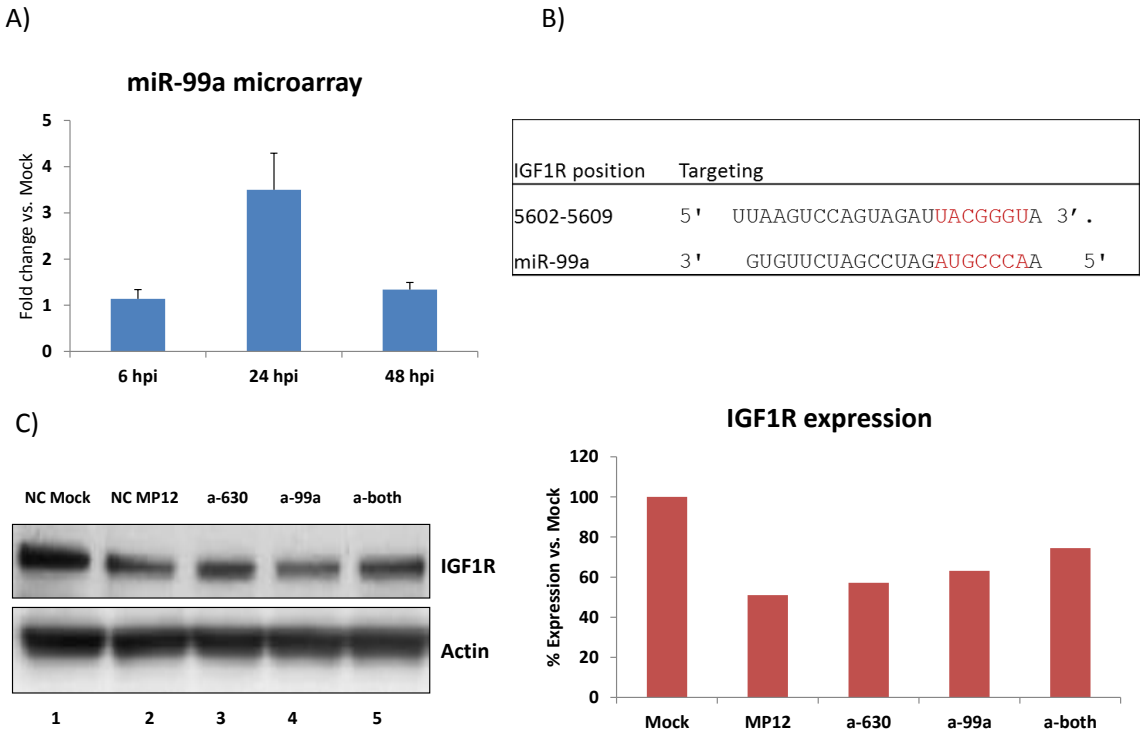

Figure 13: Co-transfection with a-mir-630 and a-miR-99a induces partial rescue of IGF1R in RVFV infection. A series of infections were performed in the presence of NC or a-mir-630, a-miR-99a, or both (a-both). Samples were collected at 24 hpi and assessed by Western blot. Panel A: Microarray results for miR-99a expression in HSAECs infected with RVFV at MOI=3. Panel B: Predicted targeting of IGF1R by miR-99a as determined by TargetScan Panel C, left: Western blot showing expression of IGF1R following treatment with miRNA inhibitors as described (single representative blot shown). Panel C, right: Quantitation of band intensities for each condition (duplicate samples) as percent expression vs. mock value.

7.4 Results—miR-17-92 cluster

7.4.1 Repression of miR-17-92 cluster in RVFV infection is NSs dependent

As previously discussed, the miR-17-92 cluster is reportedly suppressed by p53[256, 257], a pro-apoptotic protein known to be activated in RVFV infection through the action of NSs[5]. Both microarray data and qRT-PCR showed downregulation of this cluster during RVFV infection of HSAECs; therefore it was hypothesized that the suppression was NSs dependent. To test this hypothesis, cultures of Vero cells were mock-infected or infected with wild-type strain MP12, a strain lacking the ORF for NSs (ΔNSs), or lacking the ORF for NSm (ΔNSm). Vero cells were chosen due to their

deficient interferon response, which enables similar growth in strains both competent and deficient in NSs production. A growth curve was performed first, infecting cells at MOI=3 and collecting at 8, 16, 24, or 48 hpi (Figure 14). Replication was determined by plaque assay. Although there were several statistically significant differences between mutant strains and MP12, the differences were less than 1 $\log_{10}$ at 24 hpi, and growth was considered generally equivalent across the three strains.

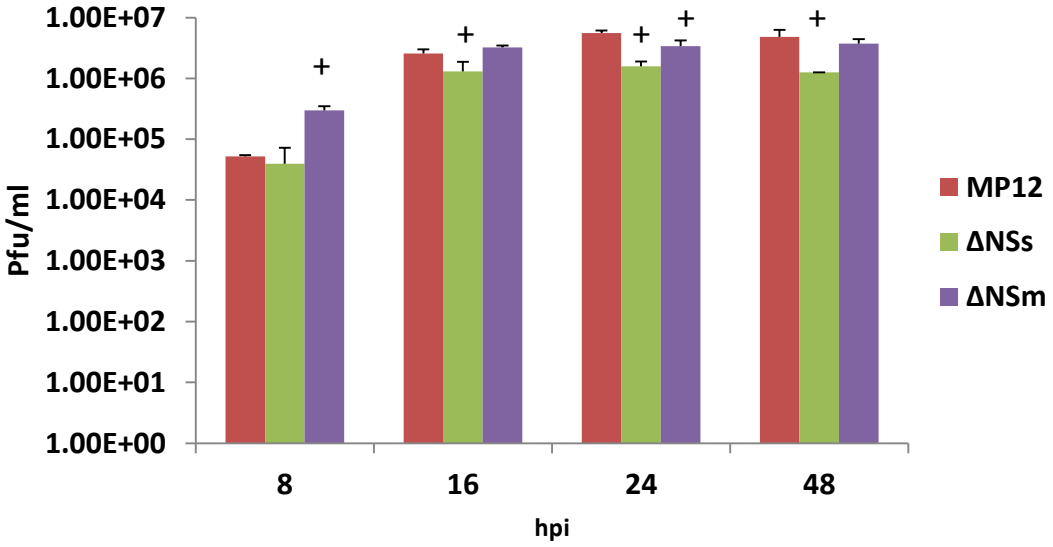

Figure 14: Growth curve of three RVFV strains in Vero cells.
Vero cells were infected at MOI=3 with one of three strains of RVFV as shown, and replication assessed by plaque assay. Plus sign (+) indicates statistical significance from MP12 when $P \leq 0.05$.

A second set of infections was performed in Veros, with samples collected at 24 hrs and processed to yield both miRNA and full-length RNA. Regulation of miRNA was assessed first, by qRT-PCR. As shown in Figure 15, all cluster members tested were

repressed in the presence of NSs (MP12 samples), from approximately 40% of mock levels in miR-17-5p to approximately 7% of mock levels in miR-92a-1-5p. Additionally, all showed some degree of recovery in the absence of NSs, with all except miR-20a-5p recovering to a level at or above the mock. miR-92a-1-5p showed the greatest recovery, to approximately 3.8 times the level seen in mock infected cells. Results for ΔNSm were similar to MP12 as expected in miR-17-5p and 19b-1-5p, but decreased in and miR-92a-1-5p to a level of approximately 38% of mock levels, respectively. Taken together, this supports the hypothesis that suppression of miR-17-92 in RVFV infection is NSs-dependent.

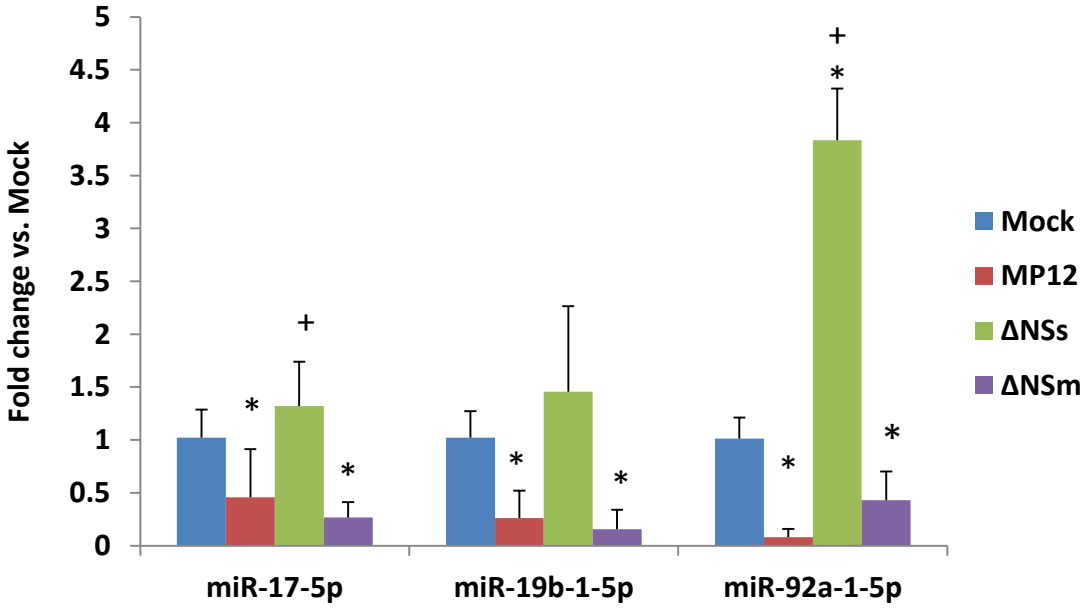

Figure 15: miR-17-92 cluster members are suppressed by NSs.
Vero cells were mock-infected or infected with variant strains of RVFV at MOI=3. Samples were collected at 24 hpi and expression of selected miR-17-92 cluster members was assessed by qRT-PCR. Values were considered significant when P=0.05 or less. Asterisk (*) indicates significant difference from Mock; plus sign (+) indicates significant difference from MP12.

7.4.2 Expression of mir-17-92 targets is suppressed by NSs

As discussed in Chapter 5, loss of miR-17-92 leads to increased apoptosis during cancer, and is associated with significant developmental abnormalities including skeletal malformations in humans and embryonic lethality in mice. As these effects mirror the increased apoptosis and developmental dysregulations associated with RVFV infection, it was hypothesized that downregulation of miR-17-92 would correlate with upregulation of genes associated with these processes.

To narrow the focus, a search was performed using literature and two databases, miR-db (www.mirdb.org) to identify predicted targets, and miRTarBase (http://mirtarbase.mbc.nctu.edu.tw), to identify validated targets. Through this search, seven targets were identified for further testing: BCL11B (B-cell CLL/Lymphoma 11B) and BIM (BCL2-like 11), both involved in the apoptosis pathway; BMPR2 (Bone Morphogenic Protein Receptor 2), an important developmental protein; CCND1 (Cyclin D1), a regulator of the cell cycle; DDIT4 (DNA-damage-inducible Transcript 4); a marker of DNA damage response; and EIF4G2 (Eukaryotic Translation and Initiation Factor Gamma 2), and PTEN (Phosphatase and Tensin Homolog), both important in embryonic development. To test the regulation of these targets *in vitro*, HSAECs were mock-infected or infected at MOI=3, and collected at 8, 16, 24, or 48 hpi. RNA was extracted and assessed by qRT-PCR. Overall, the target mRNAs were down-regulated in a time-dependent manner (Figure 16a), which does not support the hypothesis of regulation by targeting miRNA, but does suggest the action of NSs.

To test this, Vero cells were mock-infected or infected at MOI=3 with MP12, ΔNSs, or ΔNSm, and analyzed by qRT-PCR for target expression at 24 hpi (Figure16b). BCL2, BMPR2, CCND1, EIF4G2, and PTEN expression in MP12 infected cells showed statistically-significant decreases from mock infected cells, and a recovery of expression in ΔNSs infected cells. Overall, these results indicate that expression of miR-17-92 targets is also subject to regulation by NSs. However, there were two exceptions. BIM showed no statistically significant difference between mock and MP12 samples, and an increase of approximately 4.5-fold in ΔNSs and 2.4-fold in ΔNSm samples. Remarkably, DDIT4 showed statistically-significant increases above mock levels in all infection conditions, to levels of 3.7-fold, 6.8-fold, and 5.6-fold in MP12, ΔNSs, and ΔNSm samples, respectively. As the results in HSAECs showed significantly decreased expression in MP12 at the same timepoint, this suggests that differences between the two cell types could account for the lack of suppression of BIM and the upregulation of DDIT4. While Veros are used here due to their deficiency in interferon, literature search reveals no direct connection between interferon deficiency and increased expression of BIM or DDIT4. Instead, this may be a factor of differences in interspecies response, or even between lung and kidney cells.

Taken together, this suggests that both miRNA and targets are subject to NSs-induced repression. However, given the wide range of potential target genes for this cluster, there may be additional factors not suppressed by NSs through which specific regulation by miR-17-92 could more easily be determined.

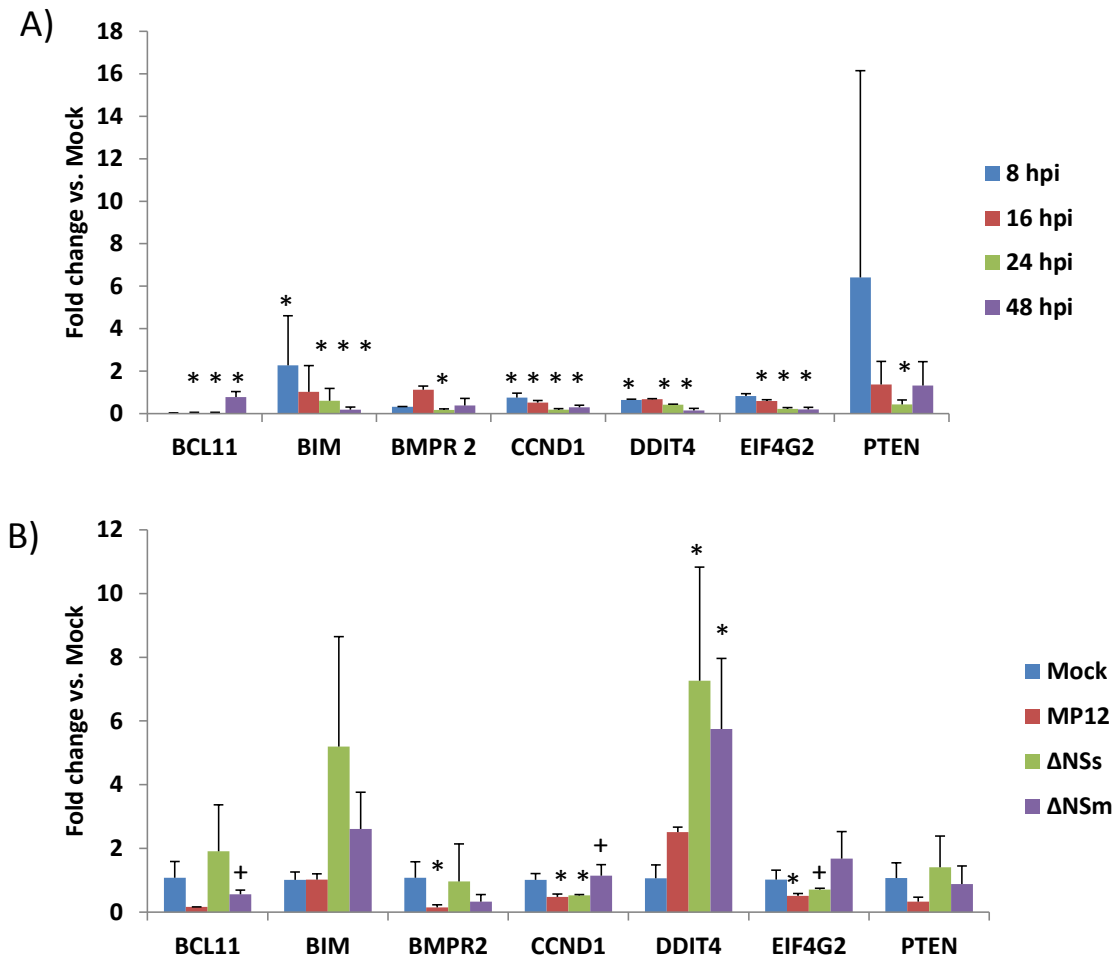

Figure 16: Expression of miR-17-92 targets is suppressed by NSs.
Panel A: HSAECs were mock-infected or infected with RVFV MP12 at MOI=3 and samples were collected at 24 hpi. RNA was extracted, and target expression was determined by qRT-PCR. Panel B: Veros were mock-infected or infected with variant strains of RVFV at MOI=3. RNA was extracted, and target expression determined by qRT-PCR. . Asterisk (*) denotes statistical significance where P=0.05 or less.

7.4.3 Transfection with miR-17-92 plasmid reduces viral replication.

Although the repression of miR-17-92 members and their target RNA suggests a general rather than a specific effect, it is possible that the repression confers some benefit to the virus which would otherwise impair its replication. Therefore, it was hypothesized that overexpression of these miRNA would result in decreased viral replication. To test

this hypothesis, cultures of HSAECs were infected at MOI=0.1 in the presence of NC or miRNA mimics, collected at 24 hpi, and assessed for viral replication by plaque assay. Overexpression of individual miR-17-92 cluster members miR-19b-1-5p and miR-92a-1-5p did not result in decreased replication (data not shown). Therefore, it was hypothesized that cluster members working in concert would be able to decrease RVFV replication.

To test this, cultures of HSAECs were transfected for 16 hours with plasmids containing the miR-17-92 sequence or a negative control, prior to infection with RVFV for 16 hrs (timeline, Figure 17A). Analysis by qRT-PCR demonstrated successful transfection, showing a general trend of upregulation in transfected samples at 0 hpi (Figure 17 B-D), though not to the same degree for all miRNAs tested. The most highly up-regulated miRNA was miR-19b-1-5p (Figure 17C), with an increase of approximately 6-fold at 0 hpi, 14-fold at 16 hpi in mock samples, and 7-fold at 16 hpi in RVFV samples. miR-92a-1-5p showed the same trend of upregulation, though not to the same degree (Figure 17D). In contrast, miR-17-5p showed decreases at 16 hpi in both mock and RVFV samples. These results could potentially be due to differing half-lives between the mature miRNA, or as some factor of each member's distance from the promoter, as previously described for downregulation. This experiment also confirmed the expected downregulation of miR-17-92 members in RVFV infection in pcDNA samples, and that transfection with miR-17-92 plasmid has the ability to induce a measure of increase, even in the presence of NSs. Specifically, the significant upregulation of miR-19b-1-5p, located near the end of the cluster, suggests that transcription from the plasmid is able to

progress through the elongation stage, which does not appear to be the case during endogenous miR-17-92 expression in RVFV infection. This could be due to the difference in NSs susceptibility between the endogenous promoter used in host-based transcription vs. the CMV promoter used to drive plasmid-based transcription.

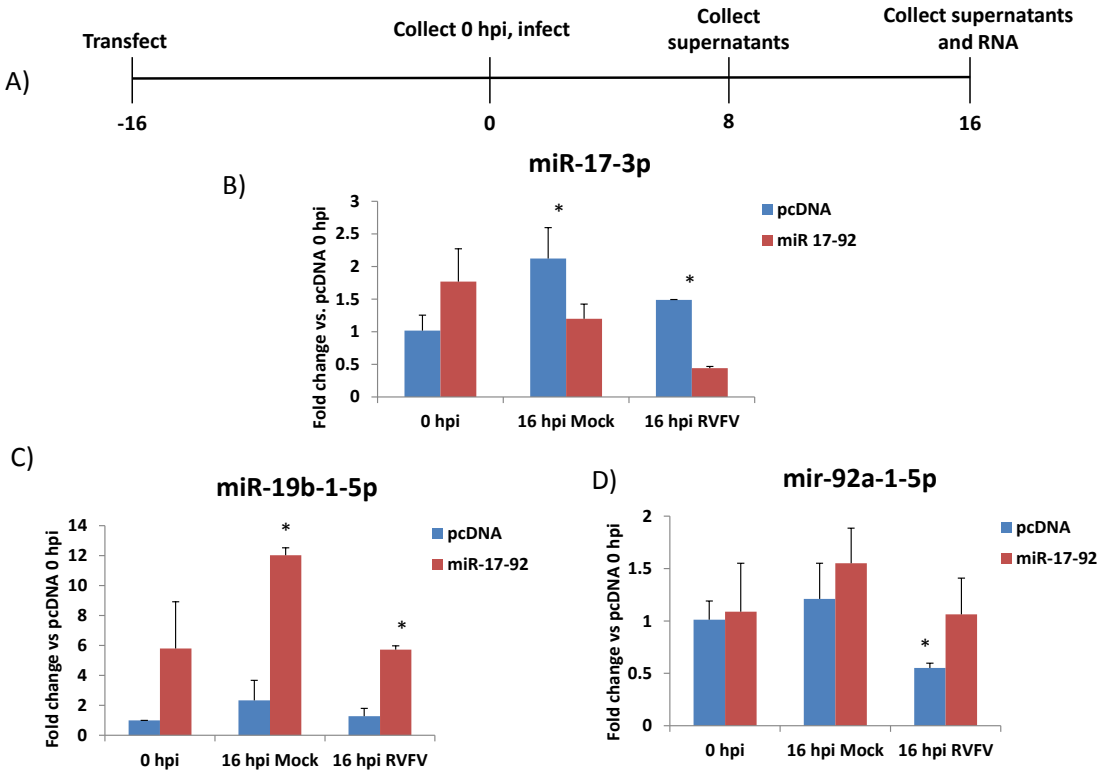

Figure 17: Transfection with miR-17-92 plasmid increases expression of cluster members.
Panel A: timeline shows order of operations and sample collection. Panel B-D: Selected cluster members were assessed by qRT-PCR following 16 hr transfection and RVFV infection at MOI=3. Asterisk (*) indicates statistical significance at P=0.05 or less.

Following confirmation, viral replication was determined at 16 hpi by qRT-PCR and at 8 and 16 hpi by plaque assay (Figure 18). The qRT-PCR showed approximately 30% decrease in viral genomic expression in miR-17-92 plasmid-treated samples

compared to the negative control (Figure 18A). Similarly, the plaque assay showed a decrease of approximately 38% following treatment with the miR-17-92 plasmid (Figure 18B). Taken together, this indicates the ability of the miR-17-92 cluster to suppress viral replication, chiefly through the actions of miR-19b-1-5p, and suggests the actions of other cluster members in concert, despite the overall moderate degree of regulation.

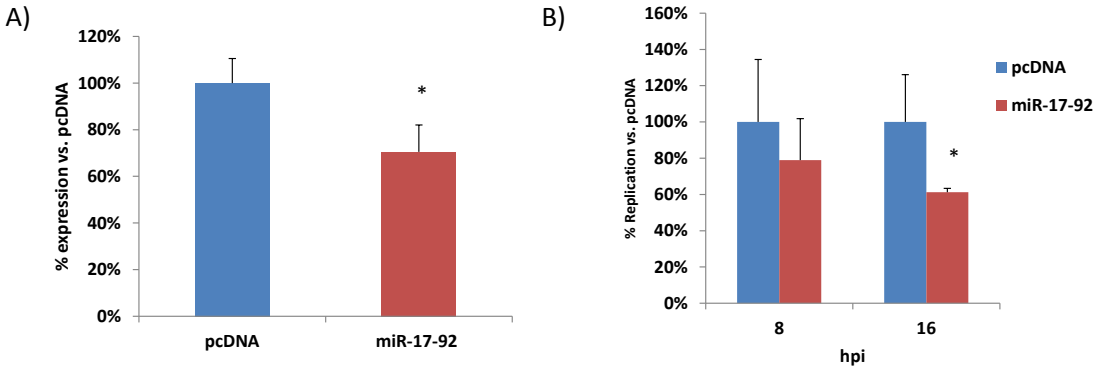

Figure 18: Transfection with miR-17-92 plasmid reduces viral replication.
HSAECs were transfected with 1.2 µg of plasmid containing miR-17-92 or pcDNA as a negative control for 16 hrs prior to infection at MOI=3. Results were assessed by qRT-PCR and plaque assay. Panel A: qRT-PCR results showing viral genomic copies following miR-17-92 transfection, 16 hpi. Panel B: Plaque assay results at 8 hpi and16 hpi following miR-17-92 transfection. Asterisk (*) indicates statistical significance where P=0.05 or less.

7.6 Conclusions

The four hypotheses for this section stated that 1) antagonism of miR-630 or overexpression of miR-17-92 would inhibit viral replication; 2) miR-17-92 was inhibited by NSs and would recover in its absence; 3) that gene targets of given miRNA would be regulated in a canonical fashion (i.e. up-regulated when miRNA is down-regulated, and vice versa), and 4) that inhibition of up-regulated miRNA would allow recovery of the target genes. In the case of miR-630, the overall data did not support the hypotheses.

Although IGF1R appeared down-regulated in RVFV infection at both the mRNA and the protein level, corresponding to the increase in miR-630 expression, antagonism of miR-630 was insufficient to reduce RVFV replication or to enable recovery of IGF1R. When combined with anti-miR-99a, there was a trend of recovery for IGF1R and a trend of decrease in viral replication.

However, it is likely that an additional factor is acting to repress IGF1R expression at both the mRNA and protein level. To address this, three future studies are suggested: first, to determine NSs binding to the IGF1R promoter through chromatin immunoprecipitation (ChIP) assays; second, to determine potential degradation of the protein through a pulse-chase or ubiquitination assay, and third, to determine translation inhibition through a ribosomal binding assay.

In the case of miR-17-92, the overall data partially supported the hypotheses. Although individual cluster members did not suppress viral replication, transfection of a plasmid encoding the full miR-17-92 cluster was sufficient to decrease viral genome expression as measured in qRT-PCR and viral replication as measured by plaque assay. The differing degrees of upregulation among cluster members suggest that inhibitory effects occur chiefly through the actions of miR-19b-1-5p, though overexpression of this miRNA alone was not sufficient to reduce RVFV replication in plaque assay. This suggests in turn that a synergistic effect is occurring through the actions of multiple cluster members, even those which appear to be less highly expressed. Therefore, the first hypothesis was partially but not fully supported.

The second hypothesis was fully supported, as removal of NSs allowed significant recovery of cluster members. However, the third hypothesis was not supported, in that mRNA targets of the cluster were also down-regulated despite the suppression of miR-17-92. This suggests the inhibitory actions of NSs above regulation by the miRNA. A proposed model is shown below (Figure 19). Therefore the fourth hypothesis, regarding expression of gene targets following miR-17-92 transfection, was not investigated.

To continue the investigation of interplay between NSs and miR-17-92, the following future directions are suggested: first, to determine the role of p53 activation on cluster suppression through siRNA knockdowns; and second, to determine the role of NSs in inhibiting elongation. This will provide additional insight into the fine-tuning of replicative processes through miRNA regulation in RVFV infection.

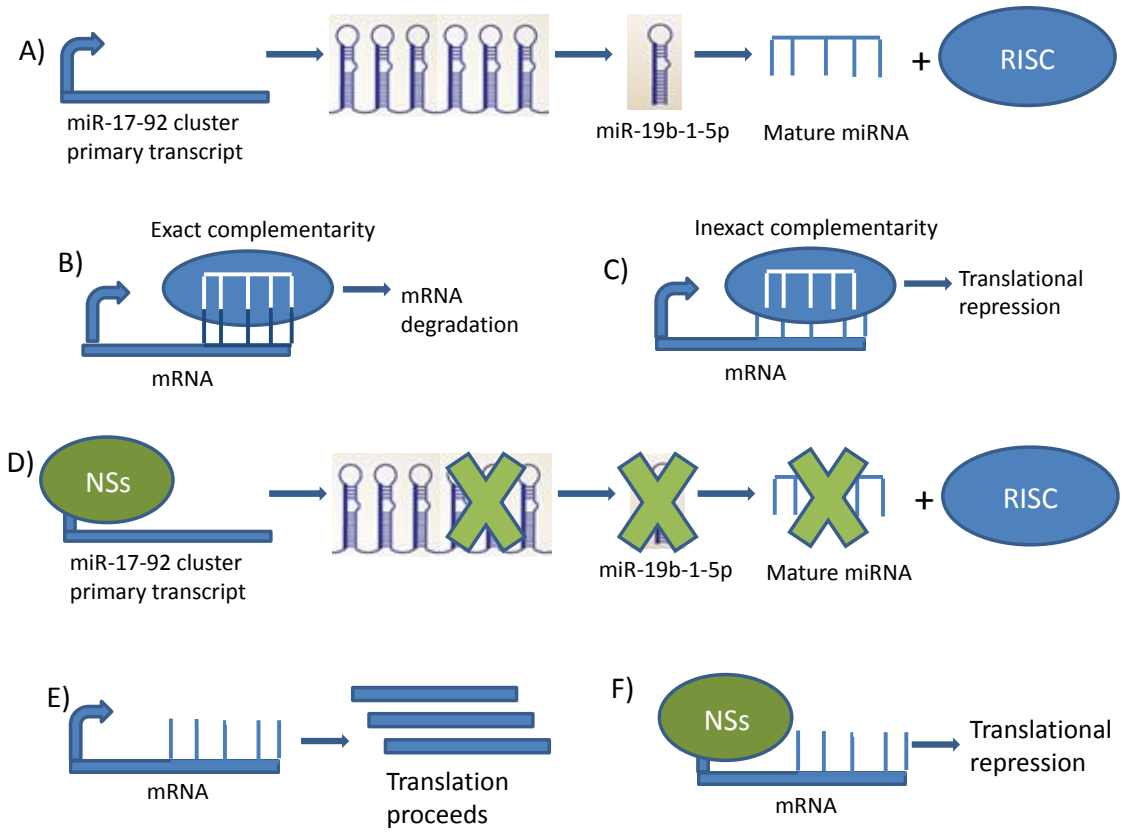

Figure 19: Proposed model of interplay between miR-17-92 cluster and NSs.
Model is based on canonical pattern of regulation. **Panel A:** Biogenesis of mature miRNA from primary transcript. Panel B: Exact complementarity between miRNA-RISC and target mRNA leads to degradation of mRNA. Panel C: Inexact complementarity leads to translational repression. Panel D: Hypothesized binding of NSs to miR-17-92 cluster promoter prevents elongation and production of mature miRNA further from promoter. Panel E: Canonical regulation suggests normal translation without binding of miRNA-RISC. Panel F: Hypothesized binding of NSs to mRNA promoter induces translational repression in absence of miRNA-RISC. Hairpin images from O'Carroll and Schaefer, 2013[269].

CHAPTER 8: VENEZUELAN EQUINE ENCEPHALITIS VIRUS INTERACTS WITH HOST MICRORNA MACHINERY TO PROMOTE VIRAL REPLICATION (AIM #3)

8.1 Introduction

VEEV, like RVFV, is an important emerging pathogen of zoonotic origin, and is of concern from both a biodefense and a public health standpoint for its severe disease course in humans and livestock. Although they can cause similar symptoms of high fever and neurological complications, the two viruses are quite different from a molecular standpoint, with VEEV having a single-stranded, non-segmented, positive-sense genome, in contrast to the single stranded, tri-segmented, negative sense genome possessed by RVFV. Therefore, the investigations into interactions of RVFV and VEEV with host miRNA and associated machinery represent a significant breadth of concept, and merit inclusion of the VEEV investigations into this study.

Early studies into miRNA regulation focused on viruses with DNA genomes, or with those which maintained latent phases after infection (HIV). However, more recent studies have examined miRNA regulation in relation to acute viral infections, such as rabies[179], pseudorabies[180], and influenza[270]. One notable study, done by Bhomia, *et al* (2010), demonstrated changed miRNA profile in the brains of VEEV-infected mice, with 32-36 miRNA differentially regulated with a distinct time-dependent change in pattern. The changed miRNA mapped to functional pathways associated with major features of

VEEV pathogenesis, notably inflammatory response and nervous system development and function[3], although they were not specifically linked to the regulation of individual target molecules. As discussed in previous chapters, a similar relationship was observed for miRNA-associated pathway mapping in RVFV, strengthening support for the breadth of concept.

To deepen the understanding of these viral processes, this investigation focused on interactions of VEEV with the miRNA machinery. As discussed in Chapter 5, canonical processing occurs through a precise set of enzymatic steps beginning with the trimming of the stem-loop precursor from the primary transcript by Drosha, and ending with incorporation of a single strand into the RISC as mediated by Ago2. Based on current understanding of miRNA in viral infections, the following hypotheses were formed: 1) that disruption of the miRNA pathway would lead to decreased replication of VEEV in culture, and 2) that similar decreases would be seen against fully-virulent strains of VEEV and related Alphaviruses. These studies could potentially identify a novel therapeutic target against VEEV infection.

8.2 Materials and methods

8.2.1 Cells and viruses

Mouse embryonic fibroblasts (MEFs), U87MG astrocytes, 293-T, and Vero cells were cultured in DMEM+++ as previously described. MEFs deficient in Ago2 (Ago2$^{-/-}$ MEFs) were obtained through Dr. G. Hannon of Cold Spring Harbor[186]. AP-7 olfactory neuronal cells, a generous gift of Dr. D. E. Griffin (Johns Hopkins University), were cultured as described by Amaya, *et al*[108]. VEEV strains Trinidad Donkey (TrD), Mena II

(Mena), 3880, and TC-83 were obtained from BEI Resources (Manassas, VA). The TrD strain, considered the model organism for the fully virulent strains, is serological subtype IAB and is associated with periodic epidemic and epizootic outbreaks. The Mena and 3880 strains are subtypes ID and IE, respectively, and, although fully virulent, are not associated with such outbreaks[67]. The TC-83 virus is a live attenuated vaccine derivative of the TrD strain propagated by 83 serial passages in guinea pig heart cells[271], resulting in 12 nucleotide substitutions which confer attenuation principally through changes within the 5'-noncoding region and E2 envelope glycoprotein[272]. All work with VEEV-TrD, VEEV-Mena, VEEV-3880, WEEV, and EEEV, was performed at BSL-3.

8.2.2 siRNA knockdowns

293-T cells were seeded in a 96-well plate and transfected concurrently with seeding, using 100 nM siRNA and Attractene transfection reagent (Qiagen, catalog #301005), according to the manufacturer's Fast-Forward protocol. Cells were subsequently mock-infected or infected with VEEV TC-83 at an MOI=0.1 at 48 hours post transfection (hpt) and collected at 24 hpi. Replication was assessed by plaque assay. To confirm knockdown, 293-T cells were seeded in a 6-well plate and transfected as described above, but were not infected. Samples were collected at 48 hpt and protein expression assessed by western blot as previously described.

8.2.3 Western blot

Protein samples of 20 µl (blue lysis buffer) were separated, transferred, and subsequently processed as described in Austin, *et al*[5]. Membranes were blocked and primary antibodies to Dicer, Drosha, DGCR8, Ago2, Exportin-5, TRBP, and VEEV

capsid were prepared in 3% bovine serum albumin (BSA) in PBST or 3% milk in PBST. β-actin conjugated with horseradish peroxidase was used as a loading control.

8.2.4 Cell viability

293-T cells were seeded in a 96-well plate and transfected without infection as described above. Samples were treated at 48 hpt using the CellTiter Glo reagent (Promega, catalog #7571) according to the manufacturer's instructions. Viability was determined via fluorescence as compared to the control sample, using a Beckman-Coulter DTX-800 Multimode Detector with Multimode Analysis Software platform.

8.2.5 Acriflavine treatment

Acriflavine (ACF) was obtained from Sigma Aldrich (catalog #8126) and a stock was prepared in DMSO. Final dilutions were performed in DMEM+++ to give the final concentrations of ACF as described below, in a maximum concentration of 0.5% DMSO. For drug treatment, cells were pre-treated with ACF of the appropriate concentrations or with a DMSO control for two hours. Cells were infected at MOI=0.1 for one hour as previously described. Drug media was replaced following infection, and samples were collected at the indicated hpi. Protein expression was assessed by western blot, and replication was assessed by plaque assay.

8.3 Results

8.3.1 RNAi machinery levels do not change after infection

To assess the interaction of VEEV with RNAi machinery, a series of infections were performed in BHK and in U87MG cells at MOI=5. Samples were collected at 4, 8,

and 16 hpi, and protein levels were assessed by western blot. Capsid protein was used as a measure of viral protein production, and actin was used as a loading control. The results showed no overt change in levels of RNAi machinery between Mock and VEEV-infected samples, either in BHK (Figure 20A) or U87MG (Figure 20B) at any given timepoint. Capsid expression showed a time-dependent increase in BHK cells, but was largely absent until 16 hpi in U87MG cells. The similar results in two cell types (kidney and astrocyte) of two species (hamster and human) indicate that overall, VEEV infection does not significantly change levels of these proteins.

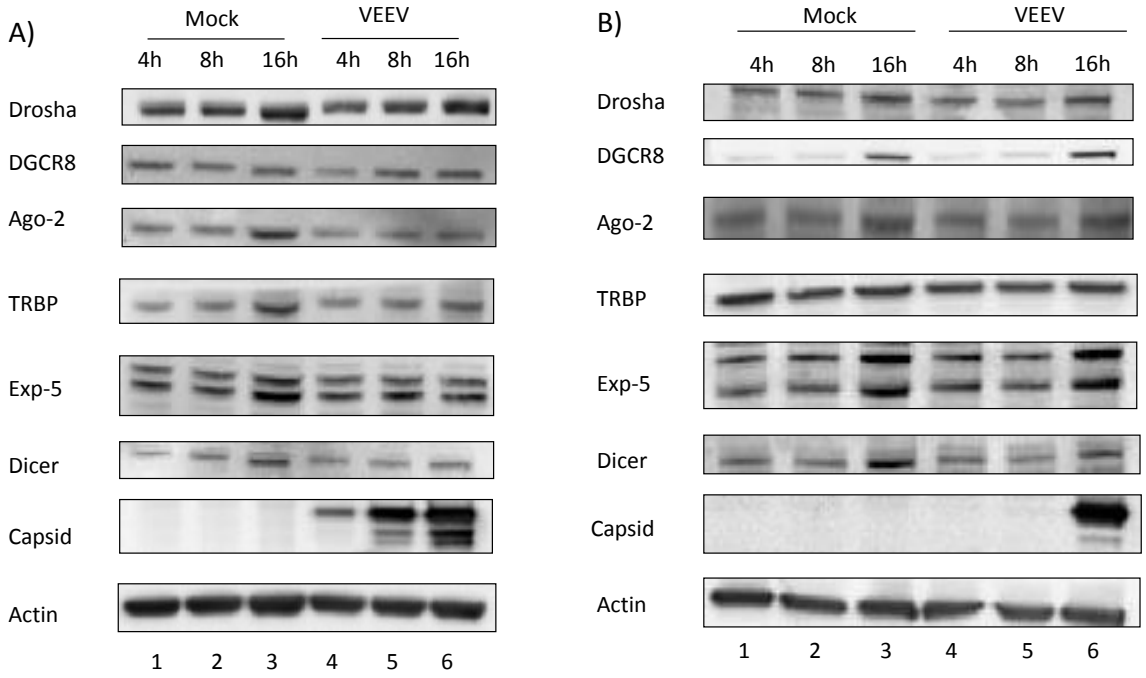

Figure 20: Levels of RNAi machinery do not change in VEEV infection.
BHK cells (Panel A) or U87MG cells (Panel B) were infected with VEEV at MOI=5 and collected at various timepoints. Protein expression was assessed by Western blot, with actin as a loading control.

8.3.2 RNAi machinery allows more efficient replication of VEEV.

To investigate the requirement for miRNA machinery in VEEV replication, cultures of 293T cells were transfected with 100 nM of specific siRNA against the major miRNA processing enzymes (Drosha, DGCR8, Exportin-5, Dicer, Ago-2, TRBP, or PIWIL4) or against a luciferase control, then subsequently infected with VEEV TC-83 at MOI=0.1. Viral supernatants were collected 24 hours post infection and viral replication was determined by plaque assay.

Knockdown of cytoplasmic components Dicer or PIWIL4 produced no significant decrease in viral replication, whereas knockdown of transport protein Exportin-5 produced a decrease of approximately 1.5 $\log_{10}$ compared to the siLuc control (Fig. 21A). Knockdown of cytoplasmic component TRBP produced a decrease of approximately 1 $\log_{10}$ compared to siLuc control (Figure 21B). Knockdown of Ago-2, an important component in binding of the small RNA to the RISC, resulted in approximately 1.5 $\log_{10}$ decrease (Figure 21B). In contrast, knockdown of Drosha produced decreases of approximately 2 $\log_{10}$ respectively (Figure 21B). As previously described, Drosha is the enzyme responsible for trimming the pre-miRNA hairpin from the primary transcript and works together with DGCR8 to form the microprocessor complex.

Western blot analysis indicated that the siRNA knockdown reduced protein levels by 40-75% depending on the siRNA (Figure 21C). Results of these knockdowns, together with those of Ago-2 and Exp-5, strongly imply that some level of miRNA processing is required for full VEEV replication. The results of the Dicer, TRBP, and PIWIL4 knockdowns indicate that such miRNA production is Dicer-independent, and

suggest a redundant system of cytoplasmic processing in which components are able to compensate for one another with little to no loss of viral replicative ability.

To ensure that results were due to direct effect on viral replication and not a function of reduced cell viability, siRNA transfected cells were assessed for changes in cell viability by the Celltiter Glo assay (Figure 21D). In all cases, the average viability following siRNA transfection was at least 90% of the siLuc value, indicating that the effects were not due to reduced cell viability.

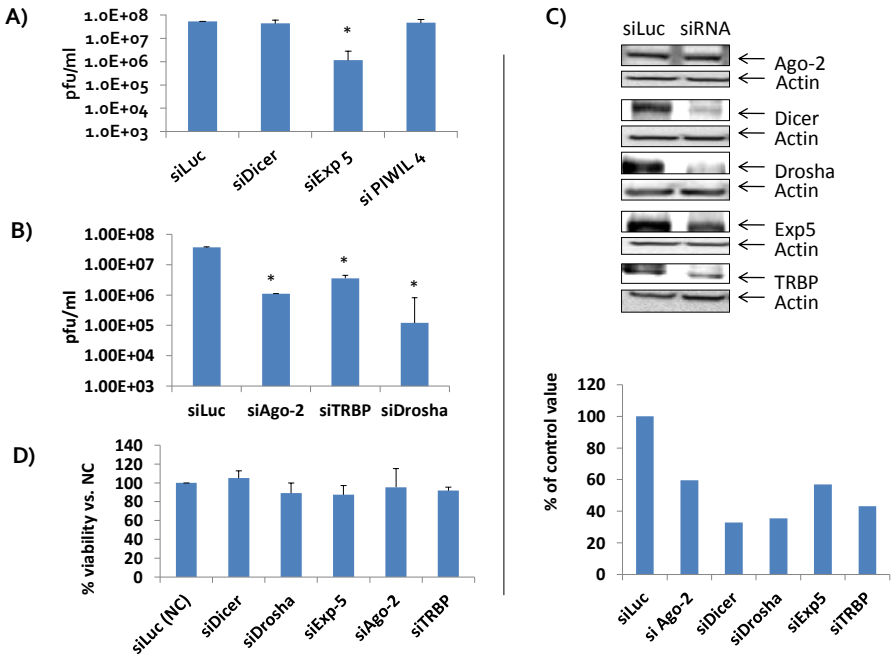

Figure 21: RNAi machinery allows more efficient replication of VEEV.
Panels A and B: Cultures of 293-T cells were infected with VEEV at MOI=0.1 in the presence of NC siRNA or siRNA targeting RNAi pathway components. Statistically significant decrease in replication was observed with knockdown of Exp-5, Drosha, or Ago2, but not other components. Panel C: Western blot confirms knockdown of components in uninfected 293-T cells; top panel shows the band intensities vs. β-actin and bottom panel shows quantitation of intensities relative to the NC value. Panel D: Luminescence assay of uninfected 293-T cells shows no significant difference between treatment with NC siRNA or siRNA targeting the RNAi pathway.

8.3.3 Inhibition of Ago2 decreases VEEV replication

Following the results above, Ago2 was chosen as the target of further investigation, as both Ago2 null cells and Ago2 inhibitors were readily available from other suppliers. To begin the investigation, wild-type (WT) or Ago2$^{-/-}$ MEFs were infected with VEEV at MOI=0.1. Viral supernatants were collected at 24 hpi to determine replication by plaque assay, and protein samples were collected at 8 and 16 hpi to determine protein expression by western blot. As shown in Figure 22A, lack of Ago2 decreased viral replication by approximately 2 $\log_{10}$ vs. WT values. Capsid expression was also decreased, to approximately 26% of WT value at 16 hpi and approximately 77% of WT value at 24 hpi (Figure 22B). These results supported the previous findings that replication efficiency decreased in the absence of Ago2.

For the next step, several inhibitors of Ago2 and/or the RISC were screened for toxicity in U87MG cells and inhibition of VEEV (described in Madsen and Hooper, *et al*)[273]. The compound which showed the greatest inhibition was acriflavine (ACF), an antimicrobial chromophore widely used to treat both internal and external infections in the pre-antibiotic era, and still occasionally prescribed against trypanosomal infections[274]. To confirm this effect, differentiated AP-7 rat neuronal cells were pre-treated with ACF at 2.5 or 1.25 μM, or a DMSO control, for two hours prior to infection with VEEV at MOI=0.1. Following the infection, drug media was replaced on the cells and samples were collected at 24 hpi. Treatment with ACF caused a dramatic decrease in viral replication (Figure 22C), approximately 6 $\log_{10}$ reduction at 1.25 μM ACF compared to DMSO control. At 2.5 μM ACF, replication had decreased to the point that no detectable

plaques were visible. The IC_{50} value, or the point at which titers had decreased to 50% of control, was determined to be approximately 0.20 µM (Figure 22D). Taken together, this confirms the previous observations of Ago2 allowing more efficient VEEV replication, and supports the further investigation of ACF as a means of controlling replication in culture.

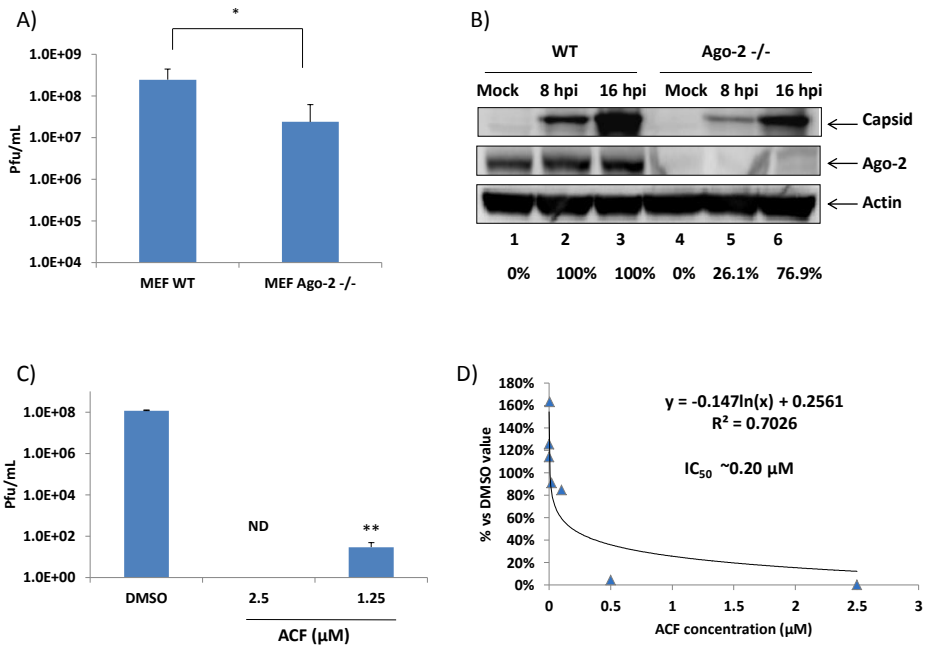

Figure 22: Inhibition of Ago2 decreases VEEV replication.
Panel A**:** WT and Ago2 -/- MEFs were infected at an MOI of 0.1 and supernatants collected at 24 hpi. Viral replication was assessed by plaque assay. *= p-value ≤0.05 (compared to WT VEEV infected cells). **Panel B:** WT and Ago2 -/- MEFs were mock-infected or infected with VEEV at an MOI of 0.1. Cells were harvested at 8 or 16 hours post infection and extracted proteins were assessed by Western Blot for the presence of VEEV capsid protein. Actin was used as a loading control. Values shown are percentage of normalized band intensity compared to WT at the same time point. Results shown are representative of two independent experiments. Panel C: Differentiated AP-7 rat neurons were pre-treated with ACF at 1.25 or 2.5 µM for 2 hours, infected with VEEV TC-83 (MOI 5), and then post-treated. Viral supernatants were collected 72 hours post-infection and analyzed by plaque assay. **=p-value ≤0.001 (compared to DMSO treated VEEV infected cells). ND=none detected (limit of detection was 10 pfu/ml). Panel D: U87MG cells were pre- and post-treated as described above, with DMSO control or with serial dilutions of ACF, and infected as described above. Viral supernatants were collected at 24 hours post infection and titers determined by plaque assay. IC_{50} was interpolated from the resulting graph to determine the concentration at which ACF induced 50% reduction of plaques compared to DMSO control. Images taken from Madsen and Hooper, *et al*, 2014[273].
.

8.3.4 Ago2 inhibitor ACF decreases replication of Alphavirus strains in culture

While ACF dramatically decreased replication of the TC-83 strain of VEEV in culture, its effects against the fully-virulent strains remained to be determined. To assess this, Vero cells were pre- and post-treated with ACF at 2.5 µM, 1.25 µM, or DMSO control as described previously, infected with VEEV-TrD at an MOI of 0.1 for one hour, and inhibition assessed by plaque assay. ACF treatment at 1.25 µM resulted in approximately 1.5- $\log_{10}$ reduction in VEEV-TrD titers at 8 hpi, and approximately 1- $\log_{10}$ reductions at 18 and 24 hpi, compared to DMSO alone. Treatment at 2.5 µM resulted in an approximately 4- $\log_{10}$ reduction compared to DMSO, consistent with the TC-83 data (Figure 23A). The responses of two additional fully-virulent VEEV strains, Mena II (Mena) and 3880, were also compared to ACF at 2.5 µM, with MOI of 0.1 in Vero cells and at a single 18-hr timepoint (Figure 23B). ACF-induced inhibition at the 18-hour timepoint was similar across all strains, approximately 4- 4.5- $\log_{10}$ compared to the DMSO control, again consistent with previous results in TrD and in TC-83.

To determine the effect of ACF against other encephalitic Alphaviruses, replication of Eastern and Western equine encephalitis viruses (EEEV and WEEV) were also measured in the presence of ACF (Figure 23C-D). Of the two, EEEV exhibited a greater sensitivity to ACF at 8 hpi, in that EEEV titers were below the level of detection in the presence of 2.5 µM ACF (Figure 23C). EEEV titers were also reduced at later time points, with the level of reduction being similar to that observed for VEEV-TrD. By comparison, WEEV showed slightly less sensitivity to ACF, with a decrease of 2- 3- $\log_{10}$ at the 2.5 µM concentration for each time point (Figure 23D). Taken together, these

findings demonstrate that ACF affects pathways which are required for optimal viral replication in encephalitic Alphaviruses, and suggests that Ago2 plays a role in these pathways.

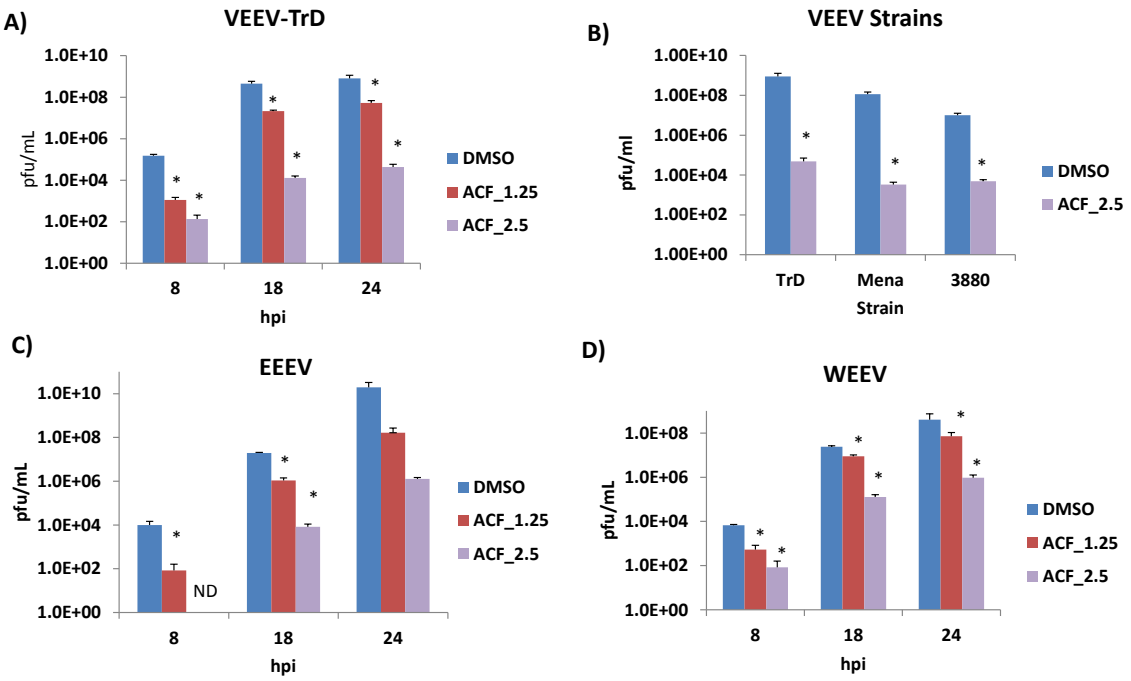

Figure 23: Ago2 inhibitor ACF inhibits Alphavirus strains in culture.
Vero cells were pre/post-treated with ACF or PLL (2.5 µM for each) or a DMSO control prior to infection with VEEV TR-D (Panel A), fully-virulent strains TrD, Mena, or 3880 (Panel B), or EEEV (Panel C), or WEEV (Panel D) at an MOI of 0.1 for 1 hour. Supernatants were collected at 8, 18 and 24 hours post infection for TC-83, and at 18 hours post infection for other viruses. Plaque assays were used to determine viral titer. *= p-value ≤0.05 (compared to DMSO treated infected cells at the corresponding time point). ND=none detected (limit of detection was 10 pfu/ml). Image from Madsen and Hooper, *et al* (2014) [273].

8.4 Conclusions

The two hypotheses predicted that a disruption of the miRNA pathway could inhibit VEEV replication in culture, and that similar inhibition would be seen in fully-virulent strains of VEEV and related Alphaviruses. The experimental data strongly

supported these hypotheses. While VEEV infection did not significantly change the expression of miRNA machinery components, targeted knockdown of Drosha, Exp-5, or Ago2 significantly inhibited replication. Confirmatory experiments in Ago2 null cells further supported this conclusion. The Ago2 inhibitor ACF, shown by Madsen and Hooper, *et al* to cause significant decreases in replication[273], was demonstrated to be similarly effective against three virulent strains of VEEV as well as related Alphaviruses EEEV and WEEV. Taken together, this indicates that VEEV and other New World Alphaviruses require an intact miRNA pathway for efficient replication, and supports the idea of pathway inhibitors as novel therapeutic drugs, though further research will be necessary to identify and screen additional drug candidates.

CHAPTER 9: DISCUSSION

miRNA regulation has traditionally been studied in cellular and biological processes, beginning with the discovery of its role in mediating developmental timing in *C. elegans*[225] and continuing through multiple investigations in higher-order eukaryotes, specifically in the area of cancer research. Its role in host-pathogen response was initially described in plants[275], though studies have not so far supported an equivalent antiviral role for miRNA in mammals[276]. Despite the lack of evidence for direct targeting, the differential regulation of miRNA during viral infections is well-established, mainly in viruses which maintain latency, such as HIV, KSHV, and the herpesviruses. HCV is also of particular interest in this context, as it not only induces upregulation of miR-122, but depends on this miRNA for efficient replication, raising the possibility that other viruses could be similarly dependent on host miRNA. miRNA regulation is also becoming increasingly well-studied in acute viral infections, and therefore it was hypothesized that this type of regulation would be a significant factor in the pathogenicity of RVFV and VEEV.

Initial analysis presents a strong case for regulation of RVFV pathogenic processes, and/or host response, by differential expression of miRNAs. A substantial subset of miRNAs were up- or down-regulated at each timepoint in infected vs. mock samples, and the pattern of regulation suggests a host-controlled early response at 6 hpi,

followed by a virally-controlled response at 24 hpi. Despite significant CPE observed at 48 hpi, this timepoint showed the greatest number of miRNAs both up- and down-regulated, and the set includes many of the same miRNAs which are highly regulated in the same direction at 24 hpi. qRT-PCR analysis of selected miRNAs largely confirms the regulation observed in microarray at both early and late timepoints. These miRNAs were predicted to target genes in several significant pathways associated with major factors of RVFV infection, including apoptosis, control of cell cycle, embryonic development, and cytokine signaling. Taken together, this supports the initial hypothesis of miRNA regulation as a sustained response to RVFV infection and as a significant factor of host-pathogen interaction.

However, preliminary pathway analysis reveals several complicating factors. First, within each pathway, regulation appears to be indirect, with less-highly regulated miRNAs targeting multiple secondary nodes, rather than direct targeting of the primary gene (e.g. IL-6). Additionally, many pathways are targeted by both up- and down-regulated miRNAs at the same timepoint, making it extremely difficult to predict the overall regulation of the pathway from the miRNA data alone. In a similar manner, a single miRNA is capable of targeting several hundred mRNAs, potentially including those with opposite functions, as was recently described for control of apoptosis by miR-630 targeting of multiple regulatory molecules[277]. With thousands of gene interactions predicted for each subset of miRNAs (e.g. 6 hpi up-regulated), the identification of relevant molecules, and the subsequent proposal of a specific mechanism, becomes challenging.

An additional factor, although not addressed by pathway analysis, is the potential for NSs-induced regulation of both miRNAs and target molecules. NSs is known to induce global downregulation of transcription through control of TFIIH[52], which would logically include downregulation of miRNAs. Additionally, as discussed in Chapter 3, NSs has been shown to interact directly with genes associated with major factors of RVFV pathogenesis, including regulators of developmental processes, neuronal functions, and inflammatory response[53], all factors identified as significant pathways targeted by miRNAs. This strongly suggests a potential interplay between NSs and miRNAs for control of host responses.

To narrow the focus of investigation, a literature and database search was conducted to identify potential mechanisms of regulation involving miRNAs, the specific roles of highly regulated miRNAs, and the potential role of NSs in these processes. This search revealed two major areas for future study: the targeting of anti-apoptotic IGF1R by miR-630 and miR-99a, and the potential for NSs-induced suppression of the miR-17-92 cluster.

IGF1R, the insulin-like growth factor 1 receptor, is associated with the insulin signaling pathway and is well-studied for its roles in mediation of cancer and apoptosis. It normally exerts an anti-apoptotic function, and decrease of IGF1R levels has been experimentally associated with upregulation of the apoptosis pathway, specifically in the decreased phosphorylation of mTOR and AKT and increase in Bax expression and caspase-3 cleavage[278]. This activity is consistent with the upregulation of the p53-

dependent apoptosis pathway in RVFV infection as previously described by this research group[5].

IGF1R is a published target of miR-630 and miR-99a, two of the highly up-regulated miRNAs at 24 hpi in microarray. Consistent with canonical regulation by miRNA, IGF1R is significantly down-regulated in RVFV infection in a time-dependent manner, and co-transfection with inhibitors of miR-630 and miR-99a induces a moderate rescue effect. Co-transfection also has the ability to inhibit RVFV replication by approximately 30% vs. transfection with a negative control. Taken together, this suggests a mechanism by which RVFV induces apoptosis through upregulation of miR-630 and miR-99a, leading to downregulation of IGF1R and ultimately to cleavage of caspase-3.

However, the inability of the miRNA inhibitors to induce a greater level of rescue suggests that IGF1R is inhibited by another factor. While NSs is the most logical candidate for transcriptional repression, it is also possible that RNA and/or protein are being degraded. Further investigations, such as the pulse-chase, ubiquitination, and ribosomal binding assays mentioned earlier, will be needed to confirm this.

In contrast to miR-630 and miR-99a, the miR-17-92 cluster is significantly down-regulated in RVFV infection. This cluster is transcribed from a common promoter on Chromosome 13, and is collectively considered to be an oncomir for its ability to induce cell proliferation; i.e. to decrease apoptosis. As such, its down-regulation during RVFV infection is entirely consistent with its published action. Notably for the context of RVFV infection, deletion of miR-17-92 is embryonic lethal in a mouse model[239]. Additionally, the miR-17-92 cluster is known to be suppressed by p53[257], which in turn is

known to be up-regulated in RVFV through the action of NSs[5]. This suggests a mechanism by which NSs induces apoptosis—and potential embryonic lethality—through repression of the miRNA predicted to target BIM and other pro-apoptotic factors. It also suggests that overexpression of miR-17-92 could reverse these effects and potentially decrease viral replication. However, experimental results did not fully support this hypothesis.

In this study, overexpression of individual miR-17-92 cluster members did not inhibit RVFV replication. However, transfection with a plasmid encoding miR-17-92 was able to reduce viral genomic expression as measured by qRT-PCR, and replication as measured by plaque assay, at 16 hpi. As previously mentioned, this strongly suggests that multiple miRNA act in concert to mitigate the effects of RVFV.

The regulation of miR-17-92 was shown to be NSs dependent, consistent with the hypothesis and with its published suppression by p53. Notably, the down-regulation of cluster members varied as a function of their respective distances from the promoter, suggesting a potential arrest or interruption of the elongation process as described in section 6.3.1. However, miR-17-92 cluster target genes, including BIM, BCL11B, BMPR2, and CCND1, were either not significantly changed or were down-regulated in RVFV infection, which is not consistent with regulation by miRNA. Studies using mutant virus in Vero cells showed that expression of these targets was also NSs dependent. While this is consistent with the role of NSs as a transcriptional repressor, it does not support the idea of apoptosis (or embryonic lethality) mediated by upregulation of BIM through p53-induced suppression of miR-17-92.

Taken together, this demonstrates the interplay between NSs and miR-17-92 as significant factor of RVFV pathogenesis, though it remains to link decrease in replication to the action of specific target genes. Given the thousands of target genes predicted for each cluster member, the ability of those genes to promote or inhibit one another, and the overall suppressive effects of NSs, this area remains ripe for further research. Two future directions, as previously discussed, are the role of p53 in this process and the potentially NSs-induced suppression of transcriptional elongation.

In contrast to the investigation in RVFV, investigation into VEEV revealed notable interaction between VEEV and host RNAi machinery, supporting the notion of miRNA regulation as an important factor for viral replication. Targeted knockdown of pathway components Drosha, Exp5, TRBP, and Ago2 induced significant decrease in VEEV replication. Consistently with these results, Ago2$^{-/-}$ cells induced a decrease of approximately 2 $\log_{10}$ vs. wild-type cells. Ago2 inhibitor ACF produced even more dramatic results, in which treatment with 2.5 µM ACF reduced replication to below the point of detectability, and treatment with 1.25 µM ACF induced a decrease of approximately 6 $\log_{10}$ compared to a DMSO control. Similar results were observed with ACF treatment of virulent strains TrD, Mena II, and 3880, as well as related Alphaviruses EEEV and WEEV. Taken together, this indicates both that Ago2 is required for efficient replication as previously stated, and that ACF acts against a pathway which is conserved at least among New World Alphaviruses.

However, the difference in reduction between the Ago2 deficient cells (null and knockdown) and the ACF model suggests that inhibition of Ago2 is not the only means

by which ACF inhibits replication. ACF is known to have pleiotropic effects, including inhibition of protein kinase C[279], inhibition of HIF dimerization[280], and breakage of single-stranded DNA[281]. However, none of these are published factors of VEEV pathogenesis. Additionally, treatment with ACF in the absence of cells does not induce a virucidal effect[273]. Therefore, although the inhibition of Ago2 contributes significantly to the decrease in VEEV replication, the exact mechanism and the identity of other potentiating factors remain to be determined.

As reviewed by Wainwright[274], the half-life of ACF in the bloodstream is reportedly less than 5 minutes, which could pose a problem for *in vivo* therapeutic usage. However, the significant effects against New World Alphaviruses in culture suggest it as a starting point for the development of more effective therapies.

The reduced replication observed following RNAi machinery knockdown also raises the possibility of VEEV and other Alphaviruses using miRNA to enhance replication, similarly to the means used by HCV. In this well-studied example, association with liver-specific miR-122 induces a closer association between the host ribosome and the viral IRES, enhancing translation of viral proteins[174, 207, 208]. Current treatments for HCV include such compounds as ribavirin and pegylated interferon-α, which carry significant risks and are frequently ineffective at clearing the virus[282]. Inhibition of miR-122, as by the novel drug candidate miravirsen, shows promise as a therapeutic in the treatment of HCV[283] and suggests that other therapies targeted against miRNA or machinery may be effective in the treatment of Alphaviruses as well.

Taken together, this study strengthens the case for miRNA involvement in multiple types of viral infections, specifically for the dependence of two distinct categories of Arbovirus on the host miRNA pathway. In the case of RVFV, multiple dysregulated miRNA were identified and linked to pathways related to known pathogenic processes. Several miRNA, including miR-99a and the miR-17-92 cluster, showed the ability to reduce viral replication when inhibited or overexpressed. However, the challenge posed by "many to many" association of miRNA and mRNA, as well as the involvement of NSs, suggests that miRNA regulation serves to fine-tune RVFV replication through indirect effects, likely against multiple host pathways.

In contrast to the findings in RVFV, findings in VEEV conclusively demonstrated that viral replication depends on an intact host miRNA pathway for maximum efficiency, and suggests that the relevant mechanism is conserved among New-world Alphaviruses. Taken together, these findings suggest that the miRNA pathway is being actively used by the virus for direct control of replication, although the specific mechanism is yet to be determined.

While further studies are needed in both virus types before conclusively linking miRNA regulation to a potential therapy, this research has strengthened the case for continued investigation of miRNA regulation in acute viral infections, an area which remains understudied.

REFERENCES

1. Fernandez, J.-C. *et al.* The Nonstructural Protein NSs Induces a Variable Antibody Response in Domestic Ruminants Naturally Infected with Rift Valley Fever Virus. *Clin. Vaccine Immunol. CVI* **19,** 5–10 (2012).

2. Baer, A. *et al.* Induction of DNA Damage Signaling upon Rift Valley Fever Virus Infection Results in Cell Cycle Arrest and Increased Viral Replication. *J. Biol. Chem.* **287,** 7399–7410 (2012).

3. Bhomia, M. *et al.* Analysis of microRNAs induced by Venezuelan equine encephalitis virus infection in mouse brain. *Biochem. Biophys. Res. Commun.* **395,** 11–16 (2010).

4. Bird, B. H. *et al.* Rift Valley Fever Virus Vaccine Lacking the NSs and NSm Genes Is Safe, Nonteratogenic, and Confers Protection from Viremia, Pyrexia, and Abortion following Challenge in Adult and Pregnant Sheep. *J. Virol.* **85,** 12901–12909 (2011).

5. Austin, D. *et al.* p53 Activation following Rift Valley Fever Virus Infection Contributes to Cell Death and Viral Production. *PLoS ONE* **7,** (2012).

6. Food and Agriculture Organization of the United Nations. Rift Valley Fever Manual. at <http://www.fao.org/ag/againfo/resources/documents/AH/RVF198.htm>

7. Daubney, R., Hudson, J. R. & Garnham, P. C. Enzootic hepatitis or rift valley fever. An undescribed virus disease of sheep cattle and man from east africa. *J. Pathol. Bacteriol.* **34,** 545–579 (1931).

8. Centers for Disease Control and Prevention. Rift Valley Fever Virus Fact Sheet. at <http://www.cdc.gov/ncidod/dvrd/spb/mnpages/dispages/Fact_Sheets/Rift_Valley_Fever_Fact_Sheet.pdf>

9. Centers for Disease Control and Prevention. Rift Valley Fever Outbreak --- Kenya, November 2006--January 2007. at <http://www.cdc.gov/mmwr/preview/mmwrhtml/mm5604a3.htm>

10. Balenghien, T. *et al.* Towards a better understanding of Rift Valley fever epidemiology in the south-west of the Indian Ocean. *Vet. Res.* **44,** 78 (2013).

11. Meegan, J. M., Hoogstraal, H. & Moussa, M. I. An epizootic of Rift Valley fever in Egypt in 1977. *Vet. Rec.* **105,** 124–125 (1979).

12. Mathiot, C., Ribot, J. J., Clerc, Y., Coulanges, P. & Rasolofonirina, N. [Rift valley fever and Zinga virus: a pathogenic arbovirus in man and animal new for Madagascar]. *Arch. Inst. Pasteur Madagascar* **51,** 125–133 (1984).

13. Davies, F. G. Rift Valley fever in the Sudan. *Trans. R. Soc. Trop. Med. Hyg.* **84,** 141 (1990).

14. Centers for Disease Control and Prevention. Outbreak of Rift Valley Fever --- Saudi Arabia, August--October, 2000. at <http://www.cdc.gov/mmwr/preview/mmwrhtml/mm4940a1.htm>

15. Sánchez-Vizcaíno, F., Martínez-López, B. & Sánchez-Vizcaíno, J. M. Identification of suitable areas for the occurrence of Rift Valley fever outbreaks in Spain using a multiple criteria decision framework. *Vet. Microbiol.* **165,** 71–78 (2013).

16. James Martin Center for Nonproliferation Studies. CNS - Chemical and Biological Weapons: Possession and Programs Past and Present. at <http://cns.miis.edu/cbw/possess.htm>

17. DSAT_brochure_July2011.pdf. at <http://www.cdc.gov/phpr/documents/DSAT_brochure_July2011.pdf>

18. Federal Select Agent Program. Select Agents and Toxins List. at <http://www.selectagents.gov/Select%20Agents%20and%20Toxins%20List.html>

19. Pendell, D., Lusk JL, Marsh TL, Coble KH & Szmania SC. Economic Assessment of Zoonotic Disease... [Transbound Emerg Dis. 2014] - PubMed - NCBI. at <http://www.ncbi.nlm.nih.gov/pubmed/25052324>

20. Bouloy, M. & Weber, F. Molecular Biology of Rift Valley Fever Virus. *Open Virol. J.* **4,** 8–14 (2010).

21. Ellis, D. S., Simpson, D. I. H., Stamford, S. & Wahab, K. S. E. A. Rift Valley Fever Virus: Some Ultrastructural Observations on Material from the Outbreak in Egypt 1977. *J. Gen. Virol.* **42,** 329–337 (1979).

22. Sherman, M. B., Freiberg, A. N., Holbrook, M. R. & Watowich, S. J. Single-particle cryo-electron microscopy of Rift Valley fever virus. *Virology* **387,** 11–15 (2009).

23. Zamoto-Niikura, A., Terasaki, K., Ikegami, T., Peters, C. J. & Makino, S. Rift Valley Fever Virus L Protein Forms a Biologically Active Oligomer. *J. Virol.* **83,** 12779–12789 (2009).

24. Ikegami, T. Molecular biology and genetic diversity of Rift Valley fever virus. *Antiviral Res.* **95,** 293–310 (2012).

25. Brennan, B., Li, P. & Elliott, R. M. Generation and characterization of a recombinant Rift Valley fever virus expressing a V5 epitope-tagged RNA-dependent RNA polymerase. *J. Gen. Virol.* **92,** 2906–2913 (2011).

26. Lopez, N., Muller, R., Prehaud, C. & Bouloy, M. The L protein of Rift Valley fever virus can rescue viral ribonucleoproteins and transcribe synthetic genome-like RNA molecules. *J. Virol.* **69,** 3972–3979 (1995).

27. Reguera, J., Weber, F. & Cusack, S. Bunyaviridae RNA Polymerases (L-Protein) Have an N-Terminal, Influenza-Like Endonuclease Domain, Essential for Viral Cap-Dependent Transcription. *PLoS Pathog* **6,** e1001101 (2010).

28. Ferron, F. *et al.* The Hexamer Structure of the Rift Valley Fever Virus Nucleoprotein Suggests a Mechanism for its Assembly into Ribonucleoprotein Complexes. *PLoS Pathog* **7,** e1002030 (2011).

29. Carnec, X., Ermonval, M., Kreher, F., Flamand, M. & Bouloy, M. Role of the cytosolic tails of Rift Valley fever virus envelope glycoproteins in viral morphogenesis. *Virology* **448,** 1–14 (2014).

30. Rusu, M. *et al.* An Assembly Model of Rift Valley Fever Virus. *Front. Microbiol.* **3,** (2012).

31. Huiskonen, J. T., Överby, A. K., Weber, F. & Grünewald, K. Electron Cryo-Microscopy and Single-Particle Averaging of Rift Valley Fever Virus: Evidence for GN-GC Glycoprotein Heterodimers. *J. Virol.* **83,** 3762–3769 (2009).

32. Gerrard, S. R. & Nichol, S. T. Characterization of the Golgi Retention Motif of Rift Valley Fever Virus GN Glycoprotein. *J. Virol.* **76,** 12200–12210 (2002).

33. Overby, A. K., Pettersson, R. F. & Neve, E. P. A. The Glycoprotein Cytoplasmic Tail of Uukuniemi Virus (Bunyaviridae) Interacts with Ribonucleoproteins and Is Critical for Genome Packaging. *J. Virol.* **81,** 3198–3205 (2007).

34. Shi, X., Kohl, A., Li, P. & Elliott, R. M. Role of the Cytoplasmic Tail Domains of Bunyamwera Orthobunyavirus Glycoproteins Gn and Gc in Virus Assembly and

Morphogenesis. *J. Virol.* **81,** 10151–10160 (2007).

35. Won, S., Ikegami, T., Peters, C. J. & Makino, S. NSm and 78-Kilodalton Proteins of Rift Valley Fever Virus Are Nonessential for Viral Replication in Cell Culture. *J. Virol.* **80,** 8274–8278 (2006).

36. Kading, R. C. *et al.* Deletion of the NSm Virulence Gene of Rift Valley Fever Virus Inhibits Virus Replication in and Dissemination from the Midgut of Aedes aegypti Mosquitoes. *PLoS Negl. Trop. Dis.* **8,** (2014).

37. Weingartl, H. M. *et al.* Rift Valley Fever Virus Incorporates the 78 kDa Glycoprotein into Virions Matured in Mosquito C6/36 Cells. *PLoS ONE* **9,** (2014).

38. Gerrard, S. R., Bird, B. H., Albarino, C. G. & Nichol, S. T. The NSm proteins of Rift Valley fever virus are dispensable for maturation, replication and infection. *Virology* **359,** 459–465 (2007).

39. Won, S., Ikegami, T., Peters, C. J. & Makino, S. NSm Protein of Rift Valley Fever Virus Suppresses Virus-Induced Apoptosis. *J. Virol.* **81,** 13335–13345 (2007).

40. Terasaki, K., Won, S. & Makino, S. The C-Terminal Region of Rift Valley Fever Virus NSm Protein Targets the Protein to the Mitochondrial Outer Membrane and Exerts Antiapoptotic Function. *J. Virol.* **87,** 676–682 (2013).

41. Narayanan, A. *et al.* Alteration in Superoxide Dismutase 1 Causes Oxidative Stress and p38 MAPK Activation Following RVFV Infection. *PLoS ONE* **6,** (2011).

42. Crabtree, M. B. *et al.* Infection and Transmission of Rift Valley Fever Viruses Lacking the NSs and/or NSm Genes in Mosquitoes: Potential Role for NSm in Mosquito Infection. *PLoS Negl. Trop. Dis.* **6,** (2012).

43. Raymond, D. D., Piper, M. E., Gerrard, S. R. & Smith, J. L. Structure of the Rift Valley fever virus nucleocapsid protein reveals another architecture for RNA encapsidation. *Proc. Natl. Acad. Sci. U. S. A.* **107,** 11769–11774 (2010).

44. Le May, N., Gauliard, N., Billecocq, A. & Bouloy, M. The N Terminus of Rift Valley Fever Virus Nucleoprotein Is Essential for Dimerization. *J. Virol.* **79,** 11974–11980 (2005).

45. Olal, D. *et al.* Structural insights into RNA encapsidation and helical assembly of the Toscana virus nucleoprotein. *Nucleic Acids Res.* **42,** 6025–6037 (2014).

46. Ikegami, T., Won, S., Peters, C. J. & Makino, S. Rift Valley Fever Virus NSs mRNA Is Transcribed from an Incoming Anti-Viral-Sense S RNA Segment. *J. Virol.*

79, 12106–12111 (2005).

47. Habjan, M. *et al.* NSs Protein of Rift Valley Fever Virus Induces the Specific Degradation of the Double-Stranded RNA-Dependent Protein Kinase. *J. Virol.* **83,** 4365–4375 (2009).

48. Ikegami, T., Won, S., Peters, C. J. & Makino, S. Rescue of Infectious Rift Valley Fever Virus Entirely from cDNA, Analysis of Virus Lacking the NSs Gene, and Expression of a Foreign Gene. *J. Virol.* **80,** 2933–2940 (2006).

49. Mansuroglu, Z. *et al.* Nonstructural NSs Protein of Rift Valley Fever Virus Interacts with Pericentromeric DNA Sequences of the Host Cell, Inducing Chromosome Cohesion and Segregation Defects. *J. Virol.* **84,** 928–939 (2010).

50. Le May, N. *et al.* A SAP30 Complex Inhibits IFN-? Expression in Rift Valley Fever Virus Infected Cells. *PLoS Pathog.* **4,** (2008).

51. Ikegami, T. *et al.* Dual Functions of Rift Valley Fever Virus NSs Protein: Inhibition of Host mRNA Transcription and Post-transcriptional Downregulation of Protein Kinase PKR. *Ann. N. Y. Acad. Sci.* **1171,** E75–E85 (2009).

52. Kainulainen, M. *et al.* Virulence Factor NSs of Rift Valley Fever Virus Recruits the F-Box Protein FBXO3 To Degrade Subunit p62 of General Transcription Factor TFIIH. *J. Virol.* **88,** 3464–3473 (2014).

53. Benferhat, R. *et al.* Large-Scale Chromatin Immunoprecipitation with Promoter Sequence Microarray Analysis of the Interaction of the NSs Protein of Rift Valley Fever Virus with Regulatory DNA Regions of the Host Genome. *J. Virol.* **86,** 11333–11344 (2012).

54. García, M. A., Meurs, E. F. & Esteban, M. The dsRNA protein kinase PKR: Virus and cell control. *Biochimie* **89,** 799–811 (2007).

55. Copeland, A. M., Altamura, L. A., Van Deusen, N. M. & Schmaljohn, C. S. Nuclear Relocalization of Polyadenylate Binding Protein during Rift Valley Fever Virus Infection Involves Expression of the NSs Gene. *J. Virol.* **87,** 11659–11669 (2013).

56. Lozach, P.-Y. *et al.* DC-SIGN as a Receptor for Phleboviruses. *Cell Host Microbe* **10,** 75–88 (2011).

57. Harmon, B. *et al.* Rift Valley Fever Virus Strain MP-12 Enters Mammalian Host Cells via Caveola-Mediated Endocytosis. *J. Virol.* **86,** 12954–12970 (2012).

58. de Boer, S. M. *et al.* Acid-activated structural reorganization of the Rift Valley fever virus Gc fusion protein. *J. Virol.* **86,** 13642–13652 (2012).

59. Ferron, F. *et al.* The Hexamer Structure of the Rift Valley Fever Virus Nucleoprotein Suggests a Mechanism for its Assembly into Ribonucleoprotein Complexes. *PLoS Pathog* **7,** e1002030 (2011).

60. Pepin, M., Bouloy, M., Bird, B. H., Kemp, A. & Paweska, J. Rift Valley fever virus (Bunyaviridae: Phlebovirus): an update on pathogenesis, molecular epidemiology, vectors, diagnostics and prevention. *Vet. Res.* **41,** (2010).

61. Ellis, D. S., Shirodaria, P. V., Fleming, E. & Simpson, D. I. Morphology and development of Rift Valley fever virus in Vero cell cultures. *J. Med. Virol.* **24,** 161–174 (1988).

62. Benedict, A. *et al.* Repurposing FDA-approved drugs as therapeutics to treat Rift Valley fever virus infection. *Virology* **6,** 676 (2015).

63. Casals, J., Curnen, E. C. & Thomas, L. Venezuelan Equine Encephalomyelitis in Man. *J. Exp. Med.* **77,** 521–530 (1943).

64. Morrison, A. C. *et al.* Venezuelan Equine Encephalitis Virus in Iquitos, Peru: Urban Transmission of a Sylvatic Strain. *PLoS Negl Trop Dis* **2,** e349 (2008).

65. Taylor, K. G. & Paessler, S. Pathogenesis of Venezuelan equine encephalitis. *Vet. Microbiol.* **167,** 145–150 (2013).

66. Weaver, S. C. *et al.* Re-emergence of epidemic Venezuelan equine encephalomyelitis in South America. *The Lancet* **348,** 436–440 (1996).

67. Powers, A. M. *et al.* Repeated emergence of epidemic/epizootic Venezuelan equine encephalitis from a single genotype of enzootic subtype ID virus. *J. Virol.* **71,** 6697–6705 (1997).

68. Deardorff, E. R. & Weaver, S. C. Vector Competence of Culex (Melanoconion) taeniopus for Equine-Virulent Subtype IE Strains of Venezuelan Equine Encephalitis Virus. *Am. J. Trop. Med. Hyg.* **82,** 1047–1052 (2010).

69. Deardorff, E. R. *et al.* Experimental Infection of Potential Reservoir Hosts with Venezuelan Equine Encephalitis Virus, Mexico. *Emerg. Infect. Dis.* **15,** 519–525 (2009).

70. Aguilar, P. V. *et al.* Endemic Venezuelan equine encephalitis in the Americas: hidden under the dengue umbrella. *Future Virol.* **6,** 721–740 (2011).

71. Muñiz, A. E. Venezuelan equine encephalitis in a teenager visiting Central America. *Pediatr. Emerg. Care* **28,** 372–375 (2012).

72. Vilcarromero, S. *et al.* Venezuelan Equine Encephalitis and 2 Human Deaths, Peru. *Emerg. Infect. Dis.* **16,** 553–556 (2010).

73. Adams, A. P. *et al.* Venezuelan Equine Encephalitis Virus Activity in the Gulf Coast Region of Mexico, 2003-2010. *PLoS Negl. Trop. Dis.* **6,** (2012).

74. Steele, K. E. & Twenhafel, N. A. REVIEW PAPER Pathology of Animal Models of Alphavirus Encephalitis. *Vet. Pathol. Online* **47,** 790–805 (2010).

75. Rusnak, J. M. *et al.* Risk of Occupationally Acquired Illnesses from Biological Threat Agents in Unvaccinated Laboratory Workers. *Biosecurity Bioterrorism Biodefense Strategy Pract. Sci.* **2,** 281–293 (2004).

76. Atasheva, S. *et al.* Pseudoinfectious Venezuelan Equine Encephalitis Virus: a New Means of Alphavirus Attenuation. *J. Virol.* **87,** 2023–2035 (2013).

77. Alevizatos, A. C., McKinney, R. W. & Feigin, R. D. Live, Attenuated Venezuelan Equine Encephalomyelitis Virus Vaccine I. Clinical Effects in Man. *Am. J. Trop. Med. Hyg.* **16,** 762–768 (1967).

78. Carossino, M., Thiry, E., la Grandière, A. de & Barrandeguy, M. E. Novel vaccination approaches against equine alphavirus encephalitides. *Vaccine* **32,** 311–319 (2014).

79. Centers for Disease Control and Prevention. CDC | Bioterrorism Agents/Diseases (by Category) | Emergency Preparedness & Response. at <http://www.bt.cdc.gov/agent/agentlist-category.asp>

80. Foy, N. J. *et al.* Hypervariable Domains of nsP3 Proteins of New World and Old World Alphaviruses Mediate Formation of Distinct, Virus-Specific Protein Complexes. *J. Virol.* **87,** 1997–2010 (2013).

81. Her, Z., Kam, Y.-W., Lin, R. T. P. & Ng, L. F. P. Chikungunya: a bending reality. *Microbes Infect.* **11,** 1165–1176 (2009).

82. Tsetsarkin, K. A., Vanlandingham, D. L., McGee, C. E. & Higgs, S. A Single Mutation in Chikungunya Virus Affects Vector Specificity and Epidemic Potential.

PLoS Pathog **3,** e201 (2007).

83. Johansson, M. A., Powers, A. M., Pesik, N., Cohen, N. J. & Staples, J. E. Nowcasting the Spread of Chikungunya Virus in the Americas. *PLoS ONE* **9,** e104915 (2014).

84. Strauss, J. H. & Strauss, E. G. The alphaviruses: gene expression, replication, and evolution. *Microbiol. Rev.* **58,** 491–562 (1994).

85. Zhang, R. *et al.* 4.4 Å cryo-EM structure of an enveloped alphavirus Venezuelan equine encephalitis virus. *EMBO J.* **30,** 3854–3863 (2011).

86. Paredes, A., Alwell-Warda, K., Weaver, S. C., Chiu, W. & Watowich, S. J. Venezuelan Equine Encephalomyelitis Virus Structure and Its Divergence from Old World Alphaviruses. *J. Virol.* **75,** 9532–9537 (2001).

87. Jose, J., Snyder, J. E. & Kuhn, R. J. A structural and functional perspective of alphavirus replication and assembly. *Future Microbiol.* **4,** 837–856 (2009).

88. Snyder, J. E. *et al.* Functional Characterization of the Alphavirus TF Protein. *J. Virol.* **87,** 8511–8523 (2013).

89. Chung, D.-H. *et al.* Discovery of a Novel Compound with Anti-Venezuelan Equine Encephalitis Virus Activity That Targets the Nonstructural Protein 2. *PLoS Pathog.* **10,** (2014).

90. Ahola, T. *et al.* Effects of Palmitoylation of Replicase Protein nsP1 on Alphavirus Infection. *J. Virol.* **74,** 6725–6733 (2000).

91. Volkova, E., Gorchakov, R. & Frolov, I. The efficient packaging of Venezuelan equine encephalitis virus-specific RNAs into viral particles is determined by nsP1-3 synthesis. *Virology* **344,** 315–327 (2006).

92. Kinney, R. M., Johnson, B. J., Welch, J. B., Tsuchiya, K. R. & Trent, D. W. The full-length nucleotide sequences of the virulent Trinidad donkey strain of Venezuelan equine encephalitis virus and its attenuated vaccine derivative, strain TC-83. *Virology* **170,** 19–30 (1989).

93. Shin, G. *et al.* Structural and functional insights into alphavirus polyprotein processing and pathogenesis. *Proc. Natl. Acad. Sci. U. S. A.* **109,** 16534–16539 (2012).

94. Myles, K. M., Kelly, C. L. H., Ledermann, J. P. & Powers, A. M. Effects of an Opal Termination Codon Preceding the nsP4 Gene Sequence in the O'Nyong-Nyong

Virus Genome on Anopheles gambiae Infectivity. *J. Virol.* **80,** 4992–4997 (2006).

95. Zusinaite, E. *et al.* Mutations at the palmitoylation site of non-structural protein nsP1 of Semliki Forest virus attenuate virus replication and cause accumulation of compensatory mutations. *J. Gen. Virol.* **88,** 1977–1985 (2007).

96. Ahola, T. & Kaariainen, L. Reaction in alphavirus mRNA capping: formation of a covalent complex of nonstructural protein nsP1 with 7-methyl-GMP. *Proc. Natl. Acad. Sci. U. S. A.* **92,** 507–511 (1995).

97. Ahola, T., Laakkonen, P., Vihinen, H. & Kaariainen, L. Critical residues of Semliki Forest virus RNA capping enzyme involved in methyltransferase and guanylyltransferase-like activities. *J. Virol.* **71,** 392–397 (1997).

98. Sawicki, D. L., Perri, S., Polo, J. M. & Sawicki, S. G. Role for nsP2 Proteins in the Cessation of Alphavirus Minus-Strand Synthesis by Host Cells. *J. Virol.* **80,** 360–371 (2006).

99. Akhrymuk, I., Kulemzin, S. V. & Frolova, E. I. Evasion of the Innate Immune Response: the Old World Alphavirus nsP2 Protein Induces Rapid Degradation of Rpb1, a Catalytic Subunit of RNA Polymerase II. *J. Virol.* **86,** 7180–7191 (2012).

100. Garmashova, N. *et al.* The Old World and New World alphaviruses use different virus-specific proteins for induction of transcriptional shutoff. *J. Virol.* **81,** 2472–2484 (2007).

101. Lulla, V., Kim, D. Y., Frolova, E. I. & Frolov, I. The Amino-Terminal Domain of Alphavirus Capsid Protein Is Dispensable for Viral Particle Assembly but Regulates RNA Encapsidation through Cooperative Functions of Its Subdomains. *J. Virol.* **87,** 12003–12019 (2013).

102. Kim, D. Y., Atasheva, S., Frolova, E. I. & Frolov, I. Venezuelan Equine Encephalitis Virus nsP2 Protein Regulates Packaging of the Viral Genome into Infectious Virions. *J. Virol.* **87,** 4202–4213 (2013).

103. Bao, H. *et al.* Nonstructural protein 2 (nsP2) of Chikungunya virus (CHIKV) enhances protective immunity mediated by a CHIKV envelope protein expressing DNA Vaccine. *Viral Immunol.* **26,** 75–83 (2013).

104. LaStarza, M. W., Lemm, J. A. & Rice, C. M. Genetic analysis of the nsP3 region of Sindbis virus: evidence for roles in minus-strand and subgenomic RNA synthesis. *J. Virol.* **68,** 5781–5791 (1994).

105. De, I., Fata-Hartley, C., Sawicki, S. G. & Sawicki, D. L. Functional Analysis of nsP3 Phosphoprotein Mutants of Sindbis Virus. *J. Virol.* **77,** 13106–13116 (2003).

106. Malet, H. *et al.* The Crystal Structures of Chikungunya and Venezuelan Equine Encephalitis Virus nsP3 Macro Domains Define a Conserved Adenosine Binding Pocket. *J. Virol.* **83,** 6534–6545 (2009).

107. Rungrotmongkol, T. *et al.* Molecular insight into the specific binding of ADP-ribose to the nsP3 macro domains of chikungunya and venezuelan equine encephalitis viruses: Molecular dynamics simulations and free energy calculations. *J. Mol. Graph. Model.* **29,** 347–353 (2010).

108. Amaya, M. *et al.* The Role of IKK? in Venezuelan Equine Encephalitis Virus Infection. *PLoS ONE* **9,** (2014).

109. Shirako, Y., Strauss, E. G. & Strauss, J. H. Suppressor Mutations That Allow Sindbis Virus RNA Polymerase to Function with Nonaromatic Amino Acids at the N-Terminus: Evidence for Interaction between nsP1 and nsP4 in Minus-Strand RNA Synthesis. *Virology* **276,** 148–160 (2000).

110. Li, M.-L. & Stollar, V. Identification of the amino acid sequence in Sindbis virus nsP4 that binds to the promoter for the synthesis of the subgenomic RNA. *Proc. Natl. Acad. Sci. U. S. A.* **101,** 9429–9434 (2004).

111. Li, M.-L. & Stollar, V. Distinct Sites on the Sindbis Virus RNA-Dependent RNA Polymerase for Binding to the Promoters for the Synthesis of Genomic and Subgenomic RNA. *J. Virol.* **81,** 4371–4373 (2007).

112. Pisano, M. B. *et al.* Genetic and evolutionary characterization of Venezuelan equine encephalitis virus isolates from Argentina. *Infect. Genet. Evol.* **26,** 72–79 (2014).

113. Aggarwal, M., Dhindhwal, S., Kumar, P., Kuhn, R. J. & Tomar, S. Trans-protease activity and structural insights into the active form of the alphavirus capsid protease. *J. Virol.* JVI.01692–14 (2014). doi:10.1128/JVI.01692-14

114. Simmons, J. D. *et al.* Venezuelan Equine Encephalitis Virus Disrupts STAT1 Signaling by Distinct Mechanisms Independent of Host Shutoff. *J. Virol.* **83,** 10571–10581 (2009).

115. Garmashova, N. *et al.* Analysis of Venezuelan Equine Encephalitis Virus Capsid Protein Function in the Inhibition of Cellular Transcription. *J. Virol.* **81,** 13552–13565 (2007).

116. Sanz, M. A. & Carrasco, L. Sindbis Virus Variant with a Deletion in the 6K Gene Shows Defects in Glycoprotein Processing and Trafficking: Lack of Complementation by a Wild-Type 6K Gene in trans. *J. Virol.* **75,** 7778–7784 (2001).

117. Forrester, N. L., Guerbois, M., Adams, A. P., Liang, X. & Weaver, S. C. Analysis of Intrahost Variation in Venezuelan Equine Encephalitis Virus Reveals Repeated Deletions in the 6-Kilodalton Protein Gene▽. *J. Virol.* **85,** 8709–8717 (2011).

118. Choi, H.-K. *et al.* Structural Analysis of Sindbis Virus Capsid Mutants Involving Assembly and Catalysis. *J. Mol. Biol.* **262,** 151–167 (1996).

119. Paredes, A., Alwell-Warda, K., Weaver, S. C., Chiu, W. & Watowich, S. J. Structure of Isolated Nucleocapsids from Venezuelan Equine Encephalitis Virus and Implications for Assembly and Disassembly of Enveloped Virus. *J. Virol.* **77,** 659–664 (2003).

120. Lamb, K., Lokesh, G., Sherman, M. & Watowich, S. Structure of a Venezuelan equine encephalitis virus assembly intermediate isolated from infected cells. *Virology* **406,** 261–269 (2010).

121. Leung, J. Y.-S., Ng, M. M.-L. & Chu, J. J. H. Replication of Alphaviruses: A Review on the Entry Process of Alphaviruses into Cells. *Adv. Virol.* **2011,** (2011).

122. Owen, K. E. & Kuhn, R. J. Alphavirus Budding Is Dependent on the Interaction between the Nucleocapsid and Hydrophobic Amino Acids on the Cytoplasmic Domain of the E2 Envelope Glycoprotein. *Virology* **230,** 187–196 (1997).

123. Atasheva, S., Fish, A., Fornerod, M. & Frolova, E. I. Venezuelan Equine Encephalitis Virus Capsid Protein Forms a Tetrameric Complex with CRM1 and Importin ?/? That Obstructs Nuclear Pore Complex Function. *J. Virol.* **84,** 4158–4171 (2010).

124. Mukhopadhyay, S. *et al.* Mapping the Structure and Function of the E1 and E2 Glycoproteins in Alphaviruses. *Struct. Lond. Engl. 1993* **14,** 63–73 (2006).

125. Zhang, W. *et al.* Placement of the Structural Proteins in Sindbis Virus. *J. Virol.* **76,** 11645–11658 (2002).

126. Gonzalez, M. E. & Carrasco, L. Viroporins. *FEBS Lett.* **552,** 28–34 (2003).

127. Melton, J. V. *et al.* Alphavirus 6K Proteins Form Ion Channels. *J. Biol. Chem.* **277,** 46923–46931 (2002).

128. The Alphavirus 6K Protein Activates Endogenous Ionic Conductances when Expressed in Xenopus Oocytes - Springer. doi:10.1007/s00232-007-9003-6

129. McInerney, G. M., Smit, J. M., Liljeström, P. & Wilschut, J. Semliki Forest virus produced in the absence of the 6K protein has an altered spike structure as revealed by decreased membrane fusion capacity. *Virology* **325,** 200–206 (2004).

130. Ivanova, L., Le, L. & Schlesinger, M. J. Characterization of revertants of a Sindbis virus 6K gene mutant that affects proteolytic processing and virus assembly. *Virus Res.* **39,** 165–179 (1995).

131. Firth, A. E., Chung, B. Y., Fleeton, M. N. & Atkins, J. F. Discovery of frameshifting in Alphavirus 6K resolves a 20-year enigma. *Virol. J.* **5,** 108 (2008).

132. Giedroc, D. P., Theimer, C. A. & Nixon, P. L. Structure, stability and function of RNA pseudoknots involved in stimulating ribosomal frameshifting. *J. Mol. Biol.* **298,** 167–185 (2000).

133. Chung, B. Y.-W., Firth, A. E. & Atkins, J. F. Frameshifting in Alphaviruses: A Diversity of 3′ Stimulatory Structures. *J. Mol. Biol.* **397,** 448–456 (2010).

134. Ooi, Y. S., Stiles, K. M., Liu, C. Y., Taylor, G. M. & Kielian, M. Genome-Wide RNAi Screen Identifies Novel Host Proteins Required for Alphavirus Entry. *PLoS Pathog.* **9,** (2013).

135. Justman, J., Klimjack, M. R. & Kielian, M. Role of spike protein conformational changes in fusion of Semliki Forest virus. *J. Virol.* **67,** 7597–7607 (1993).

136. Spyr, C. A., Käsermann, F. & Kempf, C. Identification of the pore forming element of Semliki Forest virus spikes. *FEBS Lett.* **375,** 134–136 (1995).

137. Wahlberg, J. M., Bron, R., Wilschut, J. & Garoff, H. Membrane fusion of Semliki Forest virus involves homotrimers of the fusion protein. *J. Virol.* **66,** 7309–7318 (1992).

138. Kononchik, J. P., Hernandez, R. & Brown, D. T. An alternative pathway for alphavirus entry. *Virol. J.* **8,** 304 (2011).

139. Vancini, R., Wang, G., Ferreira, D., Hernandez, R. & Brown, D. T. Alphavirus Genome Delivery Occurs Directly at the Plasma Membrane in a Time- and Temperature-Dependent Process. *J. Virol.* **87,** 4352–4359 (2013).

140. Wengler, G. The regulation of disassembly of alphavirus cores. *Arch. Virol.* **154,** 381–390 (2009).

141. Fata, C. L., Sawicki, S. G. & Sawicki, D. L. Alphavirus Minus-Strand RNA Synthesis: Identification of a Role for Arg183 of the nsP4 Polymerase. *J. Virol.* **76,** 8632–8640 (2002).

142. Jose, J. *et al.* Interactions of the Cytoplasmic Domain of Sindbis Virus E2 with Nucleocapsid Cores Promote Alphavirus Budding. *J. Virol.* **86,** 2585–2599 (2012).

143. Martinez, M. G., Snapp, E.-L., Perumal, G. S., Macaluso, F. P. & Kielian, M. Imaging the Alphavirus Exit Pathway. *J. Virol.* **88,** 6922–6933 (2014).

144. Berri, F. *et al.* Annexin V Incorporated into Influenza Virus Particles Inhibits Gamma Interferon Signaling and Promotes Viral Replication. *J. Virol.* **88,** 11215–11228 (2014).

145. Lau, N. C., Lim, L. P., Weinstein, E. G. & Bartel, D. P. An Abundant Class of Tiny RNAs with Probable Regulatory Roles in Caenorhabditis elegans. *Science* **294,** 858–862 (2001).

146. Lee, R. C. & Ambros, V. An Extensive Class of Small RNAs in Caenorhabditis elegans. *Science* **294,** 862–864 (2001).

147. Cullen, B. R. RNAi the natural way. *Nat. Genet.* **37,** (2005).

148. Vittoria Scarpati, G. Della *et al.* Analysis of Differential miRNA Expression in Primary Tumor and Stroma of Colorectal Cancer Patients. *BioMed Res. Int.* **2014,** e840921 (2014).

149. Vincent, K., Pichler, M., Lee, G.-W. & Ling, H. MicroRNAs, Genomic Instability and Cancer. *Int. J. Mol. Sci.* **15,** 14475–14491 (2014).

150. Wang, Y., Liang, J., Di, C., Zhao, G. & Zhao, Y. Identification of miRNAs as potential new biomarkers for nervous system cancer. *Tumor Biol.* 1–8 (2014). doi:10.1007/s13277-014-2387-x

151. Zhang, Y., Yang, Q. & Wang, S. MicroRNAs: a new key in lung cancer. *Cancer Chemother. Pharmacol.* 1–7 (2014). doi:10.1007/s00280-014-2559-9

152. Mastropasqua, R. *et al.* Role of microRNAs in the modulation of diabetic retinopathy. *Prog. Retin. Eye Res.* doi:10.1016/j.preteyeres.2014.07.003

153. WANG, X., CHANG, X., LI, J., YIN, L. & SUN, K. DNA methylation of microRNA-375 in impaired glucose tolerance. *Exp. Ther. Med.* **8,** 775–780 (2014).

154. Pescador, N. *et al.* Serum Circulating microRNA Profiling for Identification of Potential Type 2 Diabetes and Obesity Biomarkers. *PLoS ONE* **8,** e77251 (2013).

155. Matkovich, S. J. MicroRNAs in the Stressed Heart: Sorting the Signal from the Noise. *Cells* **3,** 778–801 (2014).

156. Nagalingam, R. S. *et al.* Deficiency of Cardiomyocyte-specific-microRNA-378 Contributes to the Development of Cardiac Fibrosis involving a TGFβ1-dependent Paracrine Mechanism. *J. Biol. Chem.* jbc.M114.580977 (2014). doi:10.1074/jbc.M114.580977

157. Eskildsen, T. V. *et al.* The microRNA-132/212 family fine-tunes multiple targets in Angiotensin II signalling in cardiac fibroblasts. *J. Renin Angiotensin Aldosterone Syst.* 1470320314539367 (2014). doi:10.1177/1470320314539367

158. Warnica, W. *et al.* Copy Number Variable MicroRNAs in Schizophrenia and Their Neurodevelopmental Gene Targets. *Biol. Psychiatry* **0,**

159. Gorini, G., Nunez, Y. O. & Mayfield, R. D. Integration of miRNA and protein profiling reveals coordinated neuroadaptations in the alcohol-dependent mouse brain. *PloS One* **8,** e82565 (2013).

160. Contet, C. Gene Expression Under the Influence: Transcriptional Profiling of Ethanol in the Brain. *Curr. Psychopharmacol.* **1,** 301–314 (2012).

161. Shapiro, J. S. *et al.* Drosha as an interferon-independent antiviral factor. *Proc. Natl. Acad. Sci. U. S. A.* **111,** 7108–7113 (2014).

162. Ramesh, S. V., Ratnaparkhe, M. B., Kumawat, G., Gupta, G. K. & Husain, S. M. Plant miRNAome and antiviral resistance: a retrospective view and prospective challenges. *Virus Genes* **48,** 1–14 (2014).

163. Kingsolver, M. B., Huang, Z. & Hardy, R. W. Insect Antiviral Innate Immunity: Pathways, Effectors, and Connections. *J. Mol. Biol.* **425,** 4921–4936 (2013).

164. Backes, S. *et al.* Degradation of host microRNAs by poxvirus poly(A) polymerase reveals terminal RNA methylation as a protective antiviral mechanism. *Cell Host Microbe* **12,** 200–210 (2012).

165. Reynoso, R. *et al.* MicroRNAs differentially present in the plasma of HIV elite controllers reduce HIV infection in vitro. *Sci. Rep.* **4,** (2014).

166. Triboulet, R. *et al.* Suppression of MicroRNA-Silencing Pathway by HIV-1 During Virus Replication. *Science* **315,** 1579–1582 (2007).

167. Huang, J. *et al.* Cellular microRNAs contribute to HIV-1 latency in resting primary CD4+ T lymphocytes. *Nat. Med.* **13,** 1241–1247 (2007).

168. Houzet, L. *et al.* MicroRNA profile changes in human immunodeficiency virus type 1 (HIV-1) seropositive individuals. *Retrovirology* **5,** 118 (2008).

169. Bhela, S. *et al.* Critical role of microRNA-155 in herpes simplex encephalitis. *J. Immunol. Baltim. Md 1950* **192,** 2734–2743 (2014).

170. Kofman, A. V. *et al.* The p53–microRNA-34a axis regulates cellular entry receptors for tumor-associated human herpes viruses. *Med. Hypotheses* **81,** 62–67 (2013).

171. Yan, Q. *et al.* Cellular MicroRNAs 498 and 320d Regulate Herpes Simplex Virus 1 Induction of Kaposi's Sarcoma-Associated Herpesvirus Lytic Replication by Targeting RTA. *PLoS ONE* **8,** (2013).

172. Lin, Z. *et al.* Differential Expression of the miR-200 Family MicroRNAs in Epithelial and B Cells and Regulation of Epstein-Barr Virus Reactivation by the miR-200 Family Member miR-429. *J. Virol.* **84,** 7892–7897 (2010).

173. Liang, X.-S., Lian, J.-Q., Zhou, Y.-X. & Wan, M.-B. Inhibitor RNA blocks the protein translation mediated by hepatitis C virus internal ribosome entry site in vivo. *World J. Gastroenterol. WJG* **10,** 664–667 (2004).

174. Jopling, C. L., Yi, M., Lancaster, A. M., Lemon, S. M. & Sarnow, P. Modulation of hepatitis C virus RNA abundance by a liver-specific MicroRNA. *Science* **309,** 1577–1581 (2005).

175. Pedersen, I. M. *et al.* Interferon modulation of cellular microRNAs as an antiviral mechanism. *Nature* **449,** 919–922 (2007).

176. Klase, Z. *et al.* HIV-1 TAR element is processed by Dicer to yield a viral micro-RNA involved in chromatin remodeling of the viral LTR. *BMC Mol. Biol.* **8,** 63 (2007).

177. Yang, H.-J. *et al.* Comprehensive profiling of Epstein-Barr virus-encoded miRNA species associated with specific latency types in tumor cells. *Virol. J.* **10,** 314 (2013).

178. Parameswaran, P. *et al.* Six RNA Viruses and Forty-One Hosts: Viral Small RNAs and Modulation of Small RNA Repertoires in Vertebrate and Invertebrate Systems. *PLoS Pathog* **6,** e1000764 (2010).

179. Zhao, P. *et al.* Changes in microRNA expression induced by rabies virus infection in mouse brains. *Microb. Pathog.* **52,** 47–54 (2012).

180. Wu, Y.-Q. *et al.* Pseudorabies Virus Infected Porcine Epithelial Cell Line Generates a Diverse Set of Host MicroRNAs and a Special Cluster of Viral MicroRNAs. *PLoS ONE* **7,** e30988 (2012).

181. Han, J. *et al.* Molecular Basis for the Recognition of Primary microRNAs by the Drosha-DGCR8 Complex. *Cell* **125,** 887–901 (2006).

182. Faller, M. *et al.* DGCR8 recognizes primary transcripts of microRNAs through highly cooperative binding and formation of higher-order structures. *RNA* **16,** 1570–1583 (2010).

183. Takeshita, D. *et al.* Homodimeric Structure and Double-stranded RNA Cleavage Activity of the C-terminal RNase III Domain of Human Dicer. *J. Mol. Biol.* **374,** 106–120 (2007).

184. Chendrimada, T. P. *et al.* TRBP recruits the Dicer complex to Ago2 for microRNA processing and gene silencing. *Nature* **436,** 740–744 (2005).

185. Rand, T. A., Petersen, S., Du, F. & Wang, X. Argonaute2 Cleaves the Anti-Guide Strand of siRNA during RISC Activation. *Cell* **123,** 621–629 (2005).

186. Liu, J. *et al.* Argonaute2 Is the Catalytic Engine of Mammalian RNAi. *Science* **305,** 1437–1441 (2004).

187. Kawamata, T. & Tomari, Y. Making RISC. *Trends Biochem. Sci.* **35,** 368–376 (2010).

188. Liu, X., Jin, D.-Y., McManus, M. T. & Mourelatos, Z. Precursor MicroRNA-Programmed Silencing Complex Assembly Pathways in Mammals. *Mol. Cell* **46,** 507–517 (2012).

189. Kim, Y. & Kim, V. N. MicroRNA Factory: RISC Assembly from Precursor MicroRNAs. *Mol. Cell* **46,** 384–386 (2012).

190. Iwasaki, S. *et al.* Hsc70/Hsp90 Chaperone Machinery Mediates ATP-Dependent RISC Loading of Small RNA Duplexes. *Mol. Cell* **39,** 292–299 (2010).

191. Rand, T. A., Ginalski, K., Grishin, N. V. & Wang, X. Biochemical identification of Argonaute 2 as the sole protein required for RNA-induced silencing complex activity. *Proc. Natl. Acad. Sci. U. S. A.* **101,** 14385–14389 (2004).

192. Filipowicz, W. RNAi: The Nuts and Bolts of the RISC Machine. *Cell* **122,** 17–20 (2005).

193. Li, J. *et al.* Identifying mRNA sequence elements for target recognition by human Argonaute proteins. *Genome Res.* **24,** 775–785 (2014).

194. Brodersen, P. & Voinnet, O. Revisiting the principles of microRNA target recognition and mode of action. *Nat. Rev. Mol. Cell Biol.* **10,** 141–148 (2009).

195. Djuranovic, S., Nahvi, A. & Green, R. miRNA-mediated gene silencing by translational repression followed by mRNA deadenylation and decay. *Science* **336,** 237–240 (2012).

196. Eulalio, A. *et al.* Deadenylation is a widespread effect of miRNA regulation. *RNA* **15,** 21–32 (2009).

197. Berezikov, E., Chung, W.-J., Willis, J., Cuppen, E. & Lai, E. C. Mammalian Mirtron Genes. *Mol. Cell* **28,** 328–336 (2007).

198. Sibley, C. R. *et al.* The biogenesis and characterization of mammalian microRNAs of mirtron origin. *Nucleic Acids Res.* **40,** 438–448 (2012).

199. Schamberger, A., Sarkadi, B. & Orban, T. I. Human mirtrons can express functional microRNAs simultaneously from both arms in a flanking exon-independent manner. *RNA Biol.* **9,** 1177–1185 (2012).

200. Havens, M. A., Reich, A. A., Duelli, D. M. & Hastings, M. L. Biogenesis of mammalian microRNAs by a non-canonical processing pathway. *Nucleic Acids Res.* **40,** 4626–4640 (2012).

201. Chekulaeva, M. & Filipowicz, W. Mechanisms of miRNA-mediated post-transcriptional regulation in animal cells. *Curr. Opin. Cell Biol.* **21,** 452–460 (2009).

202. Down-Regulated miRNA-214 Induces a Cell Cycle G1 Arrest in Gastric Cancer Cells by Up-Regulating the PTEN Protein - Springer. doi:10.1007/s12253-011-9406-7

203. Curtale, G. *et al.* Negative regulation of Toll-like receptor 4 signaling by IL-10–dependent microRNA-146b. *Proc. Natl. Acad. Sci.* **110,** 11499–11504 (2013).

204. Chen, Z. *et al.* Hypoxia-responsive miRNAs target argonaute 1 to promote angiogenesis. *J. Clin. Invest.* **123,** 1057–1067 (2013).

205. Vasudevan, S., Tong, Y. & Steitz, J. A. Switching from Repression to Activation: MicroRNAs Can Up-Regulate Translation. *Science* **318,** 1931–1934 (2007).

206. Henke, J. I. *et al.* microRNA-122 stimulates translation of hepatitis C virus RNA. *EMBO J.* **27,** 3300–3310 (2008).

207. Jopling, C. L., Norman, K. L. & Sarnow, P. Positive and Negative Modulation of Viral and Cellular mRNAs by Liver-specific MicroRNA miR-122. *Cold Spring Harb. Symp. Quant. Biol.* **71,** 369–376 (2006).

208. Roberts, A. P. E., Lewis, A. P. & Jopling, C. L. miR-122 activates hepatitis C virus translation by a specialized mechanism requiring particular RNA components. *Nucleic Acids Res.* **39,** 7716–7729 (2011).

209. Lewis, B. P., Burge, C. B. & Bartel, D. P. Conserved Seed Pairing, Often Flanked by Adenosines, Indicates that Thousands of Human Genes are MicroRNA Targets. *Cell* **120,** 15–20 (2005).

210. Friedman, R. C., Farh, K. K.-H., Burge, C. B. & Bartel, D. P. Most mammalian mRNAs are conserved targets of microRNAs. *Genome Res.* **19,** 92–105 (2009).

211. Grimson, A. *et al.* MicroRNA Targeting Specificity in Mammals: Determinants beyond Seed Pairing. *Mol. Cell* **27,** 91–105 (2007).

212. Hsu, S.-D. *et al.* miRTarBase update 2014: an information resource for experimentally validated miRNA-target interactions. *Nucleic Acids Res.* **42,** D78–D85 (2014).

213. Geng, L. *et al.* MicroRNA-103 Promotes Colorectal Cancer by Targeting Tumor Suppressor DICER and PTEN. *Int. J. Mol. Sci.* **15,** 8458–8472 (2014).

214. Sun, L. & Li, Q. The miRNAs of herpes simplex virus (HSV). *Virol. Sin.* **27,** 333–338 (2012).

215. Jung, Y.-J., Choi, H., Kim, H. & Lee, S. K. MicroRNA miR-BART20-5p Stabilizes Epstein-Barr Virus Latency by Directly Targeting BZLF1 and BRLF1. *J. Virol.* **88,** 9027–9037 (2014).

216. Moody, R. *et al.* KSHV MicroRNAs Mediate Cellular Transformation and Tumorigenesis by Redundantly Targeting Cell Growth and Survival Pathways. *PLoS Pathog.* **9,** (2013).

217. Umbach, J. L. *et al.* MicroRNAs expressed by herpes simplex virus 1 during latent infection regulate viral mRNAs. *Nature* **454,** 780–783 (2008).

218. Feldman, E. R. *et al.* Virus-Encoded MicroRNAs Facilitate Gammaherpesvirus Latency and Pathogenesis In Vivo. *mBio* **5,** (2014).

219. Gallaher, A. M. *et al.* Proteomic Screening of Human Targets of Viral microRNAs Reveals Functions Associated with Immune Evasion and Angiogenesis. *PLoS Pathog* **9,** e1003584 (2013).

220. Narayanan, A., Kehn-Hall, K., Bailey, C. & Kashanchi, F. Analysis of the roles of HIV-derived microRNAs. *Expert Opin. Biol. Ther.* **11,** 17–29 (2010).

221. Zhang, Y. *et al.* A novel HIV-1-encoded microRNA enhances its viral replication by targeting the TATA box region. *Retrovirology* **11,** 23 (2014).

222. Blevins, T. *et al.* Massive production of small RNAs from a non-coding region of Cauliflower mosaic virus in plant defense and viral counter-defense. *Nucleic Acids Res.* **39,** 5003–5014 (2011).

223. Hussain, M. & Asgari, S. MicroRNA-like viral small RNA from Dengue virus 2 autoregulates its replication in mosquito cells. *Proc. Natl. Acad. Sci. U. S. A.* **111,** 2746–2751 (2014).

224. Léger, P. *et al.* Dicer-2- and Piwi-Mediated RNA Interference in Rift Valley Fever Virus-Infected Mosquito Cells. *J. Virol.* **87,** 1631–1648 (2013).

225. Lee, R. C., Feinbaum, R. L. & Ambros, V. The C. elegans heterochronic gene lin-4 encodes small RNAs with antisense complementarity to lin-14. *Cell* **75,** 843–854 (1993).

226. Reinhart, B. J. *et al.* The 21-nucleotide let-7 RNA regulates developmental timing in Caenorhabditis elegans. *Nature* **403,** 901–906 (2000).

227. Ambros, V. *et al.* A uniform system for microRNA annotation. *RNA* **9,** 277–279 (2003).

228. Tan, W., Li, Y., Lim, S.-G. & Tan, T. M. miR-106b-25/miR-17-92 clusters: Polycistrons with oncogenic roles in hepatocellular carcinoma. *World J.*

Gastroenterol. WJG **20,** 5962–5972 (2014).

229. Jurak, I. *et al.* Expression of Herpes Simplex Virus 1 MicroRNAs in Cell Culture Models of Quiescent and Latent Infection. *J. Virol.* **88,** 2337–2339 (2014).

230. Ambrosio, M. R. *et al.* The Epstein Barr-encoded BART-6-3p microRNA affects regulation of cell growth and immuno response in Burkitt lymphoma. *Infect. Agent. Cancer* **9,** 12 (2014).

231. Olive, V., Li, Q. & He, L. mir-17-92, a polycistronic oncomir with pleiotropic functions. *Immunol. Rev.* **253,** 158–166 (2013).

232. Mendell, J. T. miRiad roles for the miR-17-92 cluster in development and disease. *Cell* **133,** 217–222 (2008).

233. Li, Y., Choi, P. S., Casey, S. C., Dill, D. L. & Felsher, D. W. MYC through miR-17-92 Suppresses Specific Target Genes to Maintain Survival, Autonomous Proliferation, and a Neoplastic State. *Cancer Cell* **26,** 262–272 (2014).

234. Kroesen, B.-J. *et al.* Immuno-miRs: Critical regulators of T-cell development, function and ageing. *Immunology* n/a–n/a (2014). doi:10.1111/imm.12367

235. Poitz, D. M. *et al.* Regulation of the Hif-system by micro-RNA 17 and 20a – Role during monocyte-to-macrophage differentiation. *Mol. Immunol.* **56,** 442–451 (2013).

236. Carraro, G. *et al.* miR-17 family of microRNAs controls FGF10-mediated embryonic lung epithelial branching morphogenesis through MAPK14 and STAT3 regulation of E-Cadherin distribution. *Dev. Biol.* **333,** 238–250 (2009).

237. Sun, Q. *et al.* Role of miR-17 Family in the Negative Feedback Loop of Bone Morphogenetic Protein Signaling in Neuron. *PLoS ONE* **8,** (2013).

238. Garg, N. *et al.* microRNA-17-92 cluster is a direct Nanog target and controls neural stem cell through Trp53inp1. *EMBO J.* **32,** 2819–2832 (2013).

239. Ventura, A. *et al.* Targeted deletion reveals essential and overlapping functions of the miR-17~92 family of miRNA clusters. *Cell* **132,** 875–886 (2008).

240. de Pontual, L. *et al.* Germline deletion of the miR-17-92 cluster causes growth and skeletal defects in humans. *Nat. Genet.* **43,** 1026–1030 (2011).

241. Fink, S. E. K. *et al.* A Comprehensive Analysis of the Cellular and EBV-Specific MicroRNAome in Primary CNS PTLD Identifies Different Patterns Among EBV-

Associated Tumors. *Am. J. Transplant.* n/a–n/a (2014). doi:10.1111/ajt.12858

242. Tsubota, A. *et al.* Involvement of MAP3K8 and miR-17-5p in Poor Virologic Response to Interferon-Based Combination Therapy for Chronic Hepatitis C. *PLoS ONE* **9,** (2014).

243. Chugh, P. E. *et al.* Systemically Circulating Viral and Tumor-Derived MicroRNAs in KSHV-Associated Malignancies. *PLoS Pathog.* **9,** (2013).

244. Thapa, D. R., Li, X., Jamieson, B. D. & Martinez-Maza, O. Overexpression of MicroRNAs from the miR-17-92 Paralog Clusters in AIDS-Related Non-Hodgkin's Lymphomas. *PLoS ONE* **6,** (2011).

245. Liu, Y. P., Haasnoot, J., Brake, O. ter, Berkhout, B. & Konstantinova, P. Inhibition of HIV-1 by multiple siRNAs expressed from a single microRNA polycistron. *Nucleic Acids Res.* **36,** 2811–2824 (2008).

246. Zhu, Z. *et al.* Comprehensive Characterization of Serum MicroRNA Profile in Response to the Emerging Avian Influenza A (H7N9) Virus Infection in Humans. *Viruses* **6,** 1525–1539 (2014).

247. Ikegami, T. & Makino, S. The Pathogenesis of Rift Valley Fever. *Viruses* **3,** 493–519 (2011).

248. Gibson, G. Microarray Analysis. *PLoS Biol* **1,** e15 (2003).

249. Caplen, H., Peters, C. J. & Bishop, D. H. L. Mutagen-directed Attenuation of Rift Valley Fever Virus as a Method for Vaccine Development. *J. Gen. Virol.* **66,** 2271–2277 (1985).

250. Bouloy, M. *et al.* Genetic Evidence for an Interferon-Antagonistic Function of Rift Valley Fever Virus Nonstructural Protein NSs. *J. Virol.* **75,** 1371–1377 (2001).

251. Saluzzo, J. F. & Smith, J. F. Use of reassortant viruses to map attenuating and temperature-sensitive mutations of the Rift Valley fever virus MP-12 vaccine. *Vaccine* **8,** 369–375 (1990).

252. Kehn-Hall, K. *et al.* Modulation of GSK-3? Activity in Venezuelan Equine Encephalitis Virus Infection. *PLoS ONE* **7,** (2012).

253. Livak, K. J. & Schmittgen, T. D. Analysis of relative gene expression data using real-time quantitative PCR and the 2(-Delta Delta C(T)) Method. *Methods San Diego Calif* **25,** 402–408 (2001).

254. Coley, W. *et al.* Absence of DICER in Monocytes and Its Regulation by HIV-1. *J. Biol. Chem.* **285,** 31930–31943 (2010).

255. Farhana, L. *et al.* Upregulation of miR-150* and miR-630 Induces Apoptosis in Pancreatic Cancer Cells by Targeting IGF-1R. *PLoS ONE* **8,** e61015 (2013).

256. Han, C., Wan, G., Langley, R. R., Zhang, X. & Lu, X. Crosstalk between the DNA damage response pathway and microRNAs. *Cell. Mol. Life Sci. CMLS* **69,** 2895–2906 (2012).

257. Yan, H. *et al.* Repression of the miR-17-92 cluster by p53 has an important function in hypoxia-induced apoptosis. *EMBO J.* **28,** 2719–2732 (2009).

258. Osada, N. *et al.* The Genome Landscape of the African Green Monkey Kidney-Derived Vero Cell Line. *DNA Res.* dsu029 (2014). doi:10.1093/dnares/dsu029

259. Emeny, J. M. & Morgan, M. J. Regulation of the Interferon System: Evidence that Vero Cells have a Genetic Defect in Interferon Production. *J. Gen. Virol.* **43,** 247–252 (1979).

260. Desmyter, J., Melnick, J. L. & Rawls, W. E. Defectiveness of Interferon Production and of Rubella Virus Interference in a Line of African Green Monkey Kidney Cells (Vero). *J. Virol.* **2,** 955–961 (1968).

261. de Lang, A., Osterhaus, A. D. M. E. & Haagmans, B. L. Interferon-γ and interleukin-4 downregulate expression of the SARS coronavirus receptor ACE2 in Vero E6 cells. *Virology* **353,** 474–481 (2006).

262. Buchholz, U. J., Finke, S. & Conzelmann, K.-K. Generation of Bovine Respiratory Syncytial Virus (BRSV) from cDNA: BRSV NS2 Is Not Essential for Virus Replication in Tissue Culture, and the Human RSV Leader Region Acts as a Functional BRSV Genome Promoter. *J. Virol.* **73,** 251–259 (1999).

263. Kalveram, B., Lihoradova, O., Indran, S. V. & Ikegami, T. Using Reverse Genetics to Manipulate the NSs Gene of the Rift Valley Fever Virus MP-12 Strain to Improve Vaccine Safety and Efficacy. *J. Vis. Exp. JoVE* (2011). doi:10.3791/3400

264. O'Donnell, K. A., Wentzel, E. A., Zeller, K. I., Dang, C. V. & Mendell, J. T. c-Myc-regulated microRNAs modulate E2F1 expression. *Nature* **435,** 839–843 (2005).

265. Narayanan, A. *et al.* Curcumin Inhibits Rift Valley Fever Virus Replication in Human Cells. *J. Biol. Chem.* **287,** 33198–33214 (2012).

266. Yen, Y.-C. *et al.* Reciprocal regulation of MicroRNA-99a and insulin-like growth factor I receptor signaling in oral squamous cell carcinoma cells. *Mol. Cancer* **13,** 6 (2014).

267. Li, X.-J. *et al.* MicroRNA-100/99a, deregulated in acute lymphoblastic leukaemia, suppress proliferation and promote apoptosis by regulating the FKBP51 and IGF1R/mTOR signalling pathways. *Br. J. Cancer* **109,** 2189–2198 (2013).

268. Lerman, G. *et al.* MiRNA Expression in Psoriatic Skin: Reciprocal Regulation of hsa-miR-99a and IGF-1R. *PLoS ONE* **6,** (2011).

269. O'Carroll, D. & Schaefer, A. General Principals of miRNA Biogenesis and Regulation in the Brain. *Neuropsychopharmacology* **38,** 39–54 (2013).

270. Liu, Z.-P., Wu, H., Zhu, J. & Miao, H. Systematic identification of transcriptional and post-transcriptional regulations in human respiratory epithelial cells during influenza A virus infection. *BMC Bioinformatics* **15,** 336 (2014).

271. Berge, T. O., Banks, I. S. & Tigertt, W. D. Attenuation of Venezuelan Equine Encephalomyelitis Virus by in Vitro Cultivation in Guinea-Pig Heart Cells. *Am. J. Epidemiol.* **73,** 209–218 (1961).

272. Kinney, R. M. *et al.* Attenuation of Venezuelan equine encephalitis virus strain TC-83 is encoded by the 5'-noncoding region and the E2 envelope glycoprotein. *J. Virol.* **67,** 1269–1277 (1993).

273. Madsen, C. *et al.* Small molecule inhibitors of Ago2 decrease Venezuelan equine encephalitis virus replication. *Antiviral Res.* **112,** 26–37 (2014).

274. Wainwright, M. Acridine—a neglected antibacterial chromophore. *J. Antimicrob. Chemother.* **47,** 1–13 (2001).

275. Waterhouse, P. M., Wang, M.-B. & Lough, T. Gene silencing as an adaptive defence against viruses. *Nature* **411,** 834–842 (2001).

276. tenOever, B. R. RNA viruses and the host microRNA machinery. *Nat. Rev. Microbiol.* **11,** 169–180 (2013).

277. Cao, J.-X. *et al.* MiR-630 inhibits proliferation by targeting CDC7 kinase, but maintains the apoptotic balance by targeting multiple modulators in human lung cancer A549 cells. *Cell Death Dis.* **5,** e1426 (2014).

278. Hou, C., Zhu, M., Sun, M. & lin, Y. MicroRNA let-7i induced autophagy to protect T cell from apoptosis by targeting IGF1R. *Biochem. Biophys. Res. Commun.*

doi:10.1016/j.bbrc.2014.10.002

279. Kim, S. G. *et al.* Suppression of Xenobiotic-Metabolizing Enzyme Expression in Rats by Acriflavine, a Protein Kinase C Inhibitor Effects on Epoxide Hydrolase, GlutathioneS-Transferases, and Cytochromes P450. *Drug Metab. Dispos.* **26,** 66–72 (1998).

280. Shay, J. E. S. *et al.* Inhibition of hypoxia-inducible factors limits tumor progression in a mouse model of colorectal cancer. *Carcinogenesis* **35,** 1067–1077 (2014).

281. Iwamoto, Y. *et al.* Photodynamic DNA strand breaking activities of acridine compounds. *Biol. Pharm. Bull.* **16,** 1244–1247 (1993).

282. Schinazi, R. F., Bassit, L. & Gavegnano, C. HCV drug discovery aimed at viral eradication. *J. Viral Hepat.* **17,** 77–90 (2010).

283. Janssen, H. L. A. *et al.* Treatment of HCV Infection by Targeting MicroRNA. *N. Engl. J. Med.* **368,** 1685–1694 (2013).

BIOGRAPHY

Cathaleen King Madsen graduated from West Potomac High School, Alexandria, Virginia, in 1989 and received her Bachelor of Arts from Randolph-Macon Woman's College in 1995. She was employed for nine years at Covance Laboratories in Vienna, Virginia, followed by a brief stint with the Museum of Florida History before returning to Virginia. During her graduate studies, she served for five years as a laboratory instructor at George Mason University, and is the recipient of three Provost's Commendations for excellence in teaching, two Bioscience Director's Fellowships, and the Elaine Joyce Outstanding Graduate Teaching Assistant Award. She currently resides in Fairfax, Virginia with her family.